uOttawa

L'Université canadienne
Canada's university

FACULTÉ DES ÉTUDES SUPÉRIEURES ET POSTDOCTORALES

uOttawa

L'Université canadienne
Canada's university

FACULTY OF GRADUATE AND POSTDOCTORAL STUDIES

Homam Albaghdadi
AUTEUR DE LA THÈSE / AUTHOR OF THESIS

M.Sc. (Microbiology and Immunology)
GRADE / DEGREE

Department of Biochemistry and Microbiology and Immunology
FACULTÉ, ÉCOLE, DÉPARTEMENT / FACULTY, SCHOOL, DEPARTMENT

Poor intracellular proliferation delays rapid priming and influences programming of $CD8^+$ T cells during infection with *Salmonella typhimurium*

TITRE DE LA THÈSE / TITLE OF THESIS

S. Sad
DIRECTEUR (DIRECTRICE) DE LA THÈSE / THESIS SUPERVISOR

CO-DIRECTEUR (CO-DIRECTRICE) DE LA THÈSE / THESIS CO-SUPERVISOR

EXAMINATEURS (EXAMINATRICES) DE LA THÈSE / THESIS EXAMINERS

A. Kumar

K. Wright

Gary W. Slater
Le Doyen de la Faculté des études supérieures et postdoctorales / Dean of the Faculty of Graduate and Postdoctoral Studies

Poor intracellular proliferation delays rapid priming and influences programming of $CD8^+$ T cells during infection with *Salmonella typhimurium*

Homam Albaghdadi

Thesis submitted to the
Faculty of Graduate and Postdoctoral Studies
In fulfillment of the requirements
For the M.Sc degree in Immunology
Biochemistry, Microbiology and Immunology Department
Faculty of Medicine
University of Ottawa

Your file Votre référence
ISBN: 978-0-494-58206-0
Our file Notre référence
ISBN: 978-0-494-58206-0

ACKNOWLEDGMENTS

First and foremost, I would like to sincerely thank my supervisor, Dr. Subash Sad, for the great privilege of working in his laboratory. He and his wife, Dr. Lakshmi Krishnan, make for a remarkable team that will put forth immense contributions to the field of immunology. I would like to thank Renu Dudani, Sue MacLean and Marsha Russel for their generous and copious technical assistance. I would like to especially thank my wonderful and brilliant lab mates, Scott McComb, Felicity Stark, Anindita Chattopadhyay, and Rebecca Mulligan for making this experience unforgettable and extraordinarily fun. I will strive to preserve their priceless friendships forever. I would like to thank my dear brothers Ayham and Amjad for being the dysfunctional distraction that I so desperately needed to keep my sanity. Last but not least, I would like to thank my beloved heroes, my mother Mouna and my father Yassin, for supporting me, believing in me, doubting me, and loving me. I dedicate this to them. To all my friends, every one of them, thank you for your immense support, love and friendship.

ABSTRACT

Antigen-presentation to $CD8^+$ T cells normally commences immediately after infection, which facilitates their rapid expansion and control of infection. Subsequently, these antigen-primed $CD8^+$ T cells undergo rapid contraction. This paradigm is not followed during infection with virulent Salmonella typhimurium (ST), an intracellular bacterium that replicates within phagosomes of infected cells. While susceptible mice die rapidly (~ 7 days), resistant mice (129X1SvJ) harbor a chronic infection lasting ~60-90 days. Using recombinant Ovalbumin (OVA)-expressing ST (ST-OVA), I show that antigen-presentation is considerably delayed in mice infected with ST-OVA. Impairment of antigen-presentation by ST-OVA-infected macrophages and dendritic cells was not due to immuno-modulatory effects of ST virulence factors, because none of the mutants used in this study displayed enhanced priming. Instead, I propose that muted antigen presentation is a consequence of poor intracellular proliferation of ST and reduced antigen load. Proliferation of OVA-specific $CD8^+$ T cells that were induced during infection peaked around day 21, and was followed by a prolonged phase of contraction. Furthermore, the magnitude of the response was contingent upon the extent of ST virulence. $CD8^+$ T cell response against virulent ST displayed a prolonged and persistent effector-memory phenotype, while that against attenuated mutants displayed reduced numbers of effector-memory cells. Taken together, these results indicate that the muted and delayed activation of $CD8^+$ T cells during infection with ST is mainly due to poor intracellular proliferation of ST, and that pathogen virulence influences the differentiation program of $CD8^+$ T cells.

TABLE OF CONTENTS

LIST OF FIGURES

LIST OF ABBREVIATIONS

APC	Antigen presenting cell
BCR	B cell receptor
BHI	Brain Heart Infusion
BrdU	Bromodeoxyuridine
CD	Cluster of Differentiation
CFSE	Carboxyfluorescein succinimidyl ester
CTL	Cytotoxic lymphocyte
CFU	Colony Forming Units
ELISPOT	Enzyme-linked immunospot assay
FBS	Fetal Bovine Serum
GM-CSF	Granulocyte-Macrophage colony stimulating factor
HBSS	Hank's Balanced Salt Solution
IFN-α	Interferon Alpha
IFN-β	Interferon Beta
IFN-γ	Interferon Gamma
IL	Interleukin
i.p.	Intraperitoneal Cavity Injection
i.v.	Lateral Tail Vein Injection
LCMV	Lymphocytic choriomeningitis Virus
LM	*Listeria monocytogens*
LPS	Lipopolysaccharide
MHC	Major Histocompatibility Complex
MOI	Multiplicity of Infection
MTT	3-(4,5-Dimethylthiazol-2-yl)-2,5-diphenyltetrazolium bromide
MTS	3-(4,5-dimethylthiazol-2-yl)-5-(3-carboxymethoxyphenyl)-2-(4-sulfophenyl)-2H-tetrazolium
OVA	Ovalbumin
OT-1	$OVA_{257-264}$-specific TCR Transgenic Mice
PBS-T80	1x PBS with 0.05% Tween 80
pMHC	peptide-MHC complex
R8	RPMI 1640 Containing 8% Fetal Bovine Serum
R10	RPMI 1640 Containing 10% Fetal Bovine Serum
SCV	*Salmonella* containing vacuole
ST	*Salmonella typhimurium* SL 1344
SIINFEKL	amino acids 257-264 of the Chicken Ovalbumin Gene
TCR	T cell Receptor
TNF-α	Tumor Necrosis Factor Alpha
TAP	Transporter Associated with Antigen Processing

CHAPTER I:
INTRODUCTION

I. Introduction

1. Infection

Salmonella species are major contaminants of food and water which affect some 16 million people annually, 600,000 cases of which are fatal (1, 2). These bacteria infect humans and domestic animals and cause diseases ranging from self-limiting gastroenteritis to typhoid fever and systemic infection (1, 2). They fall into the category of intracellular pathogens that induce chronic infections which to date have no available effective vaccines.

Listeria monocytogenes (LM) is the causative agent of Listeriosis (3). Also a food contaminant, Listeria affects people world-wide and recent outbreaks have been reported including one in France in 2000, and Toronto, Canada in 2008 (World Health Organization (WHO), 2008) . The bacteria cause general muscle-ache, fever and can spread to the nervous system (3). Furthermore, fatality can reach 20-30% in susceptible groups (3).

a. *Salmonella* infection

Salmonella typhimurium is a gram-negative, facultative-intracellular bacterium that causes gastroenteritis in humans and typhoid-like systemic disease in mice (2, 4). ST can therefore be used as a systemic disease model of typhoid fever in humans, which is namely caused by the *Salmonella* serovars *typhi* and *paratyphi*. *Salmonella* species infect animals and humans by the oral route (1, 5) and a proportion survives the acidity of the stomach by an adaptive acid-tolerance response (4). At the intestinal brush border, *Salmonella* can be taken up by dendritic cells (DCs) that sample the luminal surface, or

can invade the microfold cells (M cells) of the Peyer's patches, and subsequently the submucosal macrophages (4, 6).

Salmonella invades host cells by inducing cytoskeletal rearrangement and membrane ruffling, a process termed bacterial-mediated endocytosis, also referred to as the "trigger mechanism" (5, 7). These submucosal macrophages and DCs transport the bacteria to spleen and liver where they proliferate (6). *Salmonella* has indeed been found to manipulate the migrational patterns of dendritic cells. Induced upregulation of CCR7 resulted in the homing of those infected DCs to lymphoid tissue (8). In the spleen, the bacteria are primarily found in the red pulp and marginal zone macrophages. In the liver, *Salmonella* localizes in the Kupffer cells and can be found in the extracellular microvasculature and parenchyma (2).

Two gene loci are of particular interest for virulence of ST, namely, salmonella pathogenecity islands 1 and 2 (SPI-1 and SPI-2) (2, 4). These two loci code for various structural and secreted components that characterize ST virulence. Notably, a unique structure called Type III Secretion System (TTSS) is a molecular syringe encoded by ST to deliver virulence factors into its host cell (2, 4, 5, 9). This is known to alter the dynamics and biogenesis of the internal host cell environment, specifically, it facilitates bacterial internalization by macropinocytosis (trigger mechanism) (7), and once inside causes the arrest of phagosome (*Salmonella* containing vacuole or SCV) maturation and lysosome fusion (10, 11).

SPI-1 genes are involved in invasion into host epithelial cells. Two factors, SopE and *SptP*, target G proteins and subsequently induce or inhibit downstream MAP kinase signaling pathways. Another protein, sipA, seems to promote actin polymerization (4, 9).

SPI-2 genes are involved with intracellular propagation of the bacteria and delivery of factors that inhibit NADPH dependent oxidases as well as inhibit reactive N and O species conferring bacterial resistance (1). The latter events are orchestrated by a two-component regulatory operon known as *PhoP/PhoQ*. This "regulon" controls the expression of many virulence genes, including *sifA* and *sipC*, both of which are critical for the maintenance of *Salmonella* containing vacuole (SCV) (4, 6). This system acts as a sensor in which *PhoP*, a membrane spanning component, responds to environmental cues and relays a signal to *PhoQ*, a cytoplasmic component that regulates bacterial gene expression (11). Without phagosomal maturation and fusion with lysosomes, which are laden with antimicrobial agents, macrophages are unable to destroy these engulfed bacteria, allowing them to propagate intracellularly and evade detection by other host immune cells. Furthermore, the *PhoP/PhoQ* system facilitates increased resistance to antimicrobial peptides by surface membrane modifications, including LPS modification making it less inflammatory (12). A hallmark of ST virulence is the purported inhibition of antigen presentation facilitated by SPI-2, and suppression of T cell proliferation by iNOS (13, 14). Studies show that mutations in SPI-2 result in enhanced T cell activation. The studies claim the mutations in SPI-2 restore lysosomal targeting of SCV and subsequent antigen presentation (13, 14). Inhibition of intracellular loading of MHCII has been reported to be also SPI-2 mediated (15). Furthermore, ST replication is typically thought to occur intracellularly and mutants defective for intracellular replication are highly attenuated *in vivo* (16). It is worth noting however that the latter observations are typically detected in epithelial cell types/lines, and may not be representative of what happens in other cell types, especially macrophages.

b. Listeria Infection

Listeria moncytogenes is a gram-positive, facultative intracellular pathogen that causes gastroenteritis and can lead to meningitis and meningo-encephalitis (3, 17, 18). Like *Salmonella*, *Listeria* also enter host by the oral route and multiply in the M cells of Peyer's patches from which they invade neighboring enterocytes and gain access to blood and lymph (17).

Unlike Salmonella, Listeria invades many cell types by a "zipper mechanism" (7), which requires host surface receptor interaction. In its simplest terms, interaction between host receptor E-cadherin and LM surface protein internalin (InlA) and/or Met/HGFR (hepatocyte growth factor receptor) with InlB culminates in the internalization of the bacteria (19). Subsequently, LM escapes the phagosome using its pore forming virulence factor Listeriolysin (*LLO*), and in the cytoplasm it replicates at a rate comparable to that of culture broth (3, 18). LM utilizes another virulence factor, *ActA*, to invade neighboring cells. *ActA* recruits actin filaments which Listeria use to move inside the cell, push through the plasma membrane and project itself into neighboring cells. Once inside a neighboring cell, the two membrane vacuole pinches off, and with a combination of *LLO* and Phospholipase C (PLC) LM escapes into the cytosol again. In macrophages (18), LM's phagosomal residence is transient; however, it has evolved some mechanisms to survive that hostile environment, including secretion of a superoxide dismutase and the factor *PgdA* that makes the pepitdoglycan coat more resilient to lysozyme (18).

2. Immune Response

a. Cytotoxic T cells

Cytotoxic lymphocytes (CTLs), namely CD8 T cells, play a very crucial role in fighting and controlling tumors (20, 21), virus infections (22, 23), parasite infections (24) and intracellular bacterial infections (25). In tuberculosis, depletion of $CD8^+$ T cells results in a switch from a resistant to a susceptible phenotype, and LM infection, an otherwise acute infection, becomes chronic in the absence of $CD8^+$ T cells (25, 26).

The T cell response is triggered by the presentation of antigen to responsive T cells see Antigen Presentation section below) and follows three phases: expansion, contraction, and memory formation (27). After Antigen encounter, antigen-specific T cells commit to clonal expansion and acquisition of effector functions (27). This stage is hallmarked by up-regulation of IL2R (CD25) and secretion of IL2 which can act in an autocrine and paracrine manner supporting increased cell division via JAK1/3 kinase pathways (28, 29). After the peak of immune response, usually day 7 after infection, 90-95% of these cells undergo apoptosis and 5-10% persist, through self-renewal, as memory cells capable of rapid response to secondary infection (27).

T cell activation is accompanied by rapid epigenetic changes. Little is known about the master regulators of $CD8^+$ T cell lineage commitment but two proteins have been implicated in maintenance of committed cells including T-bet and the T-bet paralog eomesodermin (Eomes) (30-32). Furthermore, regulatory T cells, specifically $CD4^+CD25^+$, were also found to regulate $CD8^+$ T cell activation (33).

Such epigenetic remodeling leads to expression of various molecules critical for T cell cytolytic function, namely, perforin and granzyme, and FAS ligand (30, 34). Coordinated

delivery of the pore-forming protein perforin and granules of granzyme A or B into target cells, result in cell lysis (35, 36). On the other hand, the FAS dependent mechanism results in induction of apoptosis by FAS aggregation. Both mechanisms induce the caspase death cascade in the target cell (30, 35, 36). Activated $CD8^+$ T cells also produce cytokines important for recruitment neutrophils and macrophages including IFNγ (interferon gamma) and TNFα (tumor necrosis factor alpha). IFNγ was found to be critical against intracellular (37), and intraphagosomal bacteria such as *chlamydia* (36) and *Mycobacterium tuberculosis* (38), but not the intracytosolic pathogen *Listeria monoctyogenes*(36).

Activated $CD8^+$ T cells display a different set of surface molecules that facilitate cell-adhesion and chemotaxis, as well as possibly shaping its lineage development by allowing integration of additional signals (39). Activated T cells (effector cells) express CD44, an activation marker, and downregulate L-selectin (CD62L) and IL7Rα (CD127), both of which are expressed in naïve T cells (27, 39, 39).

CD62L is an important tissue homing molecule the expression of which promotes lymphocyte migration to lymphoid organs (27), and therefore, its down-regulation ensures efficient emigration of activated T cells and surveillance in peripheral tissues. IL7, as well as the IL2 family of cytokines (IL2, IL4, IL7 and IL15), are thought to be important in the contraction-to-memory transition since they support $CD8^+$ T cells survival and proliferation (IL4 survival only) (27). Therefore, down-regulation of CD127 can be viewed as a safeguard to inhibit excessive T cell proliferation (39, 40). Furthermore, there is evidence that the TNF-family interactions (CD27-CD70 and CD40-CD40L) negatively regulate contraction and CTL death (27, 41), while perforin and IFNγ

mediate CTL death, and therefore affect the formation of memory pool (42). In fact, there is a direct correlation between the extent of cell death during contraction and the size of memory pool that forms thereafter (27).

Two prominent memory subtypes persist after clearance of the infection. This classification is based on the expression of two surface molecules, the aforementioned CD62L that binds the peripheral-node addressin (PNAd) on high endothelial venules (HEV) facilitating attachment and rolling (27), and the chemokine receptor CCR7 which binds chemokines CCL19 and CCL21 in the lumina of lymph node endothelial cells facilitating firm arrest and extravasation. Two subtypes emerge with different homing properties contingent upon the coexpression, or lack thereof, of these two molecules (34, 43). $CD62L^{hi}CCR7^{+}$ populations, or "central memory" home to lymph nodes and spleen whereas $CD62L^{lo}CCR7^{-}$ populations, or "effector memory", reside in the peripheral tissue (43). These studies have also demonstrated the functional differences between those two populations. Central memory cells exhibit superior regenerative ability and activate APC more efficiently. Effector memory cells exhibit superior ability to mediate rapid effector functions, including more cytolytic activity and IFNγ secretion. Furthermore, cytokines can influence the type of memory pool created. IL15 was found to skew memory populations towards a more central phenotype, whereas IL2 favors effector memory formation (27, 30).

There has been extensive research surrounding the roadmap of T cell differentiation. As previously mentioned, the pathways of T cell differentiation into memory and effector subsets (T_{EFF}) are largely speculative; nonetheless, several models have been postulated (44, 45). The classical linear development or uniform potential model proposes that

effector populations arise upon antigenic stimulation of naïve T cells, and that memory cells are direct descendents of these effectors that arise upon antigen withdrawal. This implies that there has to be a reversion to stem cell like potential, which has not been documented to date.

In an attempt to account for the significant heterogeneity observed in the T cell pools more models emerged. The decreasing potential hypothesis is rooted in the persistence of antigen. Effector cells are said to loose "potential" with persisting antigen, culminating in apoptosis. Along this hierarchy, removal of antigen results in formation of memory pools. Effectors at the lower end of the spectrum are likely to produce less functional and less abundant memory pools. This model encompasses the formation of effector memory (T_{EM}) and central memory (T_{CM}) subtypes, where, upon antigen withdrawal, T_{EM} arises from late effector cells, and T_{CM} arises from early effector cells.

Very recently however, memory formation was linked to the polarity of cells during their division (46, 47), suggesting that lineages are fixed as early as the first cell division, with the simultaneous emergence of memory and effector subsets (termed distal and proximal populations respectively, by virtue of their APC contact point). This occurs through the process of asymmetric division (46). A more comprehensive model has been put forth recently (44) building on previous endeavors (48). The hallmark of this model, termed fate commitment with progressive differentiation, is the existence of "transitory" memory precursor effector cells (MPECs) whose development is triggered by low strength priming, and under the appropriate conditions can develop into T_{CM}. Short-lived effector cells (SLECs) also arise in parallel under stronger priming signal, and are replenished

from the MPECs pool under the appropriate conditions. Those cells further differentiate into T_{EM} and/or die.

In support of this latest model, recent studies analyzed the differential expression of 156 genes in sorted naïve, effector, and memory CD8 T cell pools and constructed phylogentic relationships between these populations (49, 50). It was concluded that memory gene profile falls consistently between that of naïve and effectors. The study also noticed the existence of an "inter-memory" state and concluded that this state might be a gateway to memory and effector populations upon priming of naïve cells. In addition, another study found a novel, self-renewing population deemed "memory stem cells" that, like naïve cells, express low CD44 and high CD62L. They were also characterized by expression of stem-cell antigen-1 (sca-1), the anti-apoptotic protein Bcl-2, and IL2Rβ (CD122) and were capable of generating T_{CM}, T_{EM}, and T_{EFF} (30, 51). Furthermore, two candidate memory regulatory genes, namely, lymphoid enhancing binding factor-1 (Lef-1) and transcription factor 7 (Tcf-7), which maintain hematopoetic stem cells (HSCs) in a pluripotent state, have been found to be highly expressed in naïve and T_{CM} (30). This further supports the notion that memory populations predate effectors during antigen-driven T cell differentiation.

b. Antigen Presentation

Adequate $CD8^+$ T cell priming and activation is contingent upon the totality of two intrinsic signals; MHCI/TCR engagement, and co-stimulation through co-stimulatory molecules (52, 53). Unlike the MHCII pathway which captures extracellular peptides from which presentable antigen is produced and presented to $CD4^+$ T cells, the MHCI pathway is classically involved with intracellular antigenic products (53-55). MHCI is

ubiquitous and expressed on virtually all somatic cells. Endogenous intracellular peptides are continuously processed and presented, but are ignored by $CD8^+$ T cells sampling surface MHCI since self-reactive T cell clones are eliminated early during T cell development (53, 54). T cells that escape this elimination process are conducive to autoimmunity. On the other hand, if cells become infected with viruses, intracellular bacteria, or become malignant, foreign gene products are digested and processed by cytosolic proteosome and TAP (transporter associated with Ag processing) respectively and subsequently loaded onto MHCI molecules in the ER. The MHCI/peptide complexes are subsequently exported to the cell surface where they await engagement by MHC-restricted TCR to initiate $CD8^+$ T cell response (53).

More recently an alternate pathway has been characterized where exogenous antigen enter the MHCI pathway (24, 56). This well-documented, non-classical MHCI pathway is pertinent to this study because it provides an explanation as to how $CD8^+$ T cells become primed against intraphagosomal pathogens, such as *Salmonella* (57, 58). It has been shown that a membrane derivative of the endoplasmic reticulum (ER) can form at the base of the bacteria-containing phagocytic cup and donate MHCI and TAP to the phagosome. Subsequently, MHCI can be loaded with antigenic peptide either directly in the phagosome, or via TAP mediated transport of antigen that may have escaped the phagosome into the cytosol. pMHCI is subsequently transported to the cell surface to be "cross-presented" (57, 58). Alternatively, dying phagocytes can release antigen that can be taken up by bystander DCs and enter the MHCI pathway. Those bystander DCs "cross-prime" $CD8^+$ T cells (57, 58).

In the 1980s, a novel molecule, which was found to promote T cell activation, was discovered and named CD28 (59, 60). However, it was soon found that CD28 is not an orphan molecule but has many related molecules that can stimulate as well as inhibit T cell priming. Inducible co-stimulator, ICOS (or CD278), was also found to promote T cell function, but its signal was important for T cell maintenance as apposed to priming (59). Cytotoxic T lymphocyte antigen-4 (CTLA-4), which binds the same ligands as CD28 (B7.1 and B7.2), was found to negatively regulate T cell priming. It is noteworthy to mention that IL-2, in excess, can substitute for CD28 signaling (59) therefore, CD28 signaling is unnecessary under the appropriate conditions.

Recent studies have shown the necessary integration of a third signal for optimal $CD8^+$ T cell activation (61). This third complimentary signal is pathogen dependent, and current candidates are IL-12, IFN-αβ, and IFN-γ (61). There is increasing evidence for the enhancing role of IL-12 in $CD8^+$ T cell response, even when added as late as 24 hours post T cell priming (62). Consistent with this, IL-12 can function as an adjuvant in promoting full $CD8^+$ T cell activation in peptide immunization models and acts directly on T cells. The underlying mechanism seems to involve up-regulation of anti-apoptotic protein Bcl-3 and down-regulation of pro-apoptotic protein caspase-3 (62). In experiments done in various knock-out mice, it has been shown that IFNs play a critical role in $CD8^+$ T cell expansion (63). This observation was true of LCMV infection, but not LM infection. Type I interferons (IFN-αβ) are critical during viral infections, whereas type II interferons (IFN-γ) are important during bacterial infections (61).

The events during initial antigen encounter shape the T cell response and memory development. Binding affinity, as well as duration and timing of stimulation influence the

ensuing T cell response. $CD8^+$ T cells activation seems to be a function of peptide pMHC affinity to TCR and not pMHC dissociation rate (64, 65). Affinity directly influences $CD8^+$ T cell cytotoxicity and IFNγ production (64). Furthermore, the extent of stimulation seems to control the magnitude of $CD8^+$ T cell memory response, (66, 67); that is the duration of antigen stimulation as well as the timing, influence the size of the memory pool. $CD8^+$ T cells have a significantly lower activation threshold compared to $CD4^+$ cells (45), which might be inherently due to ubiquity of MHCI versus MHCII, as well as the stricter prerequisite of co-stimulation and polarizing cytokines in the case of $CD4^+$ T cells. It is also believed that short term antigenic stimulation of T cells favors central memory formation, whereas chronic, low level antigenic stimulation favors effector memory, and chronic, high antigen levels lead to dysfunctional, exhausted effectors with poor memory potential (35).

c. Immune responses to ST infection

In susceptible mice (C57BL6/J), infection with *Salmonella typhimurium* results in 100% fatality within 7 days, even with doses as low as 100 bacteria (68). Resistant mice (129SvJ), expressing the same MHC haplotype ($H\text{-}2^b$) as susceptible mice, sustain a chronic infection that lasts 60-90 days (68). The reason for this seems to be due to the expression of the natural resistance-associated macrophage protein 1 (*nramp-1*) gene, which codes for an ion transporter in macrophages (69). *nramp's* function is presumably the export of divalent cations (such as iron and manganese) outside of the phagosome making the phagosomal environment more hostile and nutrient-sparse (69), hence conferring bacterial resistance. Recent studies, however, demonstrate that this resistance is not simply due to presence or absence of *nramp*, but that *nramp* expression influences

pro-inflammatory cytokine expression by DCs and promotes a more rapid inflammatory response to ST (70). Interestingly, studies have also shown that some bacteria, including ST, express homologues of *nramp* termed *MntHs* that are thought to counter the transporter function of *nramp*, and therefore support bacterial growth (71) which lends further support to the notion that *nramp* influences inflammation.

Structural components of ST, including flagellin and LPS (lipopolysaccharide), elicit pro-inflammatory response through binding to Toll-like receptors (TLR4 and TLR5) which signal through the transcription factor NF-κB resulting in IL12 and TNFα production, respectively (72). Furthermore, chemokines such as CXCL8 (IL-8) and PEEC (pathogen elicited epithelial chemokine) are also produced and recruit phagocytes to the site of infection (73). Phagocytes, including macrophages and neutrophils, are a critical component of the early innate response to ST, with both expanding 3 and 10 fold respectively in response to infection. In addition, TNFα and IFNγ dependent activation of monocytes is critical for control of infection, with NK cells being the main source for IFNγ production early on, and possibly macrophages, and DCs. ST is capable of killing infected macrophages, however cell death is often delayed (74). What determines the latter is largely elusive but seems to be temporal and spatial in nature. In fact, SPI-5 encoded SigD protein has been shown to promote survival signals in infected cells by activating Akt kinase pathway (74). Furthermore, log-phase ST seems to induce rapid cell death via caspase-1 by means of SPI-1 SipB factor, whereas stationary-phase ST (SPI-2 inducing conditions) have been shown to induce delayed apoptosis of infected cells (74).

Antibodies targeting many ST antigens, such as outer membrane protein (OMP), LPS, Vi, flagella, and heat shock proteins (HSP), have been described (75). In human typhoid

patients, IgG antibodies specific to porins, OMPs, and Vi antigen are detected (76). IgA plays an important role in mucosal immunity to ST presumably by inhibiting epithelial cell invasion, since mice that are deficient in functional IgA are significantly more sensitive to ST (77-79). Furthermore, B cell deficient mice are also more sensitive to primary and secondary ST infections suggesting a role for B cells in ST immunity (78).

ST induces a strong Th1 $CD4^+$ T cell response characterized by IFNγ and TNFα production (80-82). $CD4^+$ T cells are vital in controlling infection (68, 81), however, $CD8^+$ T cells also play an important, but less understood, role. These conclusions were based on T cell knockout studies, in which mice deficient in either T cell type were significantly more sensitive to ST infection (36, 81, 83). Both populations display an activated $CD44^{hi}CD62L^{lo}$ phenotype only 2-3 weeks post infection with ST, which is significantly delayed since T cell response to intracellular and extracellular bacteria, viruses, and even purified antigen in adjuvant always occurs around day 7 (84). However, those populations fail to expand adequately as measured by direct count and BrdU incorporation studies, using fluorescent activated cell sorting (FACS) (68, 82).

d. Immune responses to LM infection

In normal immuno-competent mice, the bacterial burden is eliminated within the first week of infection (3, 85)This highly immunogenic bacterium induces antigen-presentation immediately after infection. T cell response peaks at day 7 followed by rapid contraction immediately thereafter and the generation of the memory pool by day 21 (3, 85). The innate response is also well characterized. Flagellin is recognized by TLR-5 as in the case of ST resulting in TNFα production (18, 86). In addition, macrophages and hepatocytes produce the chemokine MCP-1 to attract additional monocytes to the site of

infection (87). Activated macrophages thereafter produce IL-12 and stimulate NK cells to produce IFNγ, which is also produced by DCs and macrophages. This in turn promotes Th1 type $CD4^+$ T cell response against LM characterized by TNFα and IFNγ production (88). Additionally, $CD8^+$ T cells play an important role in controlling LM infection. Indeed, there is a large number of IFNγ producing LM-specific CD8 T cells that are present early on in infection, which quickly contract as the pathogen is eliminated from the host leaving behind a memory population that is predominantly of a central phenotype that can be mobilized quickly upon secondary infection (85). Interestingly, $CD4^+$ T cells have been found to contribute to the maintenance of $CD8^+$ T cell memory during LM infection, while they are not required during the earlier stages of infection for a stable $CD8^+$ T cell memory population to develop (89). Furthermore, there is little evidence of an antibody response during LM infection as very little antibody titers are detected following infection (90).

3. Rationale

As previously discussed, the current paradigm is that T cell response to intracellular and extracellular bacteria, viruses, and even purified antigen in adjuvant always occurs around day 7 (84). Wildtype ST infection of *nramp*+/+ mice is characterized by massive, chronic splenic bacterial burden. Despite the substantial growth of ST *in vivo,* early priming of $CD4^+$ and $CD8^+$ T cells does not occur as they fail to down-regulate CD62L by day 7 (Sad S. et al., unpublished data). Consistent with this, studies attribute this delay to active, SPI2-mediated inhibition of antigen-presentation by ST (13, 14). However, ST-specific $CD8^+$ T cells are ultimately mobilized (68), perhaps via non-classical "cross-

priming" by bystander DCs (91). Is this delayed mobilization of $CD8^+$ T cells indeed due to SPI-mediated inhibition of antigen presentation, or does ST intracellular localization have a direct impact on antigen-load? Interestingly, $CD4^+$ T cells specific to physiological flagellin antigen of ST fail to respond to low-dose ST infection (92). Furthermore, increasing the infectious dose of another intraphagosomal pathogen, BCG, results in an "acceleration" of an otherwise delayed $CD8^+$ T cell priming (93). This suggests that pathogen growth and burden profoundly influences T cell response (94) and prompts a more thorough investigation of the characteristics of ST intracellular proliferation.

In this study, I have comprehensively evaluated the extent of antigen presentation during infection with *Salmonella typhimurium* (ST) and revealed how this pathogen influences the $CD8^+$ T cell response. A unique aspect of this study is the use of recombinant ST and LM that express the gene for Ovalbumin (OVA), which allows for comparative analysis of antigen-presentation and $CD8^+$ T cell memory development in response to the same antigen. The epitope SIINFEKL, which is derived from the model antigen OVA, is presented in the context of H2-K^b MHC class I molecules. This allows for the use of H2-K^b tetramer technology to track OVA-specific cells as well as the use of recombinant mice in adoptive transfer models. In this manner, evaluating the potency of response in "relative" terms can provide thorough understanding of the overall host-pathogen interactions, and highlight what is different, and what is important for protective response against each pathogen

4. Hypothesis

During infection, ST establishes its niche within the phagosome (Salmonella-containing vacuole or SCV) of infected host cells, effectively evading immune detection. Studies suggest that ST actively inhibits antigen presentation by means of secreted virulence factors. Instead, I propose that muted antigen presentation can be viewed as a passive, rather than direct, effect of ST virulence, which aims to preserve its phagosomal niche. Therefore I hypothesize that muted antigen presentation during ST infection is due to its poor intracellular proliferation and reduced antigenic load, not due to its virulence or active inhibition of antigen presentation.

5. Aims and Objectives

a. Antigen Presentation

ST selectively subverts antigen-presentation in the host (10). I sought to determine whether bacterial virulence factors are actively involved in the process, or whether these factors indirectly influence antigen-presentation due to their role in bacterial localization, namely, in the salmonella containing vacuole (SCV). If virulence genes of ST facilitate immune evasion, infection with ST SPI-1 and SPI-2 mutants will alleviate inhibition of antigen-presentation. Furthermore, does ST inhibit presentation of externally loaded peptide, or LM antigens?

Furthermore, I sought to determine when (timing), to what extent (magnitude), and for how long (persistence) is ST-derived antigen processed and presented to T-cells. Delayed antigen presentation, and/or chronic antigen presentation, can lead to inefficient T cell

priming, or exhaustion, respectively, and consequently lead to reduced T-cell function (11). The expression levels of the same model antigen in response to LM and ST infection, as well as attenuated ST strains, *in vivo* and *in vitro,* were determined. RNA levels provide an indirect measure of antigenic load. Furthermore, the differential loading of the model antigen on MHCI in response to infection with these bacteria was also evaluated. It is not clear whether ST infection results in inadequate antigen levels, or whether it is merely delayed. As discussed previously, bioavailability of antigen as well as antigen levels influence T cell development and function.

b. T-Cell Differentiation and Phenotype

Phagosomal localization and virulence may modulate priming of T-cells (94). ST-specific $CD8^+$ T cells' expansion and contraction, in response to infection with attenuated versus virulent ST, were comparatively monitored. In addition, the phenotype of primed T-cells and their activation states were determined and the development of T-cell memory subsets was evaluated. Such kinetic analysis delineates when the cells get activated, for how long, and what proportion of them stays in an activated state. Hyper-activation of memory cells was shown to result in reduced proliferative ability and thus reduced protection (12). This study, therefore, provides a better understanding of how ST virulence might influence T cell development and phenotype.

c. T-Cell Function:

Several outcomes are feasible in an ST infection. It can generate dysfunctional T cells due to chronic antigen exposure, given ST's apparent massive proliferation *in vivo* (68). Instead, the T cells generated are functional but were weakly exposed to antigen due to

delayed antigen presentation or low antigen levels. Finally, T cells are functional but present in such low numbers that their impact is significantly reduced.

To this end, I sought to evaluate the cytolytic activity of ST-specific $CD8^+$ T cells *in vivo* in response to infection with virulent and attenuated strains of ST. Furthermore, frequency of IFNγ producing antigen-specific $CD8^+$ T cells was determined. Differences in T cell function induced by virulent and non virulent strains shed light on the mechanisms by which ST may influence T cell development and function.

CHAPTER II:
MATERIALS AND METHODS

II. Materials and Methods

1. Bacterial strains

Previously, a recombinant strain of *Listeria monocytogenes* (10403S) (LM) expressing the gene for ovalbumin (LM-OVA)) was generated (94). Briefly, the plasmid pJJD-OVA was amplified in *E. coli* strain HB101. Subsequently, plasmid DNA was introduced to the *LM* strain 10403S by electroporation. Chromosomal integration was achieved by consecutive passages of bacteria in Brain-heart infusion (BHI) agar with 5ug/ml erythromycin (selection marker) at 42°C, in BHI without erythromycin, and finally on BHI agar with 1ug/ml erythromycin at 37°C The loss of β-galactosidase activity was determined by growing the bacteria in the presence of 5-bromo-4-chloro-3-indolyl β-D-galactoside. The r*LM*-OVA was grown at OD600 = 0.4 and aliquots were stored in 20% glycerol at -70°C.

Previously also, a recombinant strain of *Salmonella Typhimurium* (SL1344) (*ST*) expressing the gene for ovalbumin (ST-OVA) was generated (94). Briefly, ST was grown in Luria-Bertani medium supplemented with 1 mg/l 2,3-dihydroxybenzoic acid and 0.5 g of glucose/L. Bacteria were washed and resuspended in LB medium (1/100 diluted in distilled water), and plasmid DNA was introduced (1–5 ul of TE, 10 mM Tris-HCl (pH 8), and 0.1 mM EDTA) into the bacterial suspension in a precooled electroporation cuvette (0.2 cm). Electroporation was done once at 2.5 kV in a gene pulser (Bio-Rad). Immediately after the pulse, the cells were gently resuspended in LB medium described above and allowed to grow for 1 h at 37°C before plating on LB medium agarose plates containing ampicillin (10 ug/ml). Single colonies were used to inoculate liquid cultures that were incubated at 37°C under constant shaking in brain-heart infusion (BHI) medium

(Difco Laboratories). Expression of OVA by ST-OVA was confirmed by Western blot analysis using an anti-OVA mAb. At mid-log phase (OD600 = 0.8), bacteria were harvested and frozen at -80°C (in 20% glycerol). Dr. Brett Finlay (UBC, Canada) generously provided us with numerous strains of ST with mutation in key virulence genes. The *invA* mutation in the Salmonella pathogenicity island (SPI)-1 results in defective invasion. The *ssaR* mutation in SPI-2 results in defective intracellular survival. The *phoP* mutation disrupts the inhibition of phagosomal maturation and the intracellular survival of ST. Finally, the mutant *SifA* of SPI-2 replicates in the cytosol as opposed to phagosome of dendritic cells and epithelial cells. OVA was expressed successfully in all of these mutants of ST as described for the strain SL1344. The naturally occurring strain SL3261 (*aroA*), an attenuated strain that lacks the enzyme aromase that is necessary for synthesis of aromatic compounds from simple precursors, was also used. SL3261 is a vaccine candidate and induces little inflammation compared to SL1344 (95). All CFUs were enumerated by diluting bacteria in 0.9% saline and plating aliquots on BHI agar plates.

2. Mice and immunizations

C57BL/6 mice and 129X1SvJ mice were obtained from The Jackson Laboratory (Bar Harbor, ME, USA). C57BL/6-Tg (TcraTcrb) 1100Mjb mice (also known as OT-1 mice), were also obtained from the Jackson Laboratory (Bar Harbor, ME, USA). In these mice, 90% of CD8+ T cells encode $OVA_{257-264}$-specific TCRs. OT-1 mice were also bred in-house. B6129F1 mice were bred in-house in the animal facilities at the Institute of Biological Sciences of the National Research Council Canada (NRC) (Ottawa, Ontario,

Canada) by mating 129XsvJ female mice with C57BL/6 male mice. SJL-OT1 mice were also bred in-house by mating OT-1 male mice with wt-BL6/SJL female mice, or OT.1+B6-SJL (CD45.1+CD45.2+) male mice and wt-B6/SJL females. The outcome is F1 OT1-SJL (CD45.1+CD45.2+) and F2 OT1-SJL (CD45.1+CD45.2-) mice respectively. All the mice used were housed in pathogen-free conditions at the animal facilities at the Institute of Biological Sciences of the National Research Council Canada (Ottawa, Ontario, Canada) in accordance with the guidelines of the Canadian Council on Animal Care. For immunizations, bacterial stocks were diluted in 0.9% saline to the desired number of CFUs in an injection volume of 200ul, and mice were injected intravenously (i.v) via the lateral tail vein. For adoptive transfer experiments, OT1 cells were resuspended in HBSS at 10^6 cells/200ul and injected i.v. via the lateral tail vein. In lymphocyte and IFNγ depletion experiments, mice were injected – 5 times, once every 3-4 days – with antibodies intraperitoneally (i.p) at the appropriate concentrations (1-2 ug/ul).

3. Tissue culture

Two cell lines were used in this study for *in vitro* experiments. IC-21 is an adherent cell-line derived from C57BL/6 mice peritoneal-macrophages. These cells were typically passaged 1 in 2 every 2-3 days, and maintained in RPMI1640 supplemented with 10% FBS (R10). JAWSII is a mixed (adherent and suspension) dendritic cell-line derived from the bone marrow of C57BL/6 mice. These cells were typically passaged 1 in 4 every 3-4 days by lifting off in PBS, and maintained in RPMI1640 supplemented with 8% FBS and 5ng/ml murine GM-CSF.

4. Assessment of bacterial burden in spleens

Spleen cell suspensions were prepared by homogenizing infected spleens using sterile frosted slides in RPMI1640. CFUs were determined by plating 100ul aliquots of serial 10-fold dilutions in 0.9% saline on BHI agar plates. BHI plates were incubated for 24h at 37°C and colonies were counted thereafter.

5. Assessment of intracellular bacterial proliferation

IC21 cells were seeded at $1x10^5$ cells/well frequency in 24-well flat-bottom plates. Cells were infected with ST-OVA or LM-OVA at desired MOI by adding bacteria directly to wells, centrifuging the plate to promote bacterial adsorption, and incubating the cells at 37°C for 20-30 minutes. Subsequently, cells were washed vigorously with R8-50 (50 ug/ml gentamicin) media 2-3 times, and cells were reconstituted in R8-50 media and incubated for 1-2 hours at 37°C to ensure all extracellular bacteria were eliminated. Afterwards, media was aspirated off, and cells were incubated in R8-1 (1 ug/ml gentamicin). At the appropriate time-point, cells were centrifuged; media aspirated, and cells were lysed using cell-lysis buffer (1% tritonX, 0.1% SDS in PBS, pH 7.2). Appropriate dilutions were made in 0.9% saline and aliquots were plated on BHI plates.

6. Assessment of antigen presentation *in vitro*

IC21 cells were seeded at $1x10^5$ cells/well frequency in 24-well flat-bottom plates. Cells were infected with LM-OVA, ST-OVA or the various ST-OVA mutants described previously at a range of MOIs by adding bacteria directly to wells, centrifuging the plate

to promote bacterial adsorption, and incubating the cells at 37°C for 30-60 minutes. Subsequently, cells were washed vigorously with R8-50 media 2-3 times, and cells were reconstituted in R8-50 media and incubated for 1-2 hours at 37°C to ensure all extracellular bacteria were eliminated. Afterwards, media was aspirated off, and cells were incubated in R8-5 (5 ug/ml gentamicin). CFSE-labeled naïve OT-1 TCR transgenic splenocytes were added to the culture ($1x10^6$ cells/well). Labeling was accomplished by reconstituting OT-1 cells in PBS containing 0.25 μM CFSE for 8 min with shaking. Subsequently, cells are quenched with heat inactivated equine serum for 5 min, and resuspended in R8 media. After four days of co-incubation, cells are harvested, stained with PerCP-Cy5.5 conjugated anti-CD8α antibody and reduction in the expression of CFSE on OT-1 cells is evaluated by gating on $CD8^+$ $CFSE^+$ cells using flow cytometry. Degree of Reduction in CFSE staining reflects the degree of cell proliferation in response to antigenic stimulation (96).

7. Assessment of antigen presentation *in vivo*

Spleens from male OT1-SJL mice were harvested and processed as described previously. OT1-SJL splenocytes were stained with 0.5 μM CFSE in PBS, as described above. Cells were reconstituted in 1x HBSS at $<1x10^7$ cells/200μl. Male F1 recipient mice were injected *i.v.* with these CFSE-labeled OT1-SJL cells (<10 million cells/mouse), and on the following day, these F1 mice were again injected with bacteria at the appropriate dose (see results section). Five days following infection, spleens from the F1 mice were harvested, processed and stained with PerCP-Cy5.5 conjugated anti-CD8α antibody and APC conjugated anti-CD45.1 antibody and analyzed by FACS. A splenic aliquot was

also collected and diluted appropriately in 0.5% saline and plated on BHI agar plates to verify bacterial burden. Activated antigen-specific cells were identified by gating on CD45.1+ CD8+ cells and determining the degree of CFSE reduction (96).

8. Cytotoxicity Assays

a. MTT Cytotoxicity Bioassay

IC21 cells were seeded at a $1x10^4$ cells/well in a 96 flat bottom culture plate. Cells were infected at various MOIs with ST-OVA, LM-OVA, or a combination of both for 1 hour at 37°C. Infection media was removed and cells were washed with R8-50 for an hour, after which the cells were incubated with R8-5 media for 24 hours at 37°C. The MTT solution (in PBS) was added directly to the culture media to a final concentration of 0.5ug/ul, and incubated at 37°C for 3 hours. The labeling solution was subsequently discarded and 150ul/well of isopropyl alcohol was added and mixed thoroughly to solubilize the dye. The colorimetric reading is measured in a plate reader at 570nm with a reference wavelength of 650nm.

b. Neutral Red Dye Cytotoxicity Bioassay

IC21 cells were seeded at a $2x10^4$ cells/well in a 96 flat bottom culture plate. Cells were infected at various multiplicities of infection with ST-OVA, LM-OVA, or a combination of both for 1 hour at 37°C. Infection media was removed and cells were washed and subsequently incubated in R8-50 for an hour, after which the cells were incubated with R8-5 media for 24 hours at 37°C. Subsequently, the Neutral Red Dye cytotoxicity kit (Xenometrix AG, Switzerland) was used to assess cell viability following the

manufacturer's instructions. Briefly, culture media was removed and the labeling solution containing NR dye was added and incubated at 37°C for 3 hours. Cells were inspected under the microscope to insure minimal crystal formation and uptake of the dye by the cells (cells appear red in color). Subsequently, the labeling solution was aspirated and cells were washed with fixative solution (0.1% $CaCl_2$ in 0.5% Formaldehyde) for 1 minute. Finally, the fixative solution is removed and the dye is solubilized using a solubilization solution (1% acetic acid in 50% ethanol). The colorimetric reading is measured in a plate reader at 540nm with a reference wavelength of 690nm.

9. RNA extraction and quantitative real-time PCR

a. Spleens

Spleens were harvested from mice and snap frozen in a dry-ice/100% ethanol bath and stored at -70°C. The whole spleen was cut into appropriately sized pieces and each piece was lysed in 1ml lysis buffer in a mini-Beadbeater 3110BX (BioSpec Products Inc. Bartlesville, OK, USA) with glass beads (Φ = 0.5mm and Φ = 0.1mm) (BioSpec Products, Bartlesville, OK, USA). Total RNA from homogenates was extracted from spleens using the Qiagen RNeasy mini Kit (Qiagen, Mississauga, On, Canada) according to the manufactures instructions. RNA was reconstituted in 100 ul DEPC RNase free water and stored at -70°C. Total RNA was quantified using a Nanodrop ND-1000 (Nanodrop Technologies, Wilmington, DE) and the pieces from one spleen were pooled so that all the RNA from one spleen was in one tube. The total RNA was treated with turboDNAse (Ambion, Austin, TX, USA) for 30 min. at 37°C according to manufacturer's instructions. 5-10 ug of total RNA was taken for cDNA synthesis using

N8 random primers purchased from Sigma. Reverse transcription was performed using Superscript II (Invitrogen Life Technologies, Grand Island, NY) in a Thermo Cycler 9700 (Applied Biosystems, Foster City, CA, USA) according to the following scheme: Identical samples not treated with Thermo Script transcriptase were also prepared as controls to measure DNA carryover. After reverse transcription the RNA template was digested by hydrolysis with NaOH 1M at 65°C for 5 min. followed by neutralization with HCl 1M. cDNA was purified using Microcon YM-30 centrifugal filter unit (Millipore, Cambridge, On, Canada). The number of amplicons was measured by real-time PCR using gene-specific primers and qPCR SYBR green supermix (ABgene, Surrey, UK). The primers used were as follows:

LMOVA 16S rRNA: 5`-GCGCAGGCGGTCTTTTAAG-3` and 5`-CAATGACCCTCCCCGGTTA-3` spanning nucleotides 597-656

STOVA 16S rRNA: 5`-CGGGGAGGAAGGTGTTGTG-3` and 5`-GAGCCCGGGGATTTCACATC-3` spanning nucleotides 436-594

Ovalbumin: 5'-GGTTCTGGTTAATGCCATTGT-3` and 5`-TCAGGCAACAGCACCAACAT-3`spanning nucleotides 584-808

Primers were designed by inputting the gene sequence into the Beacon Designer 4.0 software and all default conditions were used. To obtain a standard curve for each primer-template set, five different PCRs were performed in parallel by using as template 10-fold dilutions of known amounts of STOVA or LMOVA chromosomal DNA (0.01 attomoles, 0.1 attomoles, 1 attomoles, 10 attomoles, and 100 attomoles), together with triplicate or duplicate reactions of the uncharacterized samples. PCR conditions were optimized based on the melting curve of each primer and its target. PCR was performed

in sealed tubes in a 96-well microtiter plate in an iCycler iQ Thermocycler (Bio-Rad Laboratories Inc., Hercules, CA, USA). The 26 ul reaction consisted of 12.5 ul qPCR SYBR green supermix (ABgene Surrey, UK), 1.2 ul of each primer, 9.1 ul DNase/RNase free doubly distilled H_2O and 1 ul of template. Thermal conditions were as follows: activation at 95°C for 15 min., followed by 40 cycles of denaturation at 95°C for 30 sec., annealing at 60°C for 30 sec., and extension at 72°C for 1min. Melting curve protocol was performed to verify that the products had the expected melting temperature. Fluorescence was measured during the annealing step and plotted against the amplification cycle. Absolute quantitative analysis of the data was extrapolated from the standard curve, and attomole quantities were mathematically converted to numbers of detectable RNA molecules. Primer efficiencies were between 98 % and 100 %.

b. IC-21 cells

$1x10^6$ IC-21 cells were infected with STOVA or LMOVA at 1 MOI as described previously (see 2.5). Cells were collected in PBS by scraping, and an equal volume of RNAlater (Qiagen, Mississauga, On, Canada) was added to prevent RNA degradation. Essentially the same protocol for RNA extraction described above was followed, with the addition of a lysozyme lysis step following the RLT buffer lysis step, as recommended by the manufacturer (Qiagen, Mississauga, On, Canada). Furthermore, vigorous vortexing was used instead of the Beadbeater. Only 50 ng of RNA were used for cDNA synthesis and ~100 ng of cDNA was used for real time PCR.

c. Liquid BHI

ST-OVA and LM-OVA were grown in liquid BHI under selective growth conditions (see section IV-1) until the culture reached an O.D of approximately 0.48-0.50 at 600nm (corresponding to the exponential growth phase). An aliquot was collected, and 2 volumes of RNAProtect Bacterial Reagent (Qiagen, Mississauga, On, Canada) were added. After 10 min incubation at RT, bacteria were pelleted by centrifugation and stored at -80°C. The same protocol for RNA extraction described above was followed with two exceptions: 250 ng of RNA were used for cDNA synthesis and ~100ng of cDNA were used to carry out rtPCR.

10. Enumeration of $H2K^b$-SIINFEKL complex

JAWSII cells were seeded in 6 well plates at $1x10^6$ cells/well density. Cells were infected with *wt* and mutant STOVA strains, or LMOVA at a multiplicity of infection (MOI) of 10 for 1 hour at 37°C. Cells were subsequently washed extensively with R8-50 and collected by centrifugation. Cells were incubated for 24h at 37°C in R8 media free of gentamicin. Cells were collected by lifting off in PBS and centrifugation, uniformly reconstituted in 1% PBS-BSA, and stained with an antibody specific for H-$2K^b$-$OVA_{257-264}$ (25D1.16) or an IGg1 isotype control for 30 min at RT. Cells were washed with PBS, reconstituted in 1% PBS-BSA, and this time stained with a goat-anti-mouse PE-conjugated antibody for 30 min at RT. Finally, cells were washed with PBS and resuspended in 0.5% fixative. The mean fluorescence intensity (MFI) was measured by FACS. In another experiment, various amounts of SIINFEKL ($OVA_{257-264}$) peptide ranging from 0.002-200 nmols were used to establish a standard plot of MFIs. In this

experiment, cells were pulsed with peptide for 1 hour after which cells were collected and processed as described above.

11. Assessment of T-cell activation and phenotype

a. Adoptive Transfer

Spleens from OT-1 mice were homogenized in RPMI 1640 (Invitrogen Life Technologies, Grand Island, NY) using the frosted ends of two glass slides, filtered through a 100 μm Falcon strainer (BD Biosciences, Mississauga, ON, Canada), centrifuged 8 min at 1600 rpm, resuspended in HBSS and enumerated by trypan Blue count. OT-1 splenocytes were injected *i.v.* into naïve B6.129 F1 mice ($1x10^6$ cells/mouse in 200 μl HBSS) 3-5 days prior to bacterial infection. To assess the phenotype of the antigen specific $CD8^+$ T cells, spleens of infected F1 mice were harvested and processed as described above. Cells were resuspended in PBS-1%BSA ($50 x10^6$ cells/ml) and $5x10^6$ spleen cells were incubated with anti-CD16/32 (Fc Block) at 4°C for 5 min. Subsequently, cells were incubated with various antibodies to markers of interest (anti-CD8α PerCP Cy5.5, anti-CD62L-PE, anti-CD127-FITC, or anti-PD1-FITC) for 5 min on ice in the dark. Finally, H-$2K^b$$Ova_{257-264}$ tetramer (Beckman Coulter, Fullerton, California) were added to the cells and incubated at room temperature for 30min in the dark. The lymphocytes were washed with PBS at room temperature and fixed with 0.5% formaldehyde and acquired on BD FACS Canto Analyzer. To assess the phenotype of the antigen specific $CD8^+$ T cells in the blood 100 ul of blood was collected in heparin coated tubes. The blood was incubated with various antibodies to markers of interest (anti-CD8α PerCP Cy5.5, anti-CD62L-PE, anti-CD127-FITC, or anti-PD1-FITC)

for 5 min at room temperature in the dark. The lymphocytes were incubated with H-2K^{b}Ova$_{257-264}$ tetramers (Beckman Coulter, Fullerton, California) at room temperature for 30min in the dark. RBCs were lysed with 1ml red blood cell lysis buffer in the dark for 8-10 min. After lysis the cells were washed with PBS at room temperature and fixed with 0.5% formaldehyde and acquired on BD FACS Canto Analyzer.

b. Endogenous Response

i. CD8 T cells purification

To asses the endogenous response to STOVA or the STOVA mutants described, spleens of infected F1 mice were harvested and processed as described above. CD8$^+$ T cells were purified by positive selection using the Dynal CELLection Biotin Binder Bead Kit. CELLection Biotin Binder Dynabeads were pre-coated as per manufacturer's instructions (Dynal Biotech, Great Neck, NY, USA), with biotin-conjugated rat anti-mouse CD8β.2 monoclonal antibody (BDbioscience, Franklin Lakes, NJ, USA). Briefly, beads were washed with PBS-tween80 (0.05%) and collected by placing samples in a magnet. Beads were incubated with the CD8β antibody (10ug/1x10^8 beads) for 1 hour at room temperature. After incubation with the antibody the beads were washed with PBS-tween 80 (0.05%) followed by washing with R8-50. Beads were stored in R8-50 until needed (for a maximum of 7 days). The pre-coated Dynabeads were added to the reconstituted cells at a ratio of five beads per cell in the appropriate volume (5-10ml), and incubated for 20-30 min at 4°C in a rotating platform. CD8β$^+$ T cells were separated by magnetic isolation. After a second round of selection, CD8β$^+$ T cell-Dynabead detachment was done using the CELLection Biotin Binder Kit Releasing Buffer (DNase; 188U/10^8

Dynabeads) and incubating at 37°C rotating for 15 min. This was followed by two to three rounds of washing and magnetic separation with R8-50.

ii. ELISPOT assay

Multiscreen IP 96 well 0.45μm hydrophobic filtration plates (Millipore, Cambridge, On, Canada) were moistened with 70% methanol and washed with $NaHCO_3$ buffer. The plates were coated with R46A2 primary anti-IFN-γ antibody at 13ug/ml in $NaHCO_3$ buffer and incubated at room temperature overnight. The following day the wells were washed with RPMI media and blocked with 1.5% skim milk powder in RPMI containing Gentamycin (50ug/ml) for 3-4 hours at 37°C. Purified CD8 T cells from infected mice (section b.i) were added, at variable densities, together with feeder cells from unimmunized mice such that the final cell density is $5x10^5$/well. Cells were incubated in R8-50 supplemented with IL-2 (0.1ng/ml) and with or without Ova peptide (5ug/ml) at 37°C for 48 hours. After stimulation, the cells were lysed with milli-Q water and the wells were washed with 0.01% PBS-T20. The wells were incubated 2 hours at 37°C with the biotinylated secondary anti-IFN-γ antibody XMG1.2 (0.6ug/ml) in 0.05% PBS-T20. The plate was washed with 0.01% PBS-T20 and the wells were incubated at room temperature for 1 hour with the peroxidase conjugated streptavidin 1ug/ml (MediCorp, Montreal Quebec Canada) in sterile 0.05% PBS-T20. The plate was again washed with 0.01% PBS-T20 followed by washing with 1x PBS. The wells were incubated with the AEC substrate (Sigma, Oakville, Ontario, Canada) prepared according to manufactures instructions for 10-12 mins at room temperature. The reaction was stopped by plunging the plate into cold tap water. The plates were dried overnight and spots were enumerated the next day under an Olympus dissecting microscope.

12. Assessment of *in vivo* cytolytic activity

In vivo cytolytic activity of Ag-specific CD8+ T cells was enumerated, according to the protocol of Barber et al. Donor (B6129F1) spleen cell suspensions were prepared, and RBCs were lysed by ammonium chloride treatment (RBC lysis buffer). Cells were split into two aliquots, and cells were incubated in R8-50 media with 10 μM SIINFEKL $OVA_{257-264}$ peptide or without peptide for 30 minutes at 37°C. Subsequently, both groups were resuspended in Diluent C buffer (Sigma Aldrich) and stained with an equal volume of 4μM PKH26 dye (in Diluent C) at RT for 4 minutes. The two populations were differentially stained with carboxyfluorescein succinimidyl ester (CFSE). Cells were resuspended in PBS, the peptide pulsed population stained with an equal volume of 5 μM CFSE (in PBS), and the control population with 0.5 μM CFSE (in PBS). Following each staining step, cells were quenched with an equal volume of heat inactivated Equine Serum. Finally, cells in the two treatments were counted, reconstituted in HBSS, and mixed 1:1 for injection into B6129F1 mice ($20x10^6$ cells/mouse) that were previously infected with various strains of STOVA as well as non-infected naïve mice. After 24 hours, spleens were harvested from recipient mice, and the relative number of peptide pulsed vs. control donor cells were determined by flow cytometry. Percent killing was calculated by comparing the ratio in infected mice to that in naïve mice according to the published formula:

$$100- \left[\frac{\%pulsed\,\mathrm{inf}\,ected\,/\,\%unpulsed\,\mathrm{inf}\,ected}{\%pulsedun\,\mathrm{inf}\,ected\,/\,\%unpulsedun\,\mathrm{inf}\,ected} x100\right]$$

13. Statistical analysis

All statistical analyses, including the student T test, one-way and two-way ANOVA, were performed using GraphPad Prism 5 software. Figure legends indicate which tests were used for the corresponding data sets. Mean +/- standard error of the mean is displayed for all data. For time course studies (e.g. Figure 26) and grouped studies with two variables (e.g. Figure 23) Two-way ANOVA was performed with Banferroni test to determine the p-value for pair combinations. One-way ANOVA was performed on grouped studied with a single variable with Banferroni test to determine the p-value for pair combinations (e.g. Figure 16). Standard unpaired t-test was used to compared expression levels of mRNA species of ST-OVA vs. LM-OVA (Figure 21). 16s and OVA levels were tested independently. T-test was elected as apposed to two-way ANOVA because we are only interested in one variable, which is the pathogen used.

CHAPTER III:
RESULTS

III. Results

1. The mouse strain 129X1SvJ is an ideal *in vivo* model for ST infection

C57BL/6J mice succumb to ST infection within 7 days (Figure 1). On the other hand 129X1SvJ mice harbor a chronic infection (Figure 1) which peaks between days 7-15 and lasts until day 60, after which the bacteria are undetectable in the spleen. These mice were crossed to obtain the F1 strain. These mice also harbor a chronic ST infection, and they express the MHC haplotype H-2^b which makes them compatible with adoptive transfer studies using OT-1 mice, also H-2^b (97). Bacterial burden was determined by visually counting colony-forming units (CFUs) on BHI agar plated with appropriate dilutions of infected spleen homogenates.

2. T cells and IFNγ play an important role in controlling ST infection

To determine the contribution of T cells and cytokines in controlling ST infection, I depleted $CD4^+$ and $CD8^+$ T cells in mice infected with ST, at early (day 1) and late (day 120) time points during infection. Depletion was carried out by injecting mice with anti-IFNγ (XMG1.2), anti-CD4 (GK1.5), or anti-CD8 (Hyb2.43), five consecutive times every 3-4 days. As evident in Figure 2, T cells seem to play a critical role in controlling ST infection in the chronic phase of infection. When $CD4^+$ and $CD8^+$ T cells were depleted in mice from day 1 onwards (Figure 2-A), there was only a mild increase in splenic bacterial burden. On the other hand, depleting $CD8^+$ T cells, $CD4^+$ T cells, or IFNγ, around day 120 of infection (Figure2-B), resulted in a pronounced increase in splenic bacterial burden. Mice that received a non-specific IgG control had no detectable bacteria

in the spleen, while depletion of $CD8^+$ and $CD4^+$ T cells resulted in a 10 and 200 fold increase in bacterial burden, respectively. In the case of IFNγ depletion, there was an even greater increase in burden, and mice were visibly ill.

3. Delayed expansion of OVA-specific effector $CD8^+$ T cells in response to ST-OVA infection.

The F1 progeny of C57BL/6J and 129X1SvJ was established as a mouse model for infection (see sub-section 1). I wanted to evaluate the induction of T cell response during infection of mice with the recombinant ST expressing Ovalbumin (OVA). Another recombinant pathogen, *Listeria monocytogenes* (LM), also expressing OVA, was used as a positive control. LM-OVA caused an acute infection in B6.129F1 mice, in which the splenic bacterial burden peaks at day 3 and is resolved by day 7 (Figure 3-A). ST-OVA infection, however, remains chronic for up to 90 days – as in 129X1SvJ mice – after which the bacteria are undetectable in the spleen (Figure 3-A). The frequency of OVA specific $CD8^+$ T cells was measured using the ELISPOT assay.

The expansion of OVA-specific, IFNγ producing $CD8^+$ T cells was delayed during ST infection. The frequency of IFNγ producing $CD8^+$ T cells peaked around day 25 during ST-OVA infection, as apposed to day 7 in the case of LM-OVA infection (Figure 3-B). In this particular experiment, $5x10^5$ IFNγ producing $CD8^+$ T cells were detectable in the spleen at day 7 following LM-OVA infection, which dropped quickly to and stabilized at around $1x10^4$ cells from day 14 onwards. In the case of ST-OVA however, effector cells were not detected until day 25 at which point $3x10^4$ IFNγ producing $CD8^+$ T cells were present stably until day 60 (Figure 3-B), at which point ST burden is declining rapidly.

Figure 1 Different outcomes of ST infection in different mice strains

129X1SvJ or C57BL/6J mice were infected i.v. with 10^3 CFUs of ST-OVA(wt). At different time-points throughout infection, spleens were harvested and spleen cell suspensions were prepared by homogenizing infected spleens using sterile frosted slides in RPMI1640. CFUs were determined by plating 100ul aliquots of serial 10-fold dilutions in 0.9% saline on BHI agar plates. BHI plates were incubated for 24h at 37°C and colonies were counted thereafter. Data representative of two experiments (n=2). Symbol indicates fatality occurring by day 7.

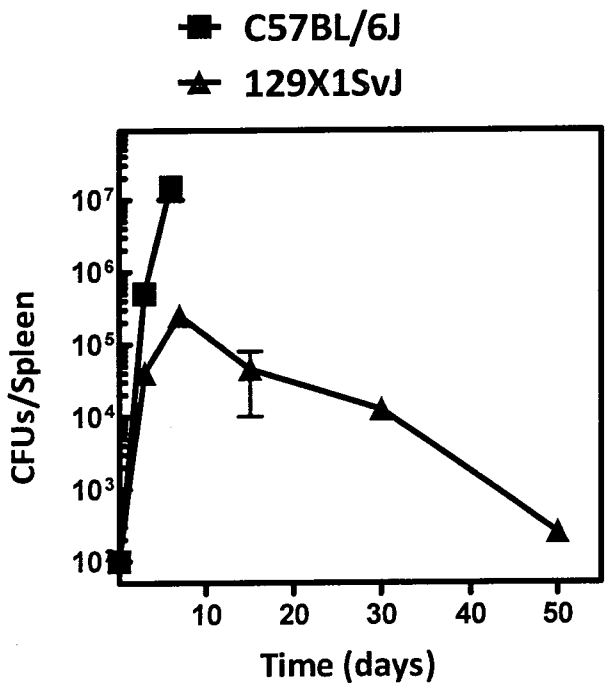
C57BL/6J
129X1SvJ
CFUs/Spleen
10^7
10^6
10^5
10^4
10^3
10
20
30
40
50
Time (days)

Figure 2 T cells and IFNγ limit bacterial burden during chronic stage of ST infection.

B6.129F1 mice were infected i.v. with 10^3 CFUs of ST-OVA (wt). At days 1 *(A)* and 120 *(B)*, mice were injected – 5 times, once every 3-4 days – with anti-IFNγ (XMG1.2), anti-CD4 (GK1.5), anti-CD8 (Hyb2.43), or IgG negative control antibodies intraperitoneally (100 μg/200 μl/mouse). Next day after the last injection, spleens were harvested and spleen cell suspensions were prepared by homogenizing infected spleens using sterile frosted slides in RPMI1640. CFUs were determined by plating 100ul aliquots of serial 10-fold dilutions in 0.9% saline on BHI agar plates. BHI plates were incubated for 24h at 37°C and colonies were counted thereafter. Data representative of two separate experiments.

A

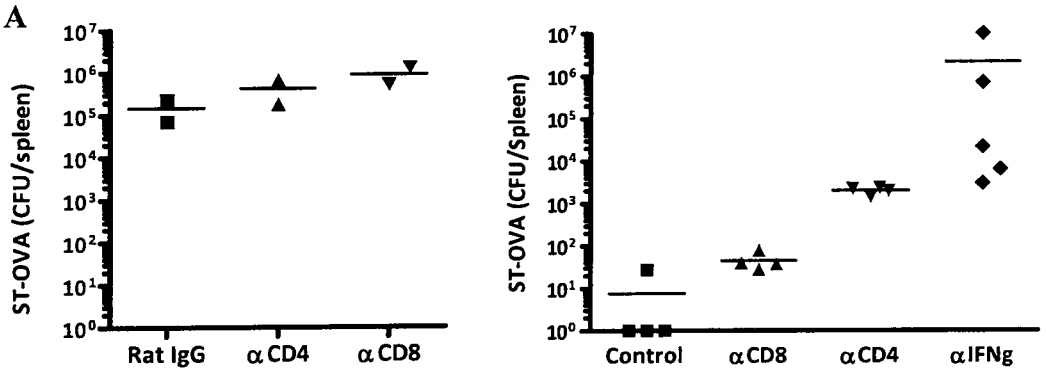
ST-OVA (CFU/spleen)
10^7
10^6
10^5
10^4
10^3
10^2
10^1
10^0
Rat IgG
αCD4
αCD8
ST-OVA (CFU/Spleen)
Control
αCD8
αCD4
αIFNg

Figure 3. Delayed expansion of OVA-specific, IFNγ-producing CD8+ T cells in response to ST-OVA infection.

B6.129F1 mice were infected intravenously with 10^3 CFUs ST-OVA or LM-OVA. At various time intervals spleens were haravested and the bacterial burden determined as described previously (A). Spleens were harvested, processed, and the frequency of OVA-specific $CD8^+$ T cells enumerated by ELISPOT assay (B). $CD8^+$ T cells were purified using the DYNAL magnetic bead system. Purified $CD8^+$ T cells (90-98% pure) were incubated for 48 hours with IL-2 (0.1 ng/ml) in the presence or absence of OVA peptide (5μg/ml), using IP plates pre-coated with anti-IFNγ Ab (R46A2; 13ug/ml in NaHCO3 buffer). Plates were washed with 0.01% PBST, incubated with biotinylated anti-IFNγ Ab (XMG1.2). Subsequently plates were washed, incubated with SA-HRP, and finally developed using AEC substrate. Dots corresponding to IFNγ producing cells were enumerated under the microscope. *(A)* Bacterial burden in the spleen as described previously. *(B)* Frequency of ova-specific CD8 T cells/spleen. Asterisks indicate statistical significance determined by two way ANOVA using graphpad prism 5 software. ($P<0.05$). Data representative of two separate experiments (n=2-3).

A

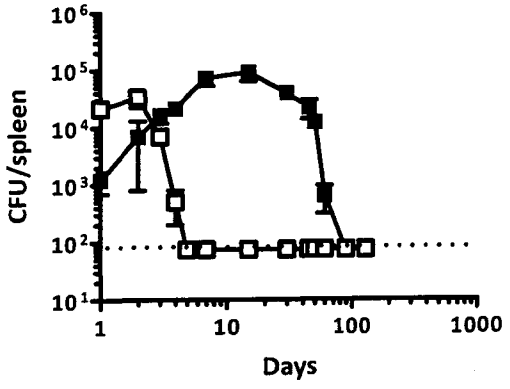
CFU/spleen
10^6
10^5
10^4
10^3
10^2
10^1
1
10
100
1000
Days

B

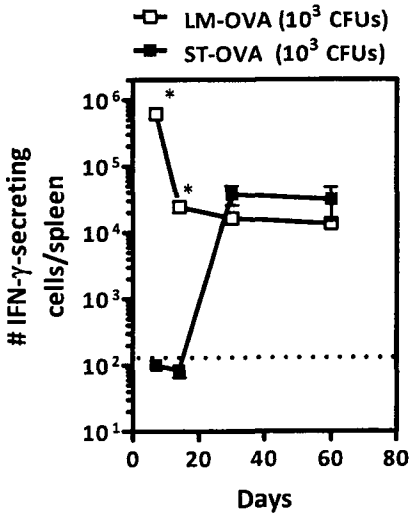
LM-OVA (10^3 CFUs)
ST-OVA (10^3 CFUs)
IFN-γ-secreting cells/spleen
10^6
10^5
10^4
10^3
10^2
10^1
*
*
0
20
40
60
80
Days

4. ST-OVA does not induce measurable antigen-presentation *in vivo*.

To assess the extent of *in vivo* antigen presentation, I adoptively transferred CFSE labeled TCR transgenic OT1 mice into bacteria-infected F1 mice and determined whether these donor cells get activated by CFSE dilution method (Figure 4). The technique rests on the premise that if antigen-presentation is happening at a given time, it should result in activation and expansion of adoptively transferred antigen-responsive T cells and consequently the progressive dilution of CFSE signal.

Recipient mice (B6.129F1) were infected with LM-OVA or ST-OVA. At various time intervals after infection, CFSE labeled B6.SJL-OT-1 cells are adoptively transferred. These mice are genetically modified such that the majority of their $CD8^+$ T cells express T-cell receptor Vα2 specific to OVA peptide 257-264 (SIINFEKL) (98). Further, these transgenic OT-1 mice are back-crossed to the B6.SJL strain so that the donor cells ($CD45.1^+45.2^-$) can be easily discriminated from the host B6.129F1 cells ($CD45.1^-$ $CD45.2^+$) by CD45.1 expression.

Four days after infection, the spleens are harvested, splenocytes isolated and stained, and FACS was used to gate on CFSE-labelled $CD8^+CD45.1^+$ T cells. In ST-OVA infected mice there was no antigen presentation to $CD8^+$ T cells in the first few days after infection (day 5) (Figure 5-A). This is in sharp contrast to LM-OVA infected mice in which a profound decrease in CFSE staining of T lymphocytes was noted (nearly 90% of donor $CD8^+$ T cells were $CFSE^{low}$). Non-recombinant controls lacking OVA display negligible decrease in CFSE staining, indicating that the response is OVA-specific. Furthermore, there was an increase in the numbers of donor OVA-specific cells (Figure 5-B) in LM-OVA infected mice relative to total $CD8^+$ T cell population (donor +

recipient). All other groups of mice did not show any such increase, further confirming that antigen presentation did not occur rapidly following ST-OVA infection. Activation and expansion of donor OT-1 cells in LM-OVA infected mice resulted in reduction of bacterial load (Figure 5-C), which did not take place in the other infected groups of mice.

5. ST-OVA does not induce measurable antigen presentation *in vitro*

Antigen presentation to $CD8^+$ T cells in response to ST infection was further tested in a controlled tissue culture setting, where MOI and cell numbers can be easily manipulated. The macrophage cell line IC-21 ($H\text{-}2^b$ background) was chosen as an *in vitro* model since it is documented ST survives and replicated in macrophages (6, 91, 99-105) (Figure 6). Before testing antigen presentation by ST-infected IC-21 cells, it was important to determine the minimal amount of antigen needed to prime T cells in this *in vitro* model. I therefore pulsed IC-21 cells with variable amounts of OVA peptide and co-cultured them with CFSE-labeled OT1 (also $H\text{-}2^b$ background) splenocytes (Figure 7) which, as indicated previously, are >90% specific to the SIINFEKL epitope. The EC50 (effective concentration resulting in 50% of maximal response) appeared to be around 0.005 nmol (Figure 7). Furthermore, higher infectious doses were used in an attempt to encourage antigen-presentation. However, all tested doses of ST-OVA, from MOI (multiplicity of infection) of 0.1 to 100, did not result in any visible T cell proliferation (Figure 8-A, B) which supports the aforementioned *in vivo* data.

Figure 4. ***In vivo*** **antigen-presentation model.**

CFSE-labeled OT1-SJL splenocytes ($CD45.1^+$) were adoptively transferred into B6.129F1 ($CD45.2^+$) mice. 24 hours later, these recipient mice were infected intravenously with bacteria at different doses (see Materials and Methods). Five days after infection, spleens were harvested, processed and spleen cell suspensions were stained with anti-CD8α, and anti-CD45.1. OVA-induced proliferation of $CD8^+$ donor T cells was evaluated by measuring CFSE dilution by flow cytometry.

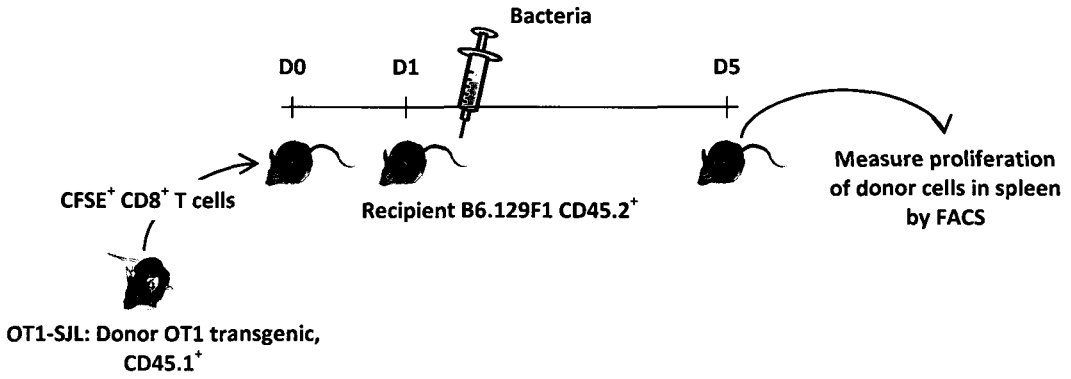
Bacteria
D0
D1
D5
Measure proliferation of donor cells in spleen by FACS
CFSE+ CD8+ T cells
Recipient B6.129F1 CD45.2+
OT1-SJL: Donor OT1 transgenic, CD45.1+

Figure 5. ST-OVA does not induce measurable antigen-presentation *in vivo*.

CFSE-labeled OT1-SJL splenocytes ($CD45.1^+$) were adoptively transferred into B6.129F1 ($CD45.2^+$) mice. 24 hours later, these recipient mice were infected intravenously with bacteria (10^3 CFUs). Five days after infection, spleens were harvested, processed and spleen cell suspensions were stained with PerCP conjugated anti-CD8α, and APC conjugated anti-CD45.1 antibodies. OVA-induced proliferation of $CD8^+$ donor T cells was evaluated by measuring CFSE dilution by flow cytometry *(A)*. The percentage of donor cells ($CD45.1^+$) in the whole $CD8^+$ population was also plotted *(B)*. The bacterial burden in the infected spleens is also shown *(C)* and was determined as described previously. Data representative of three separate experiments (n=2).

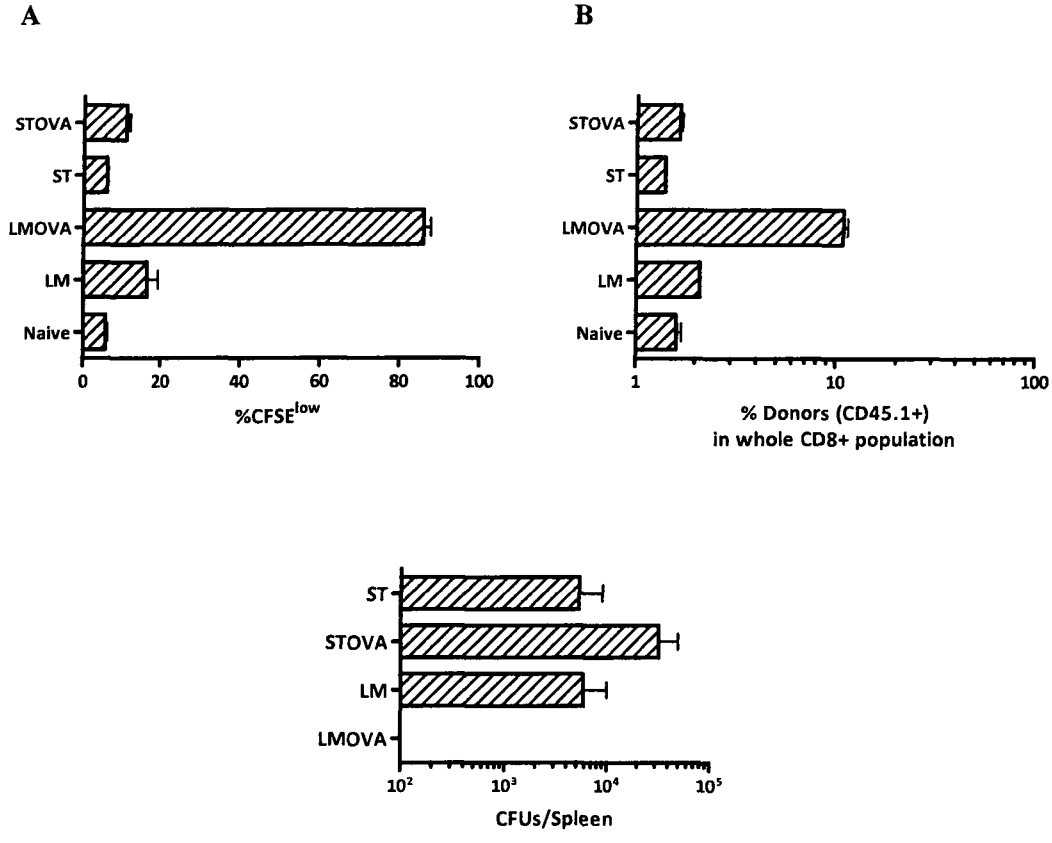
A
STOVA
ST
LMOVA
LM
Naive
0
20
40
60
80
100
%CFSE^low
B
STOVA
ST
LMOVA
LM
Naive
1
10
100
% Donors (CD45.1+)
in whole CD8+ population
ST
STOVA
LM
LMOVA
10^2
10^3
10^4
10^5
CFUs/Spleen

Figure 6. ***In vitro*** **antigen-presentation model.**

A macrophage cell-line (IC-21), and a dendritic cell-line (JAWSII) both of which are derived from C57BL/6J mice, and expressing $H2K^b$ MHCI were used. Cultured cells are seeded in well-plates and infected with bacteria at various multiplicities of infection (MOIs). Extracellular bacteria are removed by vigorous gentamicin wash, and cells co-cultured with CFSE-labeled OT1 splenocytes for 4-9 days. Cells are subsequently collected and stained with anti-CD8α. The degree of OVA-induced $CD8^+$ T cell proliferation is evaluated by measuring CFSE dilution using flow cytometry.

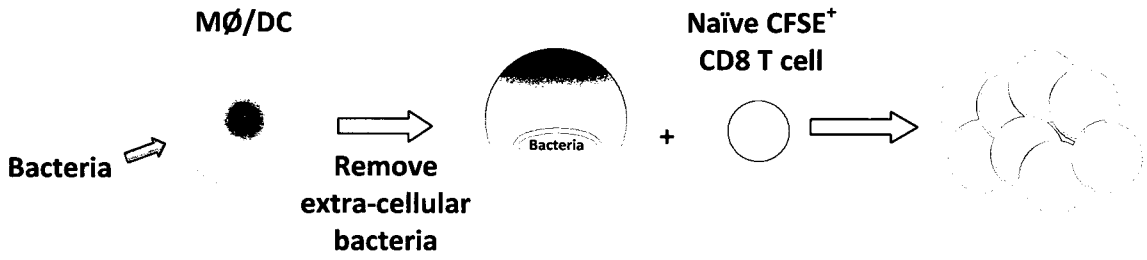
MØ/DC
Naïve CFSE+
CD8 T cell
Bacteria
Remove
extra-cellular
bacteria
Bacteria
+

Figure 7. Titration of OVA peptide required to prime $CD8^+$ T cells *in vitro*.

IC-21 cells were seeded in 24-well plates (10^5 cells/well) and pulsed with different concentrations of OVA peptide for one hour at 37°C. Cells were subsequently washed and co-cultured with CFSE-labeled OT1 splenocytes (10^6 cells). After three days of culture, cells were subsequently collected and stained with anti-CD8α. The degree of OVA-induced $CD8^+$ T cell proliferation was evaluated by measuring CFSE dilution using flow cytometry. Data representative of two separate experiments with each data point comprised of two pooled wells. Dotted line indicated concentration resulting in 50% priming (EC50 ~ 0.005 nmol)

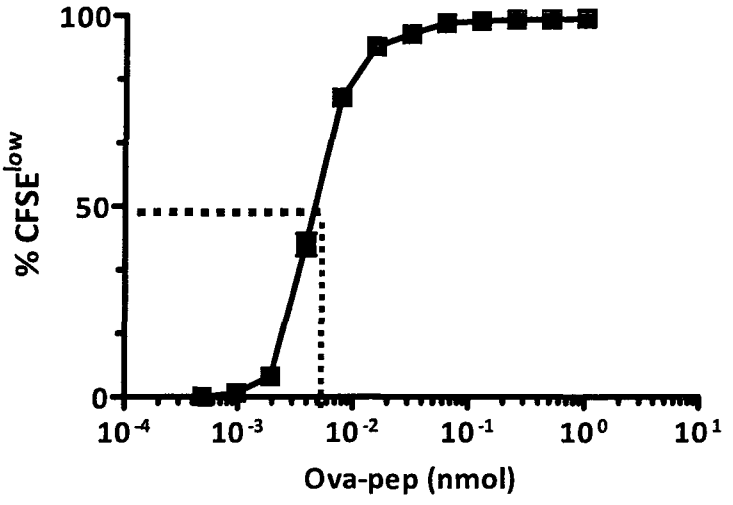
100
50
0
% CFSE^low
10^-4
10^-3
10^-2
10^-1
10^0
10^1
Ova-pep (nmol)

Figure 8. Cultured macrophages infected with ST-OVA fail to promote antigen presentation .

IC-21cells were seeded in well-plates. Bacteria were added at various MOIs, plates centrifuged to promote bacterial adsorption, and incubated at 37°C for 30-60 minutes. Cells were subsequently washed vigorously and incubated with R8-50 media for 1-2 hours. Subsequently, cells were co-cultured with CFSE-labeled OT1 splenocytes for 4 days in R8-5 media. Cells were finally collected and stained with anti-CD8α. The degree of OVA-induced $CD8^+$ T cell proliferation was evaluated by measuring CFSE dilution using flow cytometry *(A)*. A representative panel of FACS data displaying extent of CFSE down-regulation is also shown *(B)* with the percentage of $CFSE^{low}$ CD8 T cells highlighted. Data representative of two separate experiments (n=2).

A

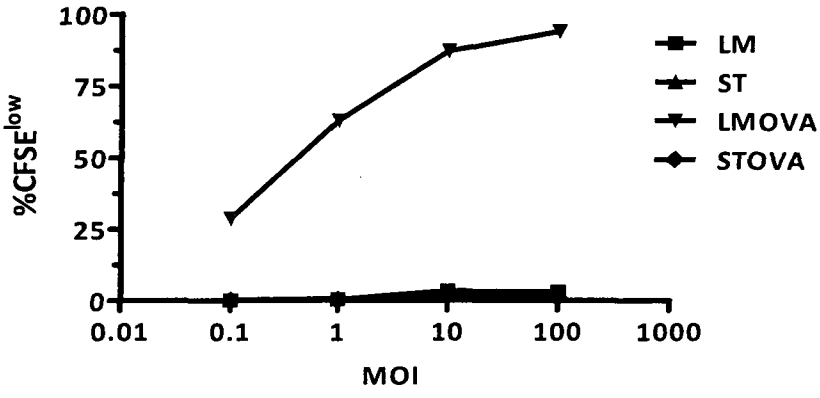
100
75
50
25
0
%CFSE^low
0.01
0.1
1
10
100
1000
MOI
LM
ST
LMOVA
STOVA

B

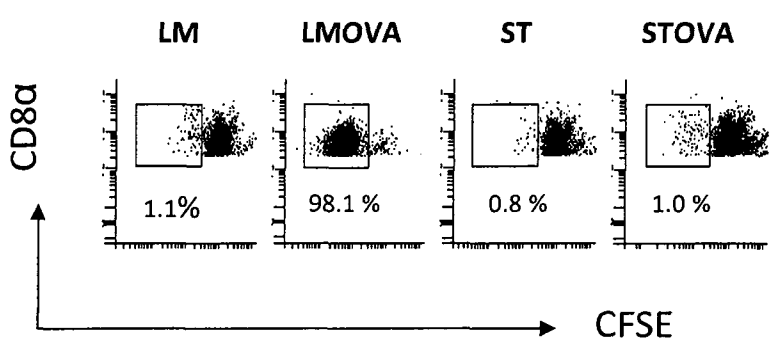
LM
LMOVA
ST
STOVA
CD8α
1.1%
98.1 %
0.8 %
1.0 %
CFSE

As expected, LM-OVA displayed a dose dependent response, with an MOI of 0.1 resulting in 30% of transferred OT1 $CD8^+$ T cells becoming activated and an MOI of 100 resulting in upwards of 95% activation. No measurable response to ST and LM controls was detected. Extending culture time did not seem to enhance antigen presentation by ST-OVA (Figure 9). Only 10% of $CD8^+$ T cells become activated on day 7 and return to below threshold levels by day 9. Whether this slight activation is antigen specific or a result of bystander effects could not be determined.

6. ST infected dendritic cells fail to promote antigen presentation

Several studies support the ability of *Salmonella* to infect dendritic cells (106, 107). I therefore wanted to test the cultured dendritic cell line JAWSII ($H\text{-}2^b$ background) to determine whether DCs can promote antigen presentation when infected with ST (Figure 10). As in IC-21 cells, OT1 $CD8^+$ T cells are not primed to proliferate by ST-OVA infected JAWSII cells. All tested MOIs displayed no reduction of CFSE staining of transferred $CD8^+$ T cells reflecting the lack of antigen presentation. LM-OVA infection , on the other hand, resulted in a dose dependent reduction in CFSE staining of transferred $CD8^+$ T cells, which recapitulates previously mentioned findings in the IC-21 cell line. Likewise, ST and LM infected controls did not result in any CFSE dilution indicating that any observed response is OVA specific.

Figure 9. ST fails to induce antigen-presentation even when the time of culture is extended.

IC-21 cells were gamma-irradiated for 8 min on ice (10,000 Rads). Cells were subsequently seeded in 24-well-plates. Bacteria were added at 10 MOIs, plates centrifuged to promote bacterial adsorption, and incubated at 37°C for 30-60 minutes. Cells were subsequently washed vigorously and incubated with R8-50 media for 1-2 hours. Subsequently, cells were co-cultured with CFSE-labeled OT1 splenocytes for up to 9 days in R8-5 media. Cells were collected at various time intervals and stained with anti-CD8α. The degree of OVA-induced $CD8^+$ T cell proliferation was evaluated by measuring CFSE dilution using flow cytometry. Data representative of three separate experiments (n=2).

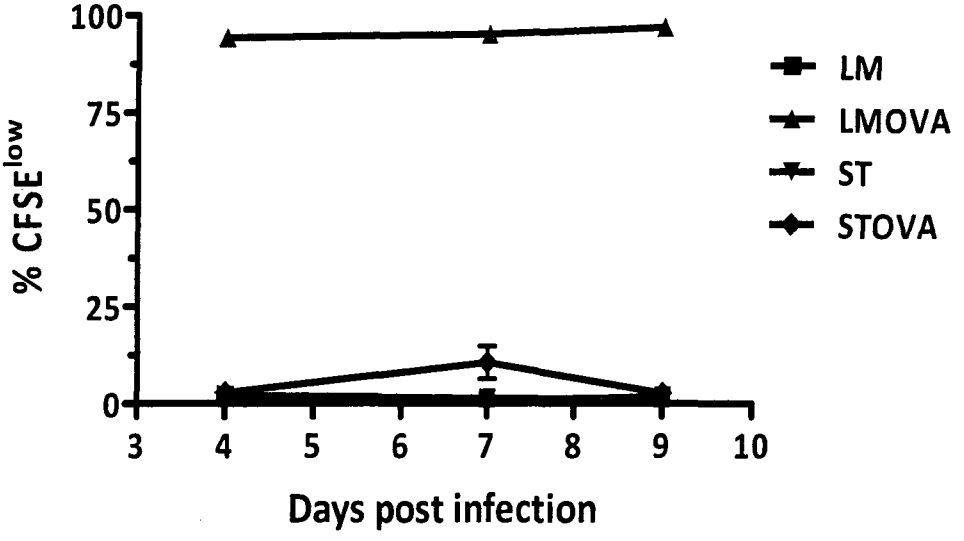
100
75
50
25
0
% CFSE low
3
4
5
6
7
8
9
10
Days post infection
LM
LMOVA
ST
STOVA

Figure 10. Cultured DCs also fail to promote antigen presentation when infected with ST-OVA.

JAWSII cells were seeded in 24-well-plates. Bacteria were added at various MOIs, plates centrifuged to promote bacterial adsorption, and incubated at 37°C for 30-60 minutes. Cells were subsequently washed vigorously and incubated with R8-50 media for 1-2 hours. Subsequently, cells were co-cultured with CFSE-labeled OT1 splenocytes for up to 4 days in R8-5 media. Cells were collected and stained with anti-CD8α. The degree of OVA-induced $CD8^+$ T cell proliferation was evaluated by measuring CFSE dilution using flow cytometry *(A)*. A representative panel of FACS data displaying extent of CFSE down-regulation is also shown *(B)* with the percentage of CFSElow CD8 T cells highlighted. Data representative of two separate experiments (n=2).

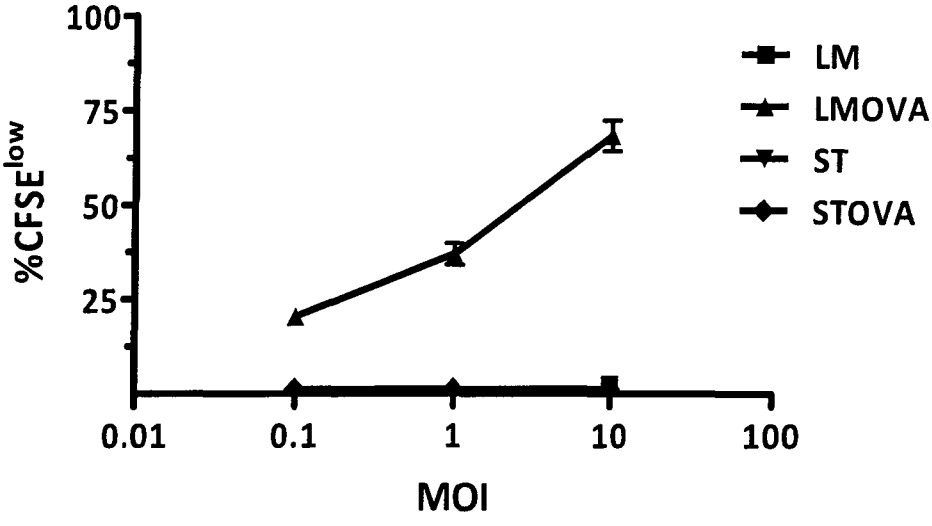
100
75
50
25
%CFSE low
0.01
0.1
1
10
100
MOI
LM
LMOVA
ST
STOVA

B

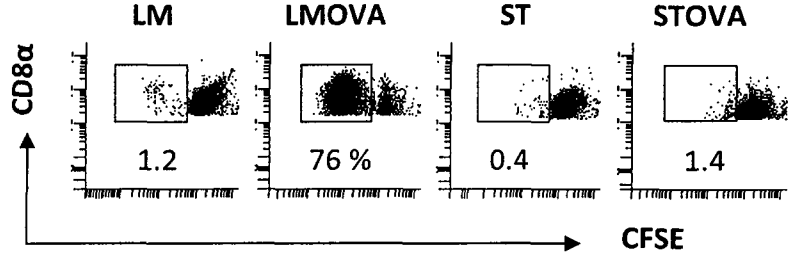
LM
LMOVA
ST
STOVA
CD8α
1.2
76 %
0.4
1.4
CFSE

7. ST fails to inhibit LM induced antigen-presentation

I have demonstrated that LM-OVA induces rapid T cell priming both *in vivo* and *in vitro*, which was absent during ST-OVA infection, due to the alleged inhibition of antigen-presentation as reported by others (13, 14). What happens if ST-OVA was co-infected with LM-OVA? Can ST-OVA impair the ongoing antigen-presentation by LM-OVA infected macrophages?

Interestingly, ST-OVA co-infection did not impair antigen-presentation by LM-OVA-infected macrophages (Figure 11). Furthermore, addition of SIINFEKL OVA peptide to ST-OVA infected macrophages also resulted in potent $CD8^+$ T cell activation indicated by extensive CFSE dilution, again suggesting that ST infection of macrophages does not result in inhibition of antigen-presentation.

To further test the validity of these results, I used multiple dose-combinations of bacteria to see whether a higher MOI of ST may result in any inhibition (Figure 12). When the percentage of $CFSE^{low}$ $CD8^+$ T cell population was measured by FACS, it was evident that only at a high MOI (100) ST inhibited LM-OVA induced antigen presentation (Figure 12-A). No such inhibition was observed when a lower MOI of ST was used (Figure 12-A). When the intracellular CFUs in these samples were measured however, it was revealed that there was a 10-fold drop in initial LM-OVA load (Figure 12-B) suggesting that ST influences LM-OVA uptake ultimately causing this apparent inhibition. Interestingly, the few LM-OVA that did gain access to the intracellular compartment under these conditions did proliferate within the 24 h period. LM-OVA, in contrast, did not influence ST uptake. A high MOI of LM-OVA did not inhibit the uptake of ST (Figure 12-C). Interestingly, no competitive inhibition between LM and ST was

observed on BHI plates (Figure 12-D) as the two types of colonies could be easily discerned visually.

It could be argued that the decline in LM-OVA uptake when cells had been infected with high doses of ST could be due to reduced viability of IC-21 macrophages. To test this theory, I measured the viability of infected macrophages by MTT and neutral red cytotoxicity assays. MTT is reduced by mitochondrial reductases to MTS which absorbs light. Therefire, the MTT assay in essence measures mitochondrial activity which reflects cell viability. The assay revealed that there was not any decrease in cell viability (Figure 13-A), but on the contrary, there was a trend of increased MTT uptake with higher MOIs of ST. Since MTT may potentially be taken up by bacteria as well and therefore cause ambiguity in signal interpretation, I used a second cytotoxicity assay to verify these results (Figure13-B). The neutral red dye assay measures lysosomal integrity, since neutral red, a vital dye, accumulates in that compartment when cells are viable. Reduced cell viability results in reduced lysosomal integrity and therefore inefficient accumulation of neutral red intracellularly. The data show that the extent of neutral red uptake is virtually identical whether or not LM-OVA is present during ST infection. These results indicate that the observed reduction in LM-OVA intracellular CFUs when ST is present at high MOIs is not due to reduced cell viability. Therefore, the failure to detect the rapid development of T cell response during infection of mice with ST is not due to ST-induced inhibition of antigen-presentation.

Figure 11. ST-OVA does not restrict antigen-presentation induced by LM-OVA infection.

IC-21cells were seeded in 24 well-plates. Bacteria were added individually or together at an MOI of 10, plates centrifuged to promote bacterial adsorption, and incubated at 37°C for 30-60 minutes. Cells were subsequently washed vigorously and incubated with R8-50 media for 1-2 hours. Subsequently, cells were co-cultured with CFSE-labeled OT1 splenocytes for 4 days in R8-5 media. Cells were finally collected and stained with anti-CD8α. The degree of OVA-induced $CD8^+$ T cell proliferation was evaluated by measuring CFSE dilution using flow cytometry. Data representative of three separate experiments (n=2).

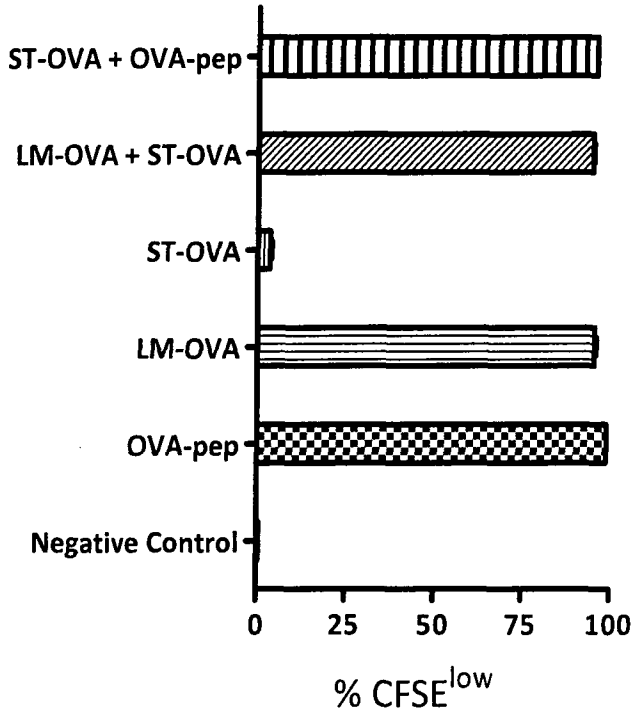
ST-OVA + OVA-pep
LM-OVA + ST-OVA
ST-OVA
LM-OVA
OVA-pep
Negative Control
0
25
50
75
100
% CFSE low

Figure 12. Suppression of LM-OVA-induced antigen presentation at high ST MOIs is due to bacterial competition, not active inhibition of antigen presentation.

IC-21cells were seeded in well-plates. Bacteria were added individually or together at various MOIs, plates centrifuged to promote bacterial adsorption, and incubated at 37°C for 30-60 minutes. Cells were subsequently washed vigorously and incubated with R8-50 media for 1-2 hours. Subsequently, cells were co-cultured with CFSE-labeled OT1 splenocytes for 4 days in R8-5 media. Cells were finally collected and stained with anti-CD8α. The degree of OVA-induced $CD8^+$ T cell proliferation was evaluated by measuring CFSE dilution using flow cytometry *(A) (n=2).* Intracellular bacterial titer for LM-OVA *(B)* and ST *(C)* in different co-infection scenarios was also determined at 1 hour and 24 hour post-infection. Cells were spun down, media aspirated, and cells were lysed using cell lysis buffer (1% tritonX, 0.1% SDS in PBS, pH 7.2). Appropriate dilutions were made in 0.9% saline and 100μl aliquots were plated on BHI plates. LM-OVA and ST bacterial colonies were clearly distinguishable *(D)* based on size and morphology. Data representative of two separate experiments (n=2).

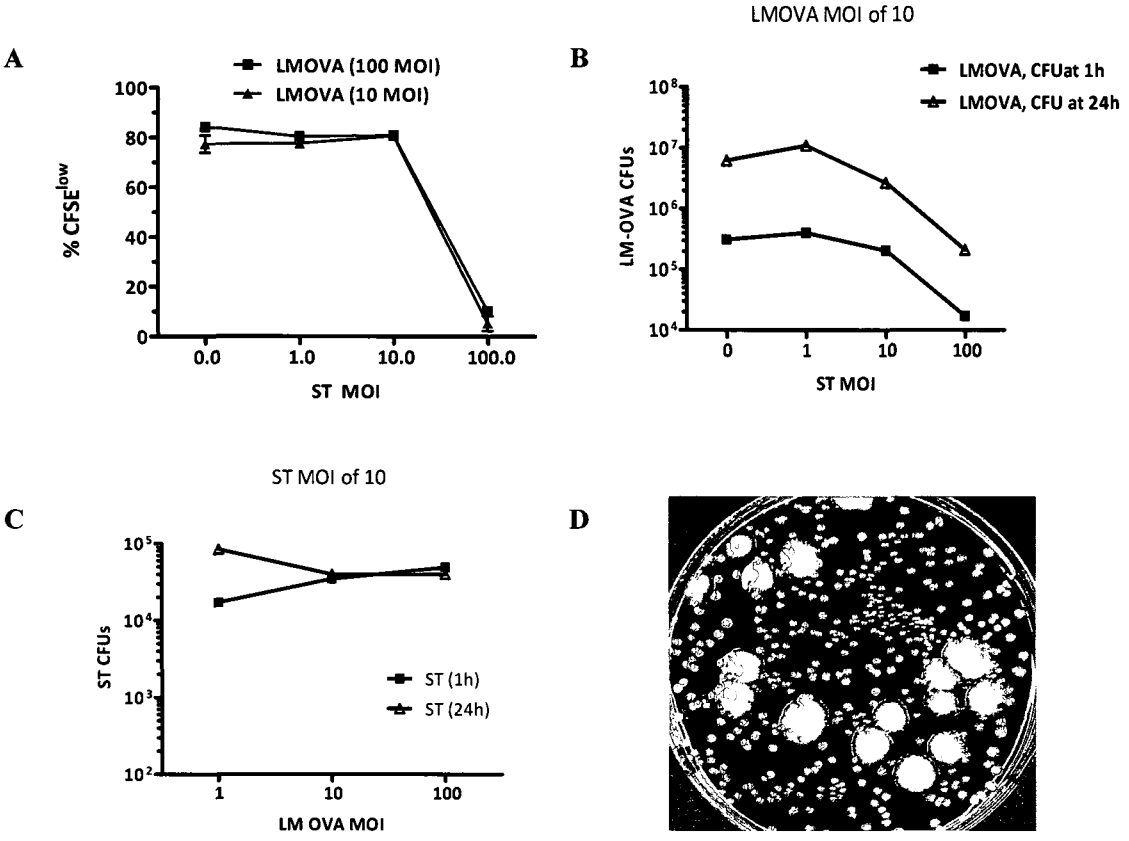
A
LMOVA (100 MOI)
LMOVA (10 MOI)
% CFSE low
100
80
60
40
20
0
0.0
1.0
10.0
100.0
ST MOI
B
LMOVA MOI of 10
LMOVA, CFUat 1h
LMOVA, CFU at 24h
LM-OVA CFUs
10 8
10 7
10 6
10 5
10 4
0
1
10
100
ST MOI
C
ST MOI of 10
ST CFUs
10 5
10 4
10 3
10 2
ST (1h)
ST (24h)
1
10
100
LM OVA MOI
D

Figure 13. The apparent suppression of LM-OVA-induced antigen presentation at high ST MOIs is not due to massively reduced viability of macrophages.

IC21 cells were seeded at a 1-2x10^4 cells/well in a 96 flat bottom culture plate. Cells were infected at various multiplicities of infection with ST-OVA, LM-OVA, or a combination of both for 1 hour at 37°C. Infection media was removed and cells were washed with R8-50 for an hour, after which the cells were incubated with R8-5 media for 24 hours at 37°C. Cell viability was assessed using the MTT assay *(A)* or the Neutral Red dye assay *(B)* according to standard protocol (see Materials and Methods). (n=3-6)

A

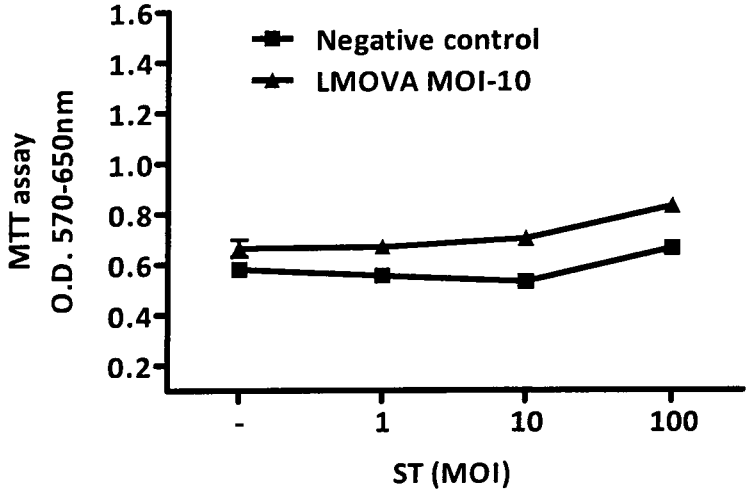
MTT assay
O.D. 570-650nm
1.6
1.4
1.2
1.0
0.8
0.6
0.4
0.2
Negative control
LMOVA MOI-10
-
1
10
100
ST (MOI)

B

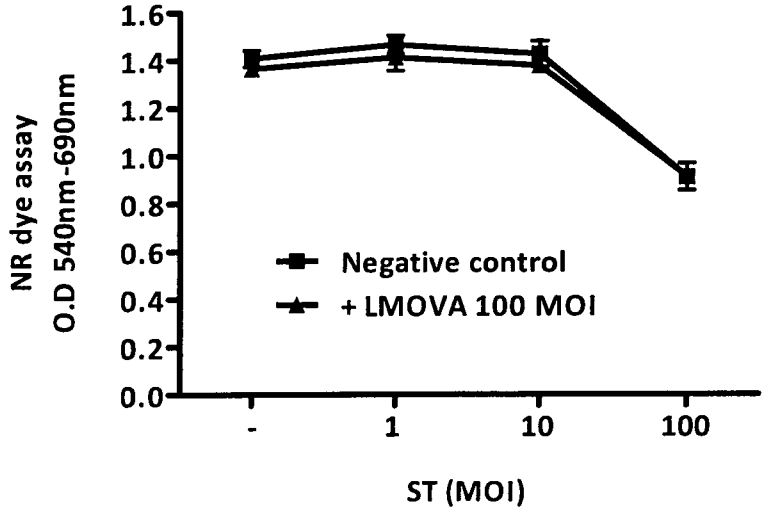
NR dye assay
O.D 540nm-690nm
1.6
1.4
1.2
1.0
0.8
0.6
0.4
0.2
0.0
Negative control
+ LMOVA 100 MOI
-
1
10
100
ST (MOI)

8. Mutations in SPI-1 and SPI-2 virulence genes do not result in increased antigen presentation.

The next question I needed to address was whether the virulence factors of ST play a role in any inhibition of antigen-presentation. To this end, I used a panel of OVA-expressing ST recombinants mutated in key genes of SPI-1 and SPI-2 pathogenecity islands (Table 1). The expression of OVA by recombinants was confirmed in aliquots of BHI grown bacteria. Samples were normalized for the number of bacteria (1.5×10^7) and loaded on SDS-12% polyacrylamide gels. Expression of OVA was measured by Western blotting using an ECL-based detection system. As shown, WT as well as the various mutants of ST express similar levels of OVA (Figure 14-A). Quantitative RT-PCR analysis was performed to determine the relative levels of OVA expressed by the virulent versus the mutants of ST-OVA. The amount of OVA mRNA was normalized to 16S rRNA expression. The relative ratio of OVA mRNA to the total bacterial RNA (16S) was similar for WT and the various mutants of ST-OVA (Figure 14-B), indicating that the various mutants of ST-OVA express similar levels of OVA. This ensures that any differences in the responses to these mutants are not due to discrepancies in OVA expression.

Do infections with these mutants result in enhanced antigen presentation? Using the *in vitro* model of antigen-presentation described previously (Figure 6), infections with these mutants did not result in effective priming of $CD8^+$ T cells since their CFSE signal remained high (Figure 15). These ST mutants were similarly tested *in vivo* (Figure 16) to determine if they induce antigen-presentation with analogous results. There was a mild increase (2 fold) in the percentage of $CFSE^{low}$ $CD8^+$ T cells in *ssaR*, *phoP*, and *invA*

infected mice. Furthermore, *aroA* infection resulted in a 3-fold increase in the number of primed T cells ($CFSE^{low}$) (Figure 16-A). However, the ratio of donor to total $CD8^+$ T cells revealed that donor T cells did not expand extensively and thus the observed CFSE dilution may be non-specific. Since some mutants display reduced replication *in vivo* (94), their infectious doses were varied to match the bacterial burden seen in mice infected with wild-type bacteria in order to ensure that any differences seen are not due to discrepancies in bacterial burden. The day 5 splenic bacterial burden was determined by plating aliquots of spleen homogenates on BHI agar to confirm the presence of bacteria (Figure 16-C).

Table1. Various bacterial strains used in this study

Inracellular bacteria	**Function of mutated gene (where applicable)**	**Intracellular localization**
Listeria monocytogenes (LM) LM (10403S)	N/A	Cytosolic
Salmonella typhimurium (ST) SL1344	N/A	Phagosomal
ST-aroA (attenuated)	Lacks the enzyme aromase required for synthesizing aromatic compound from simpler derivatives	Phagosomal
ST-invA (mutation in SPI-1)	Important for initial bacterial invasion and entry into Peyer's patches	Phagosomal
ST-ssaR (mutation in SPI-2)	Encodes a membrane-bound subunit of the type III secretion system	Phagosomal
ST-phoP (defective for intracellular survival and avoidance of lysosome)	A regulon orchestrating inhibition of lysosome-phagosome fusion	Phagosomal

Figure 14. WT and mutants of ST express similar levels of OVA.

(A) Bacteria were harvested from broth cultures, mixed with SDS sample buffer, and heated at 95°C for 5 min. Samples were normalized for cell number ($1.5x10^7$) and were loaded on SDS-12% polyacrylamide gels. ECL DualVue Western blotting markers were used. The proteins were transferred to immunoblot polyvinylidene difluoride membrane, which was blocked with 5% skim milk powder in TBST (50 mM Tris, 150 mM NaCl, and 0.05% Tween 20 v/v). OVA expression was detected using a 1/5,000 dilution of anti-OVA mAb (Sigma-Aldrich), followed by incubation with HRP-conjugated goat anti-mouse Ab (1/10,000 dilution in TBST) from Roche Applied Science. Immunoreactive bands were detected withenhanced chemiluminescence substrate (Roche Applied Bioscience) and were exposed for 30–60 s to Hyperfilm ECL (Amersham Biosciences). *(B)* Bacteria were harvested from broth cultures, and the amount of total bacterial RNA (16S rRNA) and OVA mRNA was determined by quantitative RT-PCR as explained in the *Materials and Methods* section. The ratio of OVA mRNA to the total bacterial RNA (16S RNA) was calculated. **Sad S et al. 2008. Pathogen proliferation governs the magnitude but compromises the function of CD8 T cells. *J. Immunol.* 180 : 5853-61. *Copyright 2008. The American Association of Immunologists, Inc.***

A

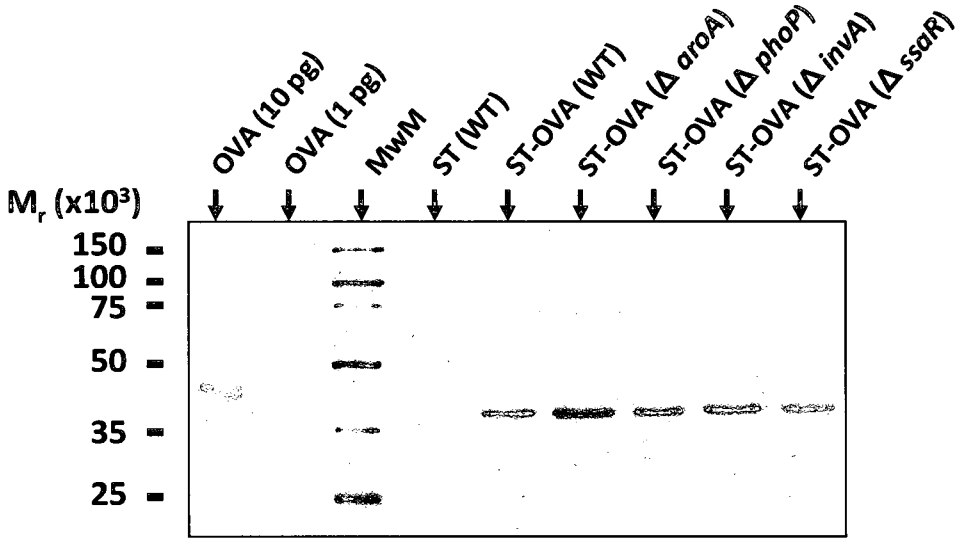
OVA (10 pg)
OVA (1 pg)
MwM
ST (WT)
ST-OVA (WT)
ST-OVA (Δ aroA)
ST-OVA (Δ phoP)
ST-OVA (Δ invA)
ST-OVA (Δ ssaR)
Mr (x10³)
150
100
75
50
35
25

B

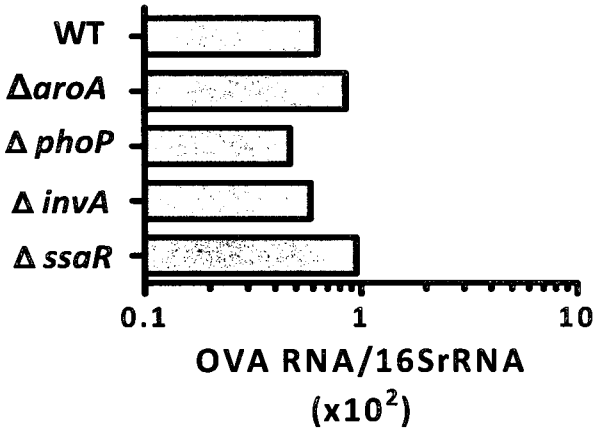
WT
ΔaroA
Δ phoP
Δ invA
Δ ssaR
0.1
1
10
OVA RNA/16SrRNA
(x10²)

Figure 15. Lack of antigen-presentation by ST infected APCs is not due to virulence effectors.

IC-21cells were seeded in well-plates. Bacteria were added at an MOI of 10, plates centrifuged - to promote bacterial adsorption, and incubated at 37°C for 30-60 minutes. Cells were subsequently washed vigorously and incubated with R8-50 media for 1-2 hours. Subsequently, cells were co-cultured with CFSE-labeled OT1 splenocytes for 4 days in R8-5 media. Cells were finally collected and stained with anti-CD8α. The degree of OVA-induced $CD8^+$ T cell proliferation was evaluated by measuring CFSE dilution using flow cytometry. Data representative of two separate experiments (n=2).

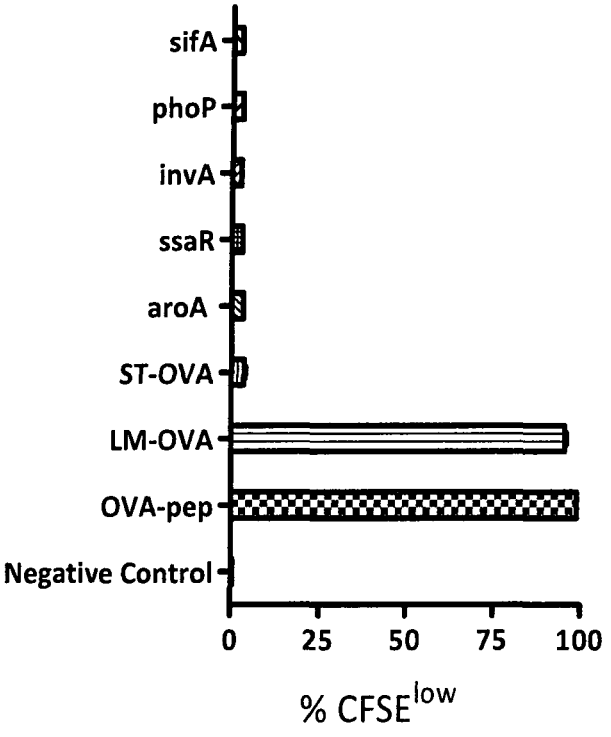
sifA
phoP
invA
ssaR
aroA
ST-OVA
LM-OVA
OVA-pep
Negative Control
0
25
50
75
100
% CFSE low

Figure 16. Virulence effectors are not the implicated in the lack of antigen presentation by ST infected APCs *in vivo*.

CFSE-labeled OT1-SJL splenocytes ($CD45.1^+$) were adoptively transferred into B6.129F1 ($CD45.2^+$) mice. 24 hours later, these recipient mice were infected intravenously with bacteria. Five days after infection, spleens were harvested, processed and spleen cell suspensions were stained with PerCP conjugated anti-CD8α, and APC conjugated anti-CD45.1 antibodies. OVA-induced proliferation of $CD8^+$ donor T cells was evaluated by measuring CFSE dilution by flow cytometry *(A)*. The percentage of donor cells ($CD45.1^+$) in the entire $CD8^+$ population was also plotted *(B)*. The bacterial burden in the infected spleens is also shown *(C)* and was determined as described previously. A representative panel of FACS data showing the percentage of $CFSE^{low}$, and therefore, primed $CD8^+$ T cells, for different strains, is also displayed *(D)*. Asterisk indicates statistical significance as determined by a one way ANOVA (* = $p<0.05$, *** = $p<0.001$) using GraphPad Prism 5 software. Data representative of three separate experiments(n=2).

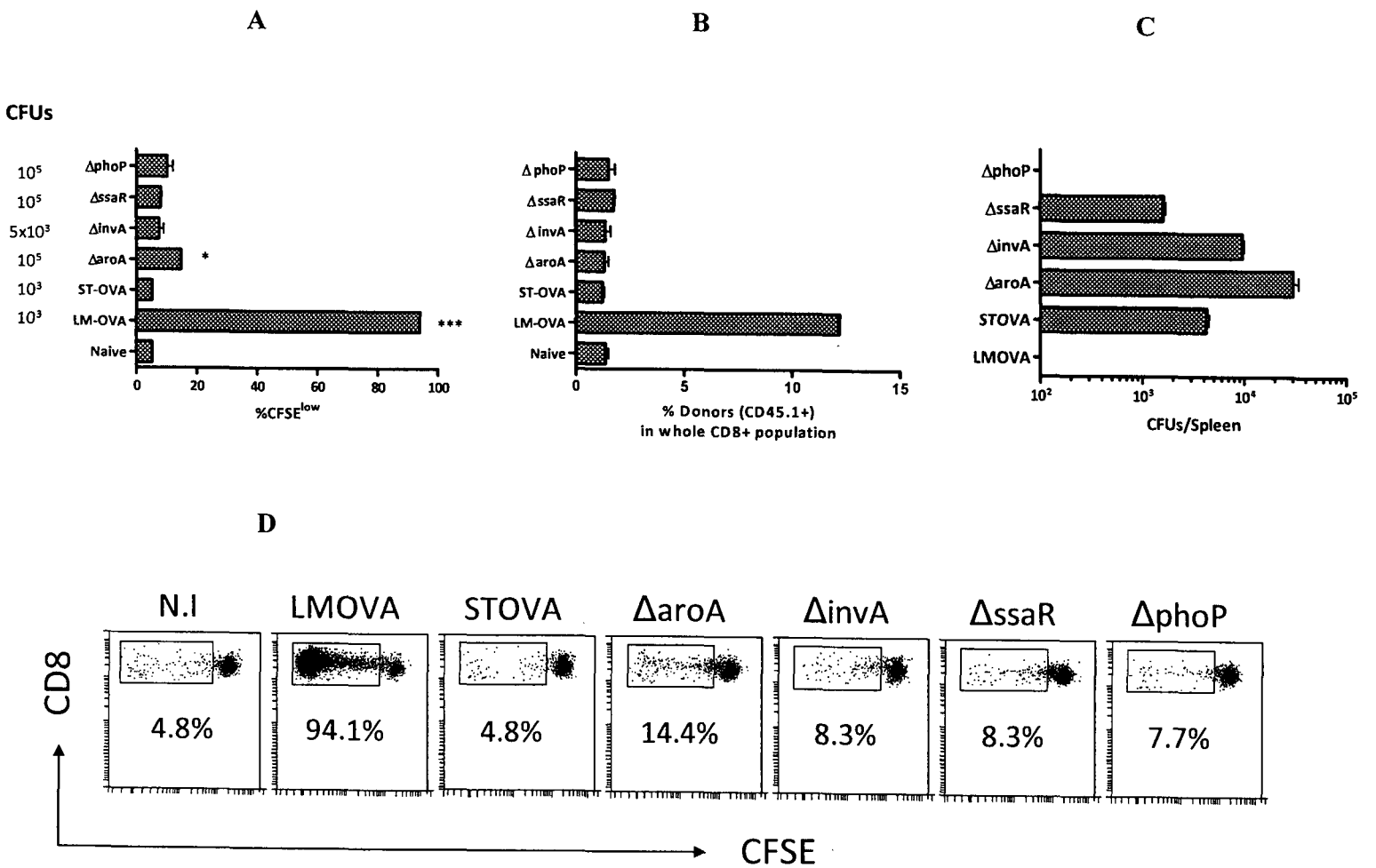
A
B
C
CFUs
10⁵
10⁵
5x10³
10⁵
10³
10³
ΔphoP
ΔssaR
ΔinvA
ΔaroA
ST-OVA
LM-OVA
Naive
*
***
0
20
40
60
80
100
%CFSE^low
0
5
10
15
% Donors (CD45.1+)
in whole CD8+ population
ΔphoP
ΔssaR
ΔinvA
ΔaroA
STOVA
LMOVA
10²
10³
10⁴
10⁵
CFUs/Spleen
D
N.I
LMOVA
STOVA
ΔaroA
ΔinvA
ΔssaR
ΔphoP
4.8%
94.1%
4.8%
14.4%
8.3%
8.3%
7.7%
CD8
CFSE

9. ST replicates at different rates in the intra- and extra- cellular compartments

Previously (68), it was established that ST doubles almost twice as fast as LM does in liquid culture (Figure 17). ST doubles every 38 minutes, while LM doubles every 55 minutes in liquid BHI. This might imply that ST is significantly more prolific *in vivo*, but there are many reports that demonstrated the limited number of bacteria intraphagosomally where ST is thought to preferentially reside (108-111). If ST is behaving *in vivo* similar to what is observed in liquid BHI, there should be sufficient amounts of antigen to prime $CD8^+$ T cells.

I set out to determine the intracellular doubling rate of ST using IC-21 macrophage cell line. After infection of IC-21 cells, extracellular bacteria were eliminated by vigorous washing and antibiotic treatment as described in the materials and methods section. I also closely monitored the infected cells visually using the microscope to ensure that they are viable and void of extracellular bacteria, which was true even at 96 hours post infection. Intracellular CFUs were determined by washing the cells at the specific time-points, aspirating the media, lysing the cells and plating appropriate dilutions of the lysate on BHI plates (Figure 18). Surprisingly, ST exhibited poor intracellular proliferation as compared to LM (Figure 18-A). The intracellular doubling time for ST was approximately 8 hours, whereas LM doubled in numbers every 2 hours. Taken together these results indicate that ST proliferates at different rates in the extracellular and intracellular compartments.

Figure 17. ST proliferates more rapidly in liquid broth.

Bacteria were grown in liquid BHI and aliquots were taken at different time intervals. The absorbance was measure in spectrophotometer at 600nm. Also indicated are the doubling time values calculated using exponential growth analysis in GraphPad Prism 5 software. **Luu RA et al. 2006. Delayed expansion and contraction of CD8+ T cell response during infection with virulent salmonella typhimurium. *J. Immunol.* 177 : 1516-25 *Copyright 2006. The American Association of Immunologists, Inc.***

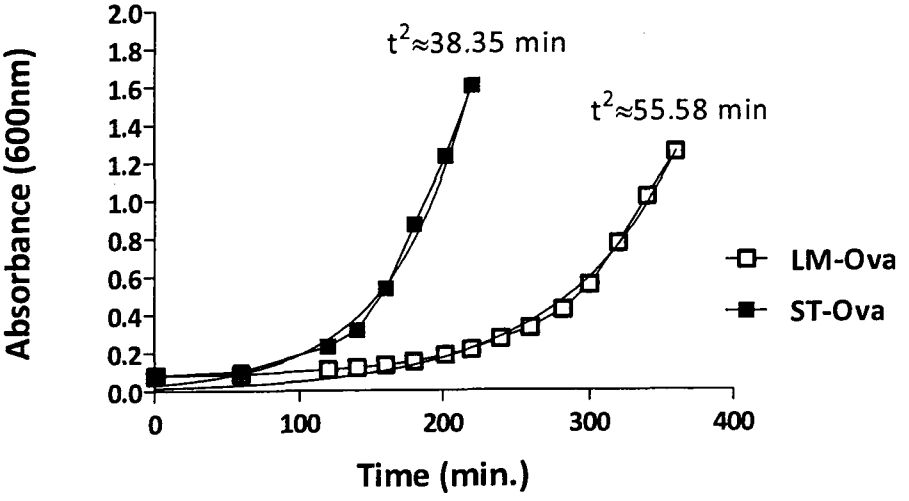
Absorbance (600nm)
2.0
1.8
1.6
1.4
1.2
1.0
0.8
0.6
0.4
0.2
0.0
0
100
200
300
400
Time (min.)
t2≈38.35 min
t2≈55.58 min
LM-Ova
ST-Ova

Figure 18. Intracellular proliferation of ST is markedly reduced compared to that of LM.

IC21 cells were seeded flat-bottom well-plates. Cells were infected with ST-OVA or LM-OVA at an MOI of 10 by adding bacteria directly to wells, centrifuging the plate to promote bacterial adsorption, and incubating the cells at 37°C for 20-30 minutes. Subsequently, cells were washed vigorously with R8-50 media 2-3 times by centrifugation, and cells were incubated in R8-50 media for 1-2 hours at 37°C to ensure all extracellular bacteria were eliminated. Afterwards, media was aspirated off, and cells were incubated in R8-1. At the appropriate time-point, cells were spun down, media aspirated, and cells were lysed using cell lysis buffer (1% tritonX, 0.1% SDS in PBS, pH 7.2). Appropriate dilutions were made in 0.9% saline and 100µl aliquots were plated on BHI plates. Intracellular CFUs are shown over the course of a 24 hour infection *(A)*. The fold increase of CFUs for both bacteria is also shown *(B)*, with the approximate doubling time calculated using exponential growth analysis in GraphPad Prism 5 software (Dotted lines). Data representative of four separate experiments (n=2).

A

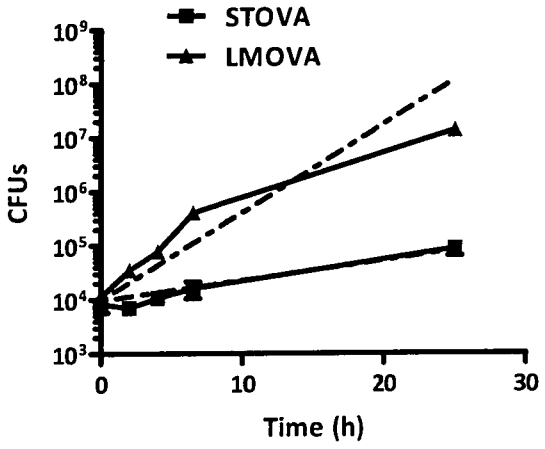
STOVA
LMOVA
CFUs
10^9
10^8
10^7
10^6
10^5
10^4
10^3
0
10
20
30
Time (h)

B

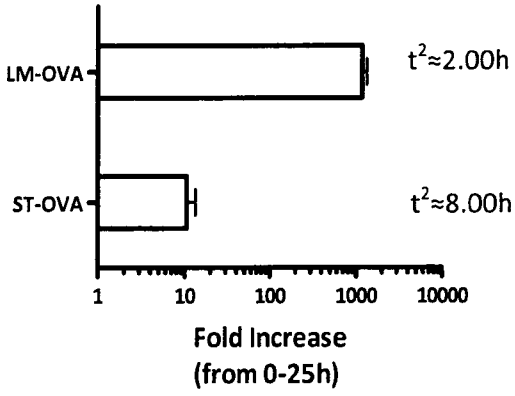
LM-OVA
ST-OVA
$t^2 \approx 2.00h$
$t^2 \approx 8.00h$
1
10
100
1000
10000
Fold Increase
(from 0-25h)

It is possible that the activation status of the macrophage may influence the relative proliferation of ST intracellularly. Therefore, IC-21 cells were stimulated *in vitro* with *E.coli* LPS for 24 hours prior to infection with ST (Figure 19). ST from LPS treated macrophages showed an identical pattern of growth to those from un-stimulated macrophages (Figure 19-A). The only difference between activated and non-activated was the initial numbers of bacteria that entered the cells (time 0), which, as expected, suggests that activated macrophages take up more bacteria. The fold change in bacterial CFUs, over 24 hours (Figure 19-B), was virtually identical.

10. Expression levels of immunodominant antigen corroborates the poor intracellular proliferation of ST

To confirm the aforementioned findings regarding the slow intracellular replication of ST, I decided to measure expression levels of the model antigen, OVA, by qRT-PCR. 16S rRNA was chosen as a positive control since its expression correlates very well with bacterial growth (112, 113). Both recombinant bacteria, LM-OVA and ST-OVA, express comparable levels of OVA in liquid broth (Figure 20). Bacteria were grown in liquid BHI under selecting conditions (see materials and methods) up to an O.D of approximately 0.45, and RNA was extracted as described. The number of OVA mRNA and 16S rRNA detectable molecules in both LM-OVA and ST-OVA were similar. This confirms that the stark difference between LM-OVA and ST-OVA in antigen-presentation potential (Figures 8, 9, 15 and 16) are not due to inconsistent OVA expression. In fact, ST-OVA produces 4 times more OVA than LM-OVA (Figure 20).

Figure 19. Activation state of macrophages does not influence intracellular proliferation of ST.

IC21 cells were stimulated with 5 ng/ml LPS overnight in flat-bottom well-plates. Cells were infected with ST-OVA at an MOI of 10 by adding bacteria directly to wells, centrifuging the plate to promote bacterial adsorption, and incubating the cells at 37°C for 20-30 minutes. Subsequently, cells were washed vigorously with R8-50 media 2-3 times by centrifugation, and cells were incubated in R8-50 media for 1-2 hours at 37°C to ensure all extracellular bacteria were eliminated. Afterwards, media was aspirated off, and cells were incubated in R8-1. At the appropriate time-point, cells were spun down, media aspirated, and cells were lysed using cell lysis buffer (1% tritonX, 0.1% SDS in PBS, pH 7.2). Appropriate dilutions were made in 0.9% saline and 100µl aliquots were plated on BHI plates. Intracellular CFUs are shown over the course of a 24 hour infection *(A)*. The fold increase of CFUs for both bacteria is also shown *(B)*, with the approximate doubling time calculated using exponential growth analysis in GraphPad Prism 5 software (Dotted line).

A

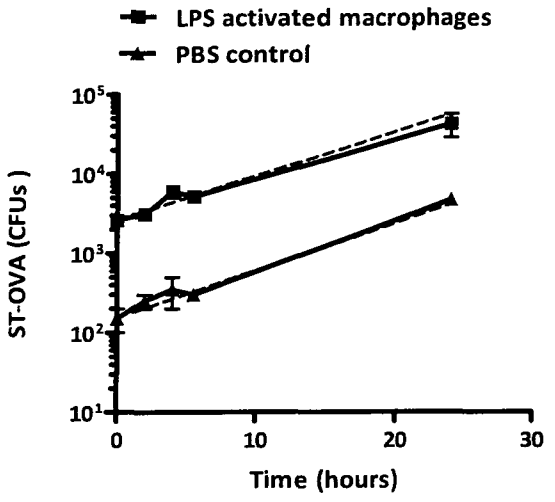
LPS activated macrophages
PBS control
ST-OVA (CFUs)
10^5
10^4
10^3
10^2
10^1
0
10
20
30
Time (hours)

B

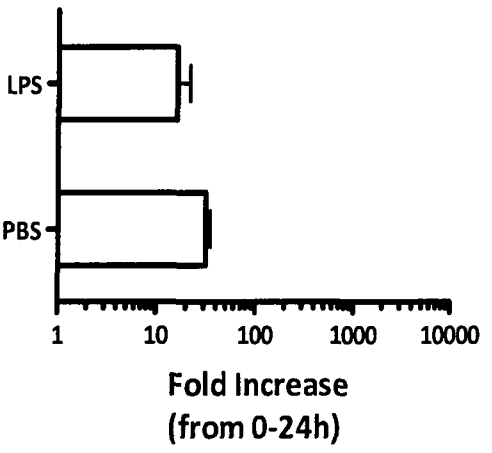
LPS
PBS
1
10
100
1000
10000
Fold Increase
(from 0-24h)

Figure 20. ST-OVA and LM-OVA show similar expression levels of *immunodominant antigen in liquid culture.*

Bacteria were grown in liquid BHI under selective growth conditions until the culture reached an O.D of approximately 0.48-0.50 at 600nm. An aliquot was collected, and 2 volumes of RNAProtect Bacterial Reagent (Qiagen) were added. After 10 min incubation at RT, bacteria were pelleted by centrifugation and stored at -80°C. RNA was extracted from these samples as described in the Materials and Methods section. Expression levels of OVA RNA and 16S rRNA in response to LM-OVA and ST-OVA infection were measured by qRT-PCR. Mole values were converted into the number of RNA molecules based on avogadro's number.

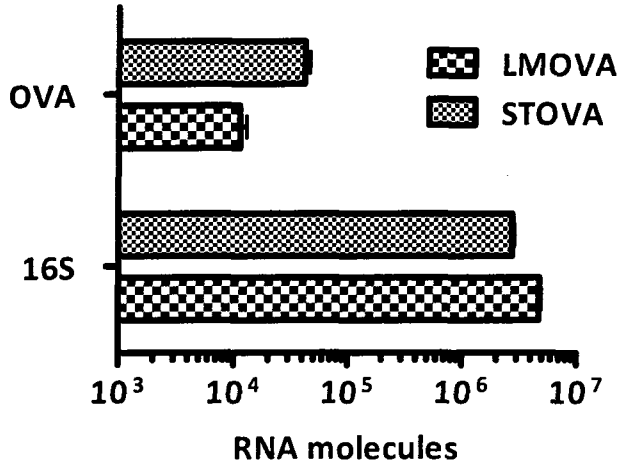
LMOVA
STOVA
OVA
16S
10^3
10^4
10^5
10^6
10^7
RNA molecules

Intracellularly, the OVA mRNA and 16S rRNA expression profiles are significantly different (Figure 21). OVA expression in LM-OVA infected IC-21 cells was 1000 fold higher than that of ST-OVA infected cells (Figure 21-A), whereas the 16S rRNA expression for LM-OVA was 200-folds higher than that of ST-OVA. The intracellular CFUs correlate very well with 16S expression (Figure 21-C) as anticipated. There were 200-fold higher numbers of intracellular CFUs for LM-OVA infected cells in comparison to ST-OVA infected cells. When the expression of OVA was normalized to 16S rRNA after 24 hours of infection, the expression ratios by LM-OVA and ST-OVA were similar (Figure 21-B) but there was still a 2-fold edge for LM-OVA.

Finally, bacterial OVA expression was measured *in vivo* (Figure 22). Spleens were isolated at specific time points post infection and frozen until RNA extraction was performed. At the maximum injectable dose of ST-OVA (10^3 CFUs), the expression of OVA falls below detection, even by qRT-PCR analysis (Figure 22-A). With LM-OVA, there is a distinct 4 fold increase in OVA expression on day 3 coinciding with the peak of infection. The expression of 16S rRNA for both bacteria closely parallels the splenic bacterial burden (Figure 22-C).

11. ST-OVA infection of macrophages does not generate detectable peptide-MHC levels.

The relative levels of pMHC complexes that engage and activate T cells defines the antigenic load (114). I therefore utilized the unique 25D1.16 monoclonal antibody which binds H-2K^b MHCI molecules only when in complex with SIINFEKL peptide to estimate the relative amounts of antigen generated by ST-OVA and LM-OVA. Before infection, I

wanted to determine the relative amount of free peptide that can be detected in complex with H-2K^b using this technique. JAWSII cells were pulsed with serial dilutions of the SIINFEKL peptide, and pMHCI levels quantified by FACS (Figure 23-A). A minimum of 1 nmol of OVA peptide was required before peptide-MHC complexes can be detected by flow cytometry. The lower end of mean fluorescence intensity (MFI) was approximately 1500. Maximal loading occurs with approximately 100 nmol at which point the mean fluorescence intensity (MFI) was approximately 7000.

LM-OVA, ST-OVA and the various mutants described earlier were used to infect JAWSII cells to determine the relative levels of pMHCI in response to infection, and whether key mutations might affect these levels. An isotype control was used in juxtaposition with 25D1.16. Only LM-OVA infection resulted in a significant increase in pMHCI numbers (~3500 MFI) (Figure 23-B,C). Infection with ST-OVA or the various mutants resulted in only mild, insignificant, increase in MFI versus the isotype control, which was in the 1000-1400 range. One exception was the infection with the naturally occurring strain *aroA*. It resulted in a noticeable increase that reached 2000 MFIs. However, when the 25D1.16 to isotype ratio is considered, the increase remains insignificant, as also determined by two-way ANOVA statistical analysis. Figure 23-C displays cytometric histogram data emphasizing the shift in fluorescence. The dotted line represents the mean fluorescence of pMHCI in response to LM-OVA, and highlights the absence of an MFI shift in response to the other infections.

Figure 21. Expression levels of immunodominant antigen corroborate the poor intracellular proliferation of ST.

Cultured IC-21 cells were seeded in well-plates and infected at an MOI of 1 with either ST-OVA or LM-OVA for 1 hour at 37°C. Cells were subsequently washed vigorously with R8-50 media by centrifugation 2-3 times, and propagated in R8-1 media for 24 hours at 37°C. Cells were collected in PBS by scraping, and an equal volume of RNAlater (Qiagen). RNA was extracted from these samples as described in the Materials and Methods section. Expression levels of OVA RNA and 16S rRNA in response to LM-OVA and ST-OVA infection are expressed as fold change to non-infected samples *(A)*. Fold expression of OVA RNA normalized to 16S rRNA expression is also shown *(B)*. Finally, the intracellular CFUs from these samples were also plotted *(C)*, correlating well with 16S rRNA expression. Asterisks indicate statistical significance based on the standard unpaired one-tailed t-test performed on GraphPad Prism 5 software (* = $p<0.05$, *** = $p<0.001$).

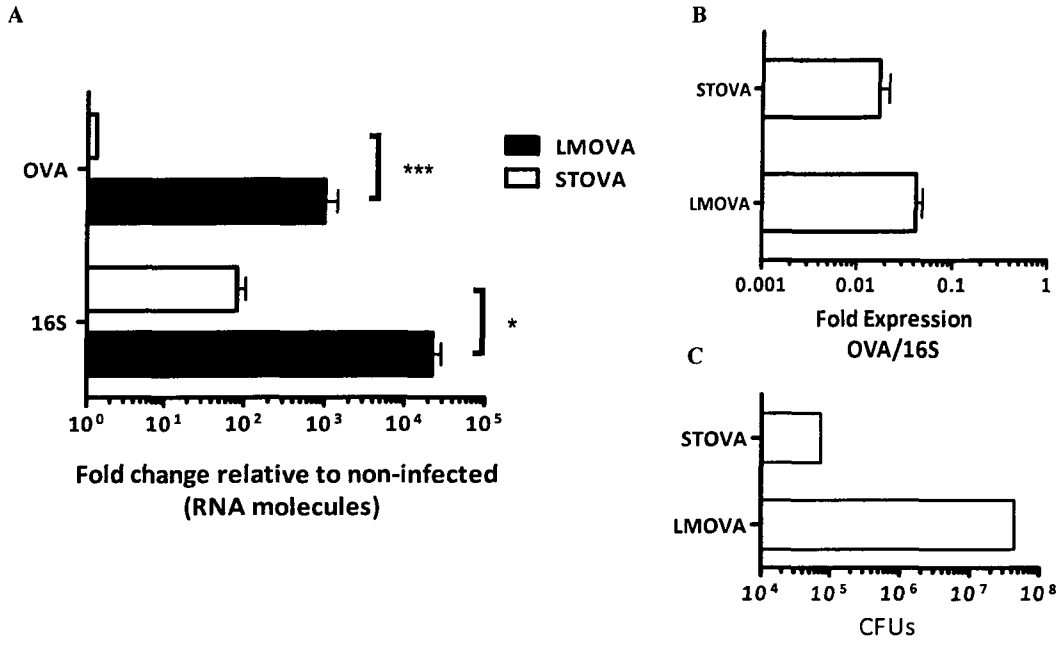
A
OVA
16S
***
*
LMOVA
STOVA
10^0 10^1 10^2 10^3 10^4 10^5
Fold change relative to non-infected
(RNA molecules)
B
STOVA
LMOVA
0.001 0.01 0.1 1
Fold Expression
OVA/16S
C
STOVA
LMOVA
10^4 10^5 10^6 10^7 10^8
CFUs

Figure 22. OVA expression during ST-OVA infection *in vivo* is undetectable.

B6129F1 mice were infected with 10^3 CFUs of ST-OVA or LMOVA intravenously. Spleens were isolated under aspetic condtions and immediately frozen in a dry ice. RNA was extracted from these samples as described in the Materials and Methods section. Expression levels of OVA RNA and 16S rRNA in response to ST-OVA *(A)* and LM-OVA *(B)* infection was determined and expressed as fold change to non-infected samples. Splenic bacterial burden is also plotted *(C)*, correlating well with 16S rRNA expression. Results are representative of two separate experiments (n=3).

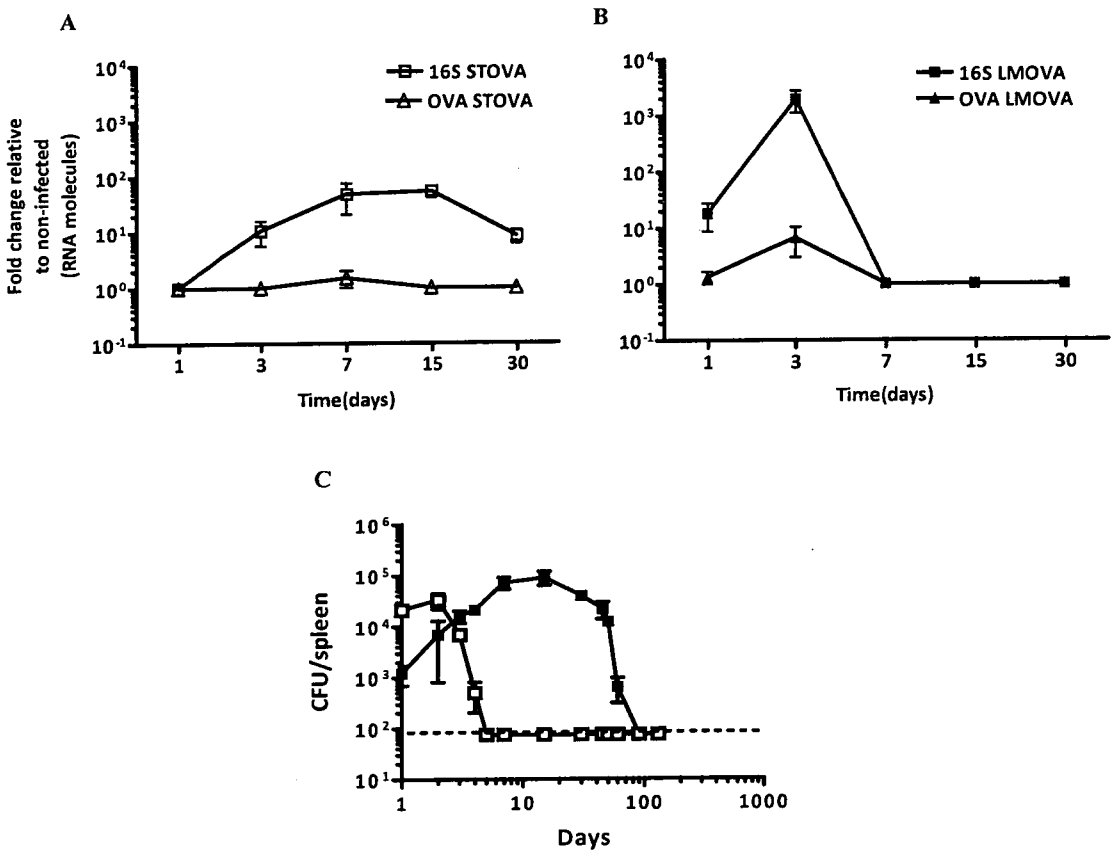
A
B
C
16S STOVA
OVA STOVA
16S LMOVA
OVA LMOVA
Fold change relative to non-infected (RNA molecules)
Time(days)
CFU/spleen
Days

Figure 23. ST-OVA infection does not result in adequate levels of pMHCI.

Cultured JAWSII cells were seeded in well-plates at $1x10^6$cells/well. Various amounts of SIINFEKL ($OVA_{257-264}$) peptide ranging from 0.002-200 nmols were used to establish a standardization plot *(A)*. In this experiment, cells were pulsed with peptide for 1 hour after which cells were collected and stained. In another experiment *(B)*, cells were infected at an MOI of 10 as described previously and incubated thereafter for 24 hours at 37°C. Subsequently, cells were collected and stained with an antibody specific for H-$2K^b$-$OVA_{257-264}$ (25D1.16) or an IGg1 isotype control. Cells were washed with PBS, reconstituted in 1% PBS-BSA, and this time stained with a goat-anti-mouse PE-conjugated antibody. Finally, cells were washed with PBS and re-suspended in 0.5% fixative. The mean fluorescence intensity was measured by FACS on PE channel. A representative panel of FACS data histograms is also shown *(C)* emphasizing the degree of shift in MFI. Asterisk indicates statistical significance as determined by a two-way ANOVA ($p<0.001$) *(B)*. A Boltzmann Sigmoidal equation was determined to be the best fit for *(B)* with and R^2 value of 0.95. Analysis was done using GraphPad Prism 5 software.(n=3)(N.I=non-infected). Data representative of two separate experiments (n=2)

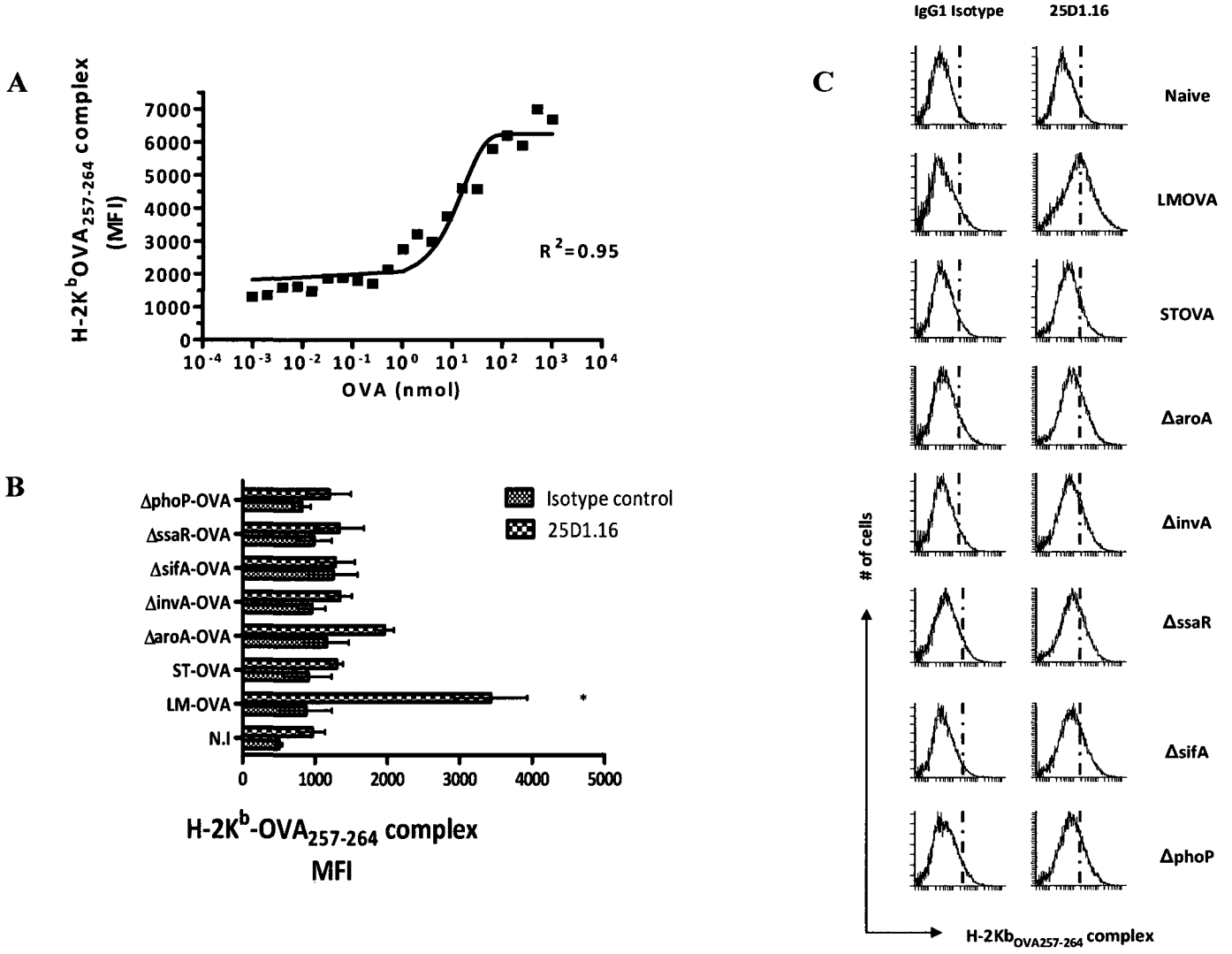
A
H-2K^{b}OVA$_{257-264}$ complex (MFI)
7000
6000
5000
4000
3000
2000
1000
0
10^{-4} 10^{-3} 10^{-2} 10^{-1} 10^{0} 10^{1} 10^{2} 10^{3} 10^{4}
OVA (nmol)
R^2=0.95
B
ΔphoP-OVA
ΔssaR-OVA
ΔsifA-OVA
ΔinvA-OVA
ΔaroA-OVA
ST-OVA
LM-OVA
N.I
Isotype control
25D1.16
*
0
1000
2000
3000
4000
5000
H-2K^b-OVA$_{257-264}$ complex MFI
C
IgG1 Isotype
25D1.16
Naive
LMOVA
STOVA
ΔaroA
ΔinvA
ΔssaR
ΔsifA
ΔphoP
# of cells
H-2Kb$_{OVA257-264}$ complex

12. Pathogen virulence influences frequency of antigen-specific $CD8^+$ T cells in the acute stage of infection

While the data presented here point to the lack of antigen-presentation during the first week of ST infection, $CD8^+$ T cell are in fact mobilized at later stages of infection, perhaps due to cross-presentation of antigen (115) (Figure 3). Here, I addressed whether the virulence of ST influences the development, magnitude and function of the T cell response. Wild-type ST versus the *aroA* mutant of ST, both expressing OVA were used for this purpose. $CD8^+$ T cells were purified from infected spleens, stimulated *in vitro* with IL-2 and SIINFEKL peptide and the frequency of OVA-specific, IFNγ–producing $CD8^+$ T cells was evaluated using the ELISPOT assay as described (Figure 24, 25). It is immediately evident that *aroA* infection results in a reduced frequency of OVA-specific, IFNγ-producing $CD8^+$ T cells compared to wildtype ST-OVA up until day 60 (Figure 25-A). The number of OVA-specific IFNγ producing $CD8^+$ T cells in the case of wildtype ST-OVA infection increased to more than half a million cells per spleen by day 30, and dropped to 10% of that by day 60. However, with *aroA*, the number of cell increased gradually to and stabilized at $2x10^5$ by day 60. From day 60 onwards, the frequency of those cells was comparable in both groups but remained about 2 folds higher in the case of *aroA* infection. There is a distinct difference in the bacterial burden for both bacteria (Figure 25-B), but as found previously by our group, bacterial virulence and not burden dictates the extent of T cell response (94). SPI-1 and SP-2 mutants, which have a characteristically reduced *in vivo* replication, induced CD8 T cells to a similar extent whether or not their bacterial burden was matched to wildtype ST by increasing their infectious dose (94).

Figure 24. Mouse infection models for measuring T cell response.

Endogenous response: B6129F1 mice are infected with recombinant bacteria expressing ovalbumin and throughout the duration of infection, the relative numbers of IFN-γ-secreting CD8 T cells are evaluated after stimulation with OVA-peptide and IL-2 for 48h. Adoptive transfer: Splenocytes from OT1 mice, whose CD8 T cells are >90% specific to SIINFEKL epitope of ovalbumin, are transferred into B6129F1 mice. Those OT1-parked mice are infected with our recombinant bacteria expressing ovalbumin. The antigen-specific CD8 T cell response is tracked in these mice using OVA-tetramers, flouropore-coated antibodies for cell markers, and flow cytometry.

Models for measuring T cell response

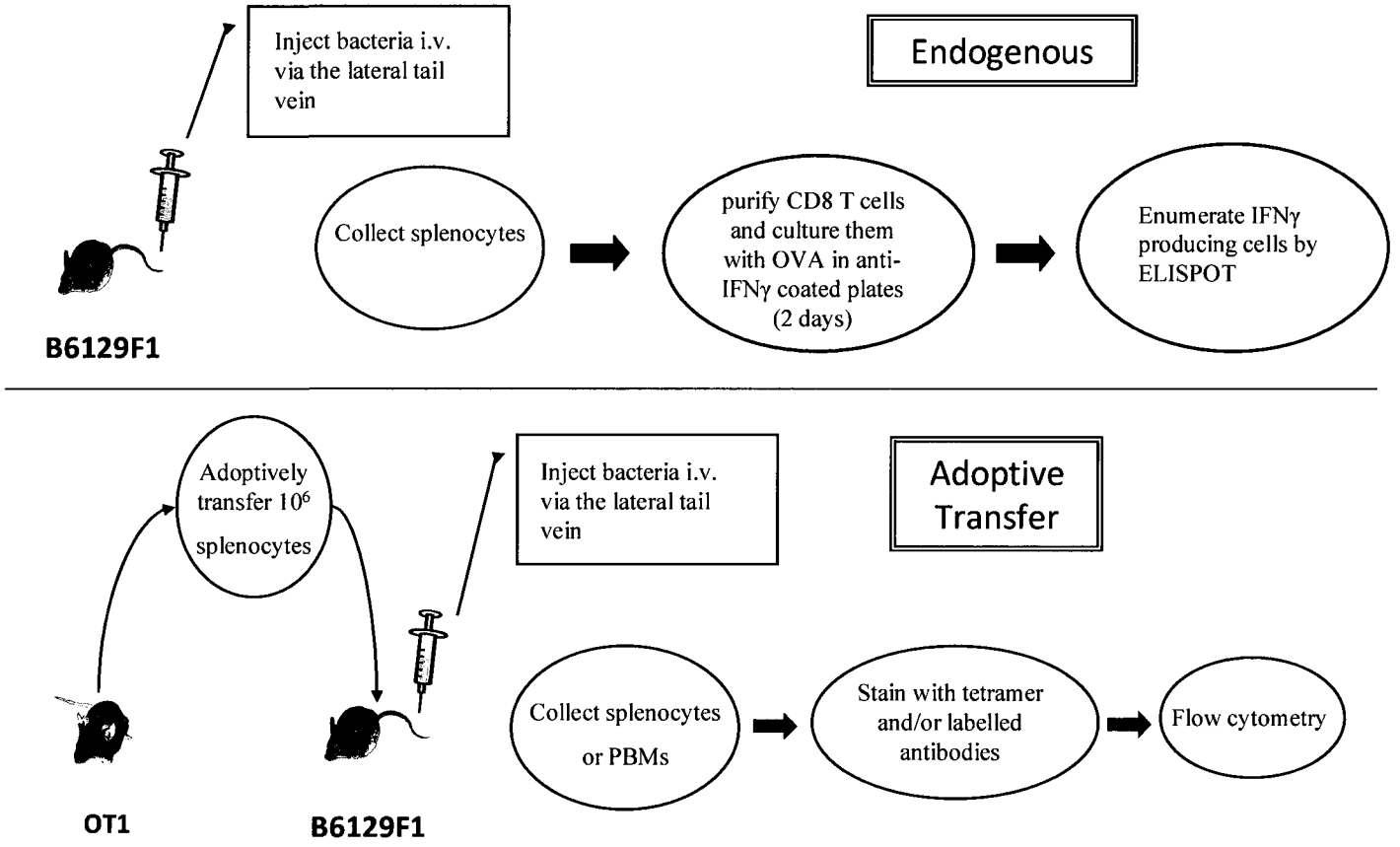

Figure 25. Attenuated ST-OVA shows reduced frequency of OVA-specific IFNγ producing CD8 T cells in the acute phase of infection.

B6.129F1 female mice were infected intravenously with 10^3 ST-OVA wt or ST-OVA *aroA*. Spleens were harvested, processed, and $CD8^+$ T cells were purified using the DYNAL magnetic bead system. Purified $CD8^+$ T cells (91-99% purity) were incubated for 48 hours with IL-2 and in the presence or absence of OVA peptide, using IP plates pre-coated with anti-IFNγ Ab (R46A2). Plates were washed with 0.01% PBST, incubated with biotinylated anti-IFNγ Ab (XMG1.2). Subsequently plates were washed, incubated with Streptavidin-HRP, and finally developed using AEC substrate. Dots corresponding to single IFNγ producing cells were enumerated under the microscope. Shown is the frequency of IFNγ producing cells throughout the course of infection *(A)*. In parallel, the bacterial burden in the spleens was determined as described previously *(B)*. Data representative of two separate experiments (n=2).

A

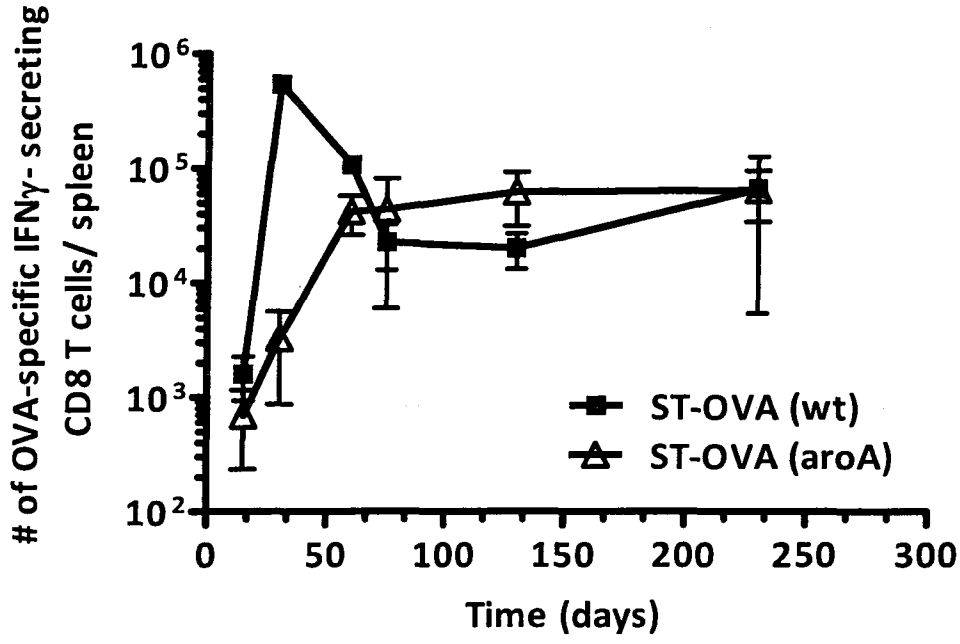
# of OVA-specific IFNγ- secreting CD8 T cells/ spleen
10 6
10 5
10 4
10 3
10 2
0
50
100
150
200
250
300
Time (days)
ST-OVA (wt)
ST-OVA (aroA)

B

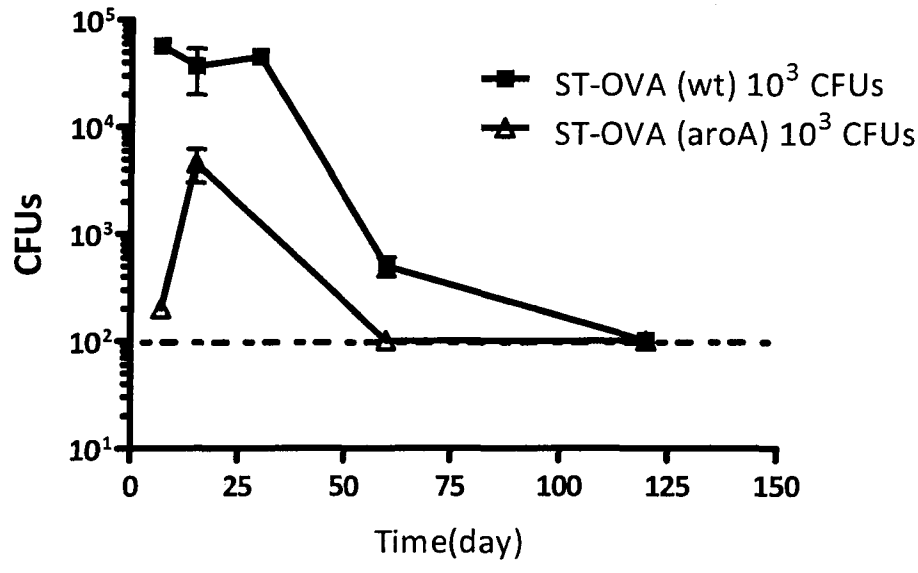
CFUs
10⁵
10⁴
10³
10²
10¹
0
25
50
75
100
125
150
Time(day)
ST-OVA (wt) 10³ CFUs
ST-OVA (aroA) 10³ CFUs

13. Magnitude of OVA-specific CD8 T cell expansion and memory correlates with extent of ST virulence

Another method of evaluating T cell response is the adoptive transfer model wherein the response can be tracked and phenotypically characterized by tetramer technology and flow cytometery for prolonged periods. In this system, OVA specific $CD8^+$ T cells derived from OT-1 mice are adoptively transferred into B6.129F1 mice that are to be infected with recombinant bacteria (Figure 24). Using H-$2K^b$ tetramers, OVA-specific $CD8^+$ T cell response can be tracked throughout the infection. Furthermore, gating on these populations using FACS, the expression profiles of certain cell markers that distinguish $CD8^+$ T cell phenotype can be uncovered using the appropriate antibodies.

Since virulence of the pathogen results in differential bacterial load *in vivo*, I injected 100-fold higher dose of *aroA* in comparison to wild-type in order to obtain similar bacterial loads. As evident in Figure 26-A, similar bacterial burden was generated in mice infected with wild-type or *aroA*-OVA. In peripheral blood (Figure 26-B), OVA-tetramer positive cells peaked at day 30 (21%) of infection with wt ST-OVA and dropped to 5% by day 60 (Figure 26-B). In the case of *aroA*, the response seems to peak earlier at day 21 (5% of total CD8 T cells) and dropped to 1% by day 60. The IL7Rα profile of OVA specific CD8 T cells also exhibits some differences after day 30 (Figure 26-C), coinciding with the memory development stage. There is a 2 fold increase in IL7Rα expression on OVA specific CD8 T cells in *aroA* infection compared to wild-type which is especially prominent on day 45.

Figure 26. Magnitude of OVA-specific CD8 T cell expansion and memory correlates with extent of ST virulence, not bacterial burden.

OT-1-parked B6.129F1 mice (10^6 cells/mouse) were infected intravenously with 10^3 cfu ST-OVA (wt) or 10^5 (*aroA*). At the respective time points, blood was collected by making a small nick in the mouse tail and drawing blood into microtainer, lithium heparin coated tubes. Samples were stained with anti-CD8α-PerCP-Cy5.5, anti-CD127-FITC, and anti-CD62L-PE Cy7, anti-PD1-FITC and H-2K^b OVA-tetramer-PE. After 30 min, RBCs were lysed using RBC lysing buffer for 8 min, and washed with PBS. Samples were finally fixed and acquired on BD Biosciences FACS Canto Analyzer, and percentages were determined by gating on the respective population. The numbers of OVA specific CD8 T cells *(B),* and the expression profiles of IL7Rα *(C),*and CD62L *(D)* over a 60 day infection period In parallel, the bacterial burden in the spleens was determined as described previously *(A)*. Asterisks denote statistical significance (* = $p<0.05$, ** = $p<0.01$) as determined by two-way ANOVA using GraphPad prism 5 software. Data shown are representative of three separate experiments (n=2).

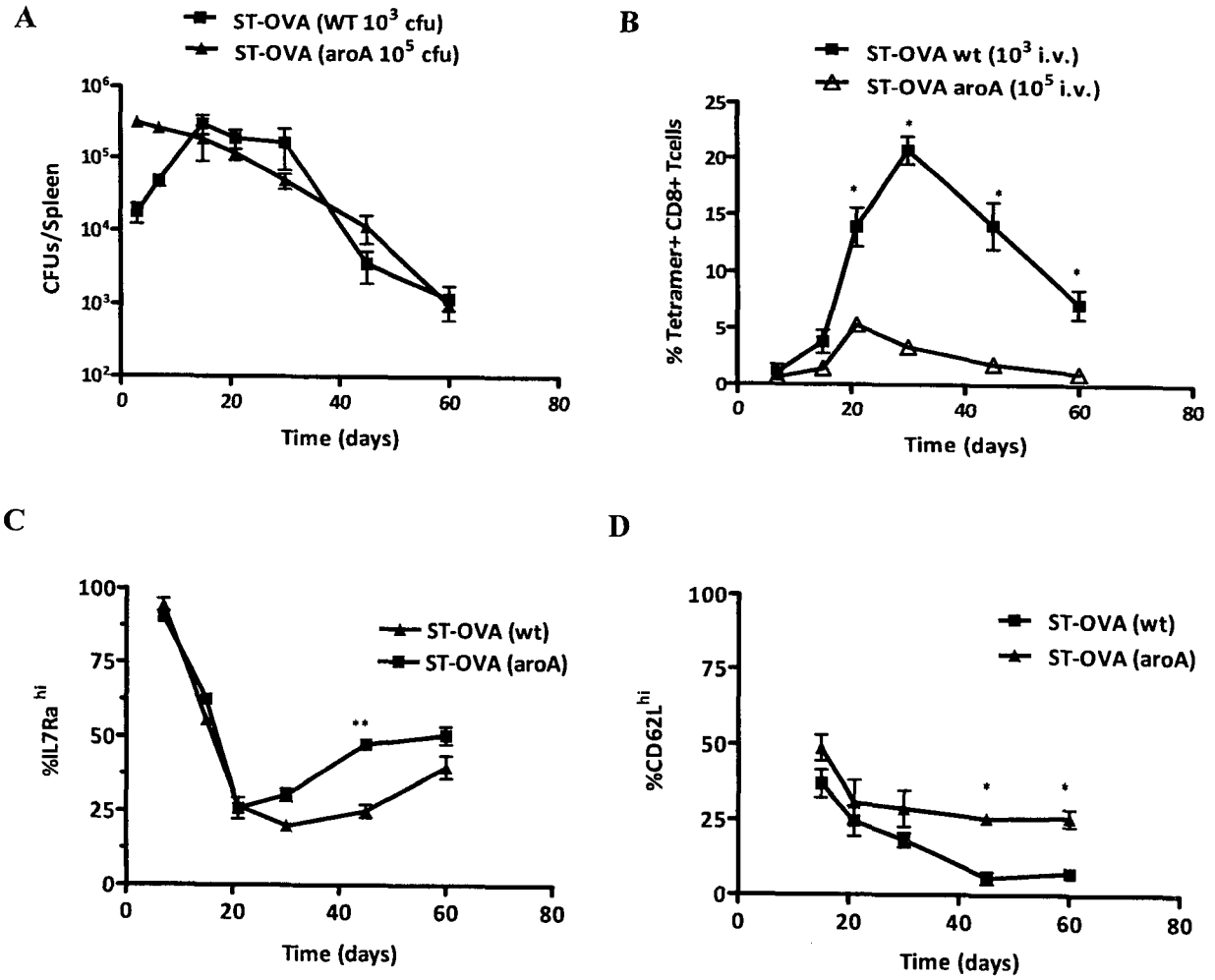
A
ST-OVA (WT 10^3 cfu)
ST-OVA (aroA 10^5 cfu)
CFUs/Spleen
Time (days)
B
ST-OVA wt (10^3 i.v.)
ST-OVA aroA (10^5 i.v.)
% Tetramer+ CD8+ Tcells
Time (days)
C
ST-OVA (wt)
ST-OVA (aroA)
%IL7Ra^hi
Time (days)
D
ST-OVA (wt)
ST-OVA (aroA)
%CD62L^hi
Time (days)

Furthermore, another memory marker CD62L shows a similar pattern with a 5 fold higher expression in OVA-specific cells generated in *aroA* infected mice (Figure 26-D). In spleen, the results recapitulate those or peripheral blood. Despite the essentially identical bacterial burden, a significant reduction in magnitude of OVA specific $CD8^+$ T cell response induced against *aroA* is observed. The percentage of tetramer positive cells after infection with wild-type ST-OVA surges to around 12% by day 21 and slowly falls below 5% by day 60. Again, there is a modest increase in tetramer positive cells in response to *aroA*, namely 4% by day 21 and dwindling to 1% by day 60 (Figure 27-A). The IL7Rα profile resembles what was seen in blood, an initial decrease in expression paralleling the expansion stage followed by a gradual increase, which is significantly higher in response to *aroA* (Figure 27-B). In this case the mean fluorescence intensity of anti-IL7Rα-FITC was measured because there are no distinct high and low populations. It is worth noting that very late in the infection (day 120), IL7Rα expression is comparable in the two groups. The expression profile for CD62L is slightly different from what was seen in blood. However, an overall decreasing trend in expression is observed. The difference between wild-type and *aroA* is negligible though still slightly higher in the case of *aroA* infection (Figure 27-C). I also evaluated the expression of PD-1 which is known to correlate with T cell exhaustion in chronic viral infections (116, 117). The expression of PD-1 in both scenarios was indistinguishable and remained relatively low throughout the infection. Only 25% of tetramer positive cells expressed high levels of PD-1 initially and this percentage dropped gradually down to 5% by day 120 (Figure 27-D).

Figure 27. Magnitude of OVA-specific CD8 T cell expansion and type of memory response correlate with extent of ST virulence.

OT-1-parked B6.129F1 mice (10^6 cells/mouse) were infected intravenously with 10^3 cfu ST-OVA or various mutants, and spleens harvested at the respective time points. Spleens were homogenized in RPMI and splenocytes were Fc blocked for 5 min and subsequently stained with anti-CD8α-PerCP-Cy5-5, anti-CD44-FITC, anti-CD62L-PE Cy7 and H-2Kb OVA-tetramer-PE. After 30 min, cells were washed, fixed, and acquired on BD Biosciences FACS Canto Analyzer, and percentages were determined by gating on the respective population. The numbers of OVA specific CD8 T cells over a 60 day infection period *(A)* and the expression profiles of IL7Rα *(B)* CD62L *(C)* and PD-1 *(D)* on OVA-specific CD8 T cells are shown. Asterisks denote statistical significance (* = $p<0.05$, *** = $p<0.001$) as determined by two-way ANOVA using GraphPad prism 5 software. Data representative of two separate experiments (n=2).

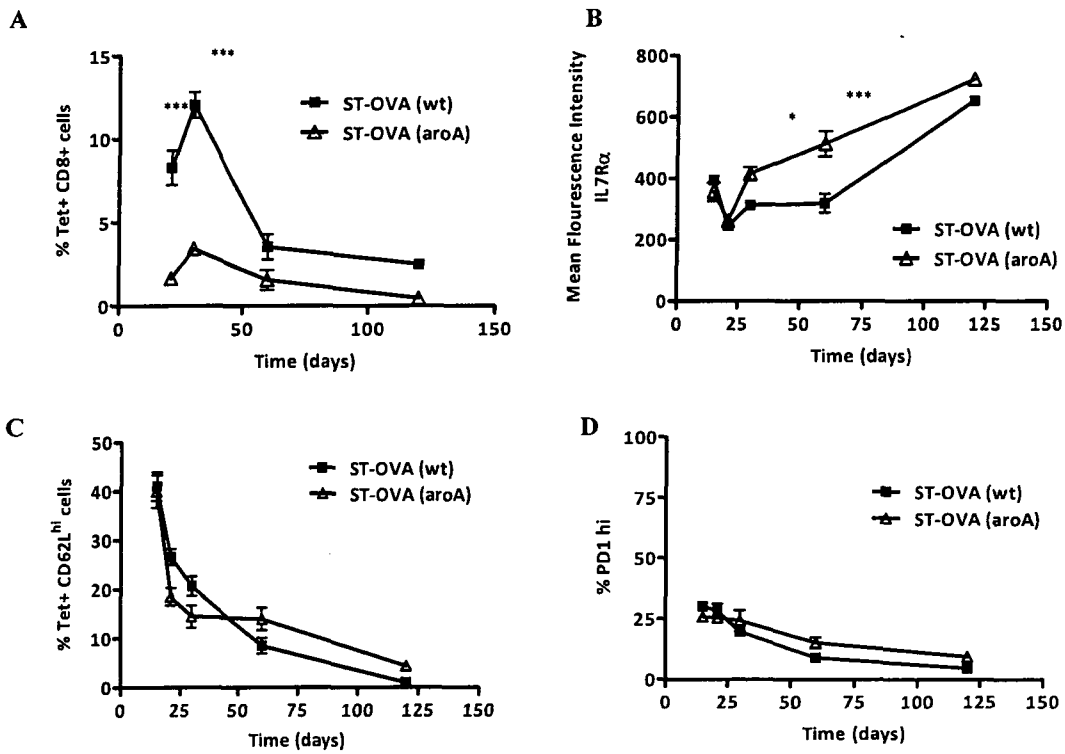
A
% Tet+ CD8+ cells
Time (days)
ST-OVA (wt)
ST-OVA (aroA)
***
***
B
Mean Flourescence Intensity IL7Rα
Time (days)
ST-OVA (wt)
ST-OVA (aroA)
*
***
C
% Tet+ CD62L^hi cells
Time (days)
ST-OVA (wt)
ST-OVA (aroA)
D
% PD1 hi
Time (days)
ST-OVA (wt)
ST-OVA (aroA)

14. Pathogen virulence influences CD8 T cell cytolytic function

Since the main function of $CD8^+$ T cells is to kill infected targets, I evaluated the cytolytic activity of $CD8^+$ T cells in response to wild-type ST-OVA and several mutants (Figure 28). This was uniquely determined *in vivo* as apposed to the more common *in vitro* CTL experiments, which are likely to be less representative, though valuable nonetheless. In short, the method utilizes differential staining to create two populations of peptide pulsed and non-pulsed cells to be introduced into previously infected mice. Those donor cells are tracked after 24 hours using FACS and the ratio of peptide pulsed to non-pulsed cells is determined. Any reduction in peptide-pulsed cells signifies the presence of functional cytotoxic $CD8^+$ T cells which can be expressed mathematically using a published formula (118). Evidently, $CD8^+$ T cells induced during wt ST-OVA exhibit minimal cytolytic function initially, supporting the notion of muted antigen-presentation early on. The cytolytic function peaks around day 30 (~95%), and only a minor loss in cytotolytic ability is observed thereafter (~85% by day 120). Increasing attenuation of ST results in reduced cytolytic activity which correlates with reduced T cell response. $CD8^+$ T cells induced in *aroA* infection display a maximum of 60% cytolytic activity on day 90, and only about 40% at the peak of infection (day 30). By day 120, activity has diminished to the levels seen on day 30. Both *ssaR* and *phoP* mutants, which are highly attenuated, induced CTLs with abrogated cytolytic activity. There is a modest 20% CTL activity measured on day 90 of infection with *ssaR* mutant, but before and beyond that time point, levels were <5%. For *phoP,* the levels were <5% throughout the duration of infection.

Figure 28. Pathogen virulence influences CD8 T cell cytolytic function.

B6.129F1 mice were infected with mutant and wiltype strains of ST-OVA, and at various time points in the cytolytic activity of T cells was evaluated using the published protocol of Barber et al. Briefly, infected mice were injected with $20x10^6$ PKH26- and 10XCFSE labeled donor B6.129F1 splenocytes that were pulsed with SIINFEKL peptide and an equal number of PKH26- and 1XCFSE splenocytes. After 24 hours, the ratio of peptide pulsed/ non-pulsed populations was determined by gating on CFSE/PKH26 positive cells using flow cytometry. Dotted line indicates expected, but unavailable data set

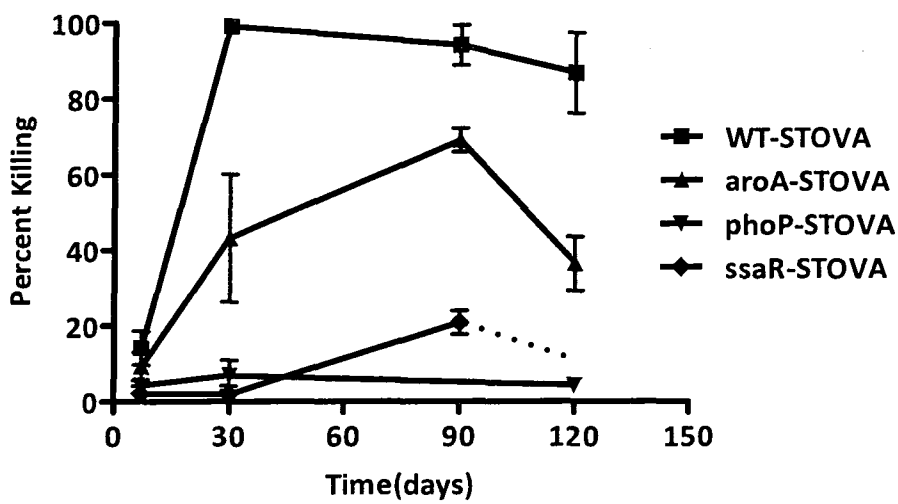
Percent Killing
100
80
60
40
20
0
0
30
60
90
120
150
Time(days)
WT-STOVA
aroA-STOVA
phoP-STOVA
ssaR-STOVA

CHAPTER IV:
DISCUSSION

IV. Discussion

1. Prelude

Antigen-presentation to $CD8^+$ T cells commences immediately after infection, which facilitates the rapid expansion of $CD8^+$ T cells, resulting in control of infection. Subsequently, the primed $CD8^+$ T cells undergo rapid and massive contraction, and only a small subset of primed cells survive as long-lived memory cells. While this is considered to be a universal paradigm, is not strictly followed during infection with *Salmonella typhimurium* (ST) (68). In this study, I have delved into the mechanisms as to why T cell response is greatly delayed during infection with ST. Using *in vitro* and *in vivo* models where antigen-presentation can be selectively measured, the results presented here offer a different perspective and indicate that poor intracellular proliferation of ST, rather than inhibition of antigen-presentation, may be the principal reason why T cell response is delayed and subdued. Furthermore, I examined how ST virulence may influence the development and function of $CD8^+$ T cells.

2. Evidence of CD8 T cell role in controlling ST infection

There is increasing evidence of the importance of $CD8^+$ T cells, otherwise known as cytotoxic lymphocytes, in controlling intracellular bacterial infections, aside from their established role in viral infections, cancer, and parasitic infection (20-24). To evaluate the importance of $CD8^+$ T cells in response to ST infection, T cells were depleted at an early and a late time point during infection. If $CD8^+$ T cells play an important role in combating ST, their depletion will exacerbate the pathology of infection.

I have demonstrated that depletion of $CD8^+$ T cells, during the chronic stage of ST infection, results in a concomitant bacterial surge in the spleen, which are otherwise undetectable at that stage of infection. This reasserts that $CD8^+$ T cells do indeed promote the control of ST in the long term. $CD4^+$ T cell depletion resulted in a greater increase in splenic bacterial burden. This suggests that $CD4^+$ T cells may play an even greater role in controlling ST. However, it is important to note that when $CD4^+$ T cells are depleted, $CD8^+$ T cell responses also decline due to the relative dependence of these cells on $CD4^+$ T cell help (42, 119, 120) (Sad et al. unpublished observations). Depletion of IFN-γ resulted in a massive surge of bacteria. Consistent with published literature, IFN-γ plays a very important role in limiting bacterial dissemination and regulating $CD8^+$ T cell homeostasis (36, 37, 121). Previously, using an oral infection route, it was shown that IFN-γ promotes the control of ST in mesenteric lymph nodes (75). Even though depletion of T cells had minimal effects early on in infection, it has been shown that they play a role in amplifying inflammatory signals, including, IFN-γ, IL-22, IL-17, macrophage inflammatory protein 2 (MIP-2), and inducible nitric oxide synthase (Nos2) in the intestinal mucosa early in infection with ST (122). Such pro-inflammatory signals are critical in promoting innate immunity against ST and the lack thereof will ultimately influence the outcome of infection and/or the onset of adaptive immunity (123). While this study supports a T cell role in controlling ST, the precise mechanisms as to how they mediate this are not clear, but may involve the expression of IFN-γ and other mediators by T cells. Interestingly, the peak of IFN-γ production by T cells is reported to coincide with the onset of bacterial elimination (82) .

3. Pathology of ST infection

Vulnerable mice strains, including C57BL/6J mice, succumb to ST infection within 7 days, even at infectious doses of 100 bacteria. On the other hand, resistant 129X1SvJ mice harbor a chronic infection lasting 60 days. This has been attributed to the function of the NRAMP1 gene (69). This gene codes for an ion transporter that helps in depleting phagosomes of critical ions, such as manganese and iron, and thereby making the phagosome environment more hostile. A cross between C57BL/6J and 129X1SvJ mice was generated (B6.129F1), which combines the benefit of NRAMP expression and B6 background. In this manner, it was possible to use these mice in adoptive transfer models using OT1 mice which are also of a B6 background. Furthermore, to determine bacterial proliferation *in vivo*, the spleens of infected mice were isolated at various points throughout the infection and whole spleen cell suspensions were plated on BHI agar plates. Bacterial counts were determined and plotted as a function of time.

B6.129F1 mice harbor a chronic ST infection resembling their parental counterpart that peaks in the spleen around day 25-30 and is undetectable by day 60-90. By comparison, LM results in an acute infection that peaks 2-3 days post infection and is rapidly cleared to undetectable levels by day 5. Unlike LM, ST infection is characterized by substantial splenomegaly and splenocyte numbers can reach over 800 million from a normal 100 million or less. However, based on the depletion experiments, ST manages to hide in small numbers possibly else where in the body and resurfaces when the host is compromised. Depletion of T cells and IFN-γ resulted in massive surge of bacteria otherwise undetectable in the spleen. Monack and colleagues have shown that even one year after oral infection of mice with a high dose of virulent ST, bacteria were found in

the mesenteric lymph nodes (MLN)(75). It is difficult to ascertain whether the plateau in bacterial growth seen in the chronic stage of infection represents a static equilibrium in which bacteria are slowly or hardly increasing in number, or whether it represents a dynamic equilibrium in which bacteria are rapidly killed while rapidly multiplying. This is a very important concept because it directly determines the amount of antigen available for APCs to present. Importantly, one group has described *Mycobacterium tuberculosis*'s *in vivo* growth as "static" (124). This bacteria has a lifestyle that is very similar to that of ST, including phagosomal residence and chronic infectivity (125). Therefore, it might be useful to keep those observations in mind as ST infection and *in vivo* proliferation is elucidated herein.

4. Delayed mobilization of $CD8^+$ T cells during ST infection

My research was focused on elucidating the $CD8^+$ T cell response against ST while critically evaluating the documented inhibition of antigen presentation by ST. A unique feature of this study is the side-by-side comparison of ST to the well-studied, also intracellular pathogen, *Listeria monocytogenes*. This is important because conclusions about ST-specific response and bacterial propagation have to be drawn in relative terms and using proper controls. A hallmark of a good CD8 T cell activation is IFNγ production (36, 82), which as demonstrated in the depletion experiments, plays a crucial role in limiting bacterial growth. I used the ELISPOT assay to quantify the frequency of IFNγ-secreting cells responding to LM-OVA or ST-OVA infection. A significant delay in the expansion of effector, OVA-specific $CD8^+$ T cells in response to ST-OVA infection is observed, at which time those mounted against LM-OVA are already undergoing

contraction. In addition, whereas the numbers of IFN-γ producing cells declined in coincidence with LM-OVA elimination, those mobilized in ST-OVA infection did not undergo contraction by day 60 at which point bacterial numbers are significantly reduced. This hints at a further delay in the contraction stage in the case of ST infection. Next, I investigated whether the delay in T cell mobilization against ST is due to inhibition of antigen-presentation, or whether the antigen presentation machinery is intact but antigen levels are suboptimal.

5. Antigen presentation in response to ST infection

Numerous studies have reported that ST selectively inhibits antigen presentation as a major constituent of its virulence; however the mechanisms surrounding these assertions are largely elusive. Using OVA as an immunodominant antigen model and adoptive transfer (Figure 5), I wanted to determine whether $CD8^+$ T cells can be primed as a result of infection with ST.

It is evident that there is no measurable OVA presentation *in vivo*, even at day 5 post-infection with ST despite the presence of over 20,000 bacteria in the spleen. Early T cell priming is a prerequisite for efficient T cell activation and pathogen clearance(67, 126-128). By contrast, LM-OVA infection resulted in extensive T cell priming and division as measured by CFSE dilution(96). Furthermore, the proportion of donor OVA-specific T cells is expected to increase relative to the whole $CD8^+$ T cell population upon activation and multiplication. This is indeed the case during LM-OVA infection, but no such increase is observed with ST-OVA.

I further tested the antigen presentation paradigm in a controlled *in vitro* model (Figure 6). This model ensures that the same numbers of bacteria are delivered to the preferred host cells, namely macrophages and dendritic cells. Gentamicin is the antibiotic of choice in the elimination of extracellular bacteria due to its low-penetration properties, meaning that it will not accumulate in the cells and therefore will not interfere with intracellular propagation(129, 130). Again, ST-OVA fails to induce measurable antigen presentation *in vitro*. The same held true even when 100 bacteria are used for every one cell, and up to nine days post infection. By referring to the loading calibration plot (Figure 7), it can inferred that even at an MOI of 1, there is 0.01 nmol of OVA peptide being produced, which is 2 fold higher than the EC50 of 0.005 nmol. By contrast at the highest tested MOI of ST-OVA (100 MOI), < 0.001 nmol of OVA is generated; which is 5 fold lower than the EC50 and therefore not enough to prime CD8 T cells. These results indicate that reduced intracellular antigen levles may be the main reason why antigen-presentation is delayed and muted during infection with *Salmonella*.

6. ST fails to induce antigen presentation in dendritic cells

Literature has shown that cross-presentation of ST antigens occurs through dendritic cells (91), and was proposed to be the primary mechanism by which T cells are primed. Cross-presentation occurs intermittently when infected macrophages die and dendritic cells pick up cellular debris and foreign antigen and incorporate it into the MHC1 pathway. Studies have shown that under SPI-1 inducing conditions, ST induces rapid apoptosis of infected macrophages, facilitated by the factor *SipB*. Furthermore, in the absence of Caspase-1 activity or under SPI-2 inducing conditions, macrophage death is greatly delayed (74). I

was curious as to whether ST-infection of dendritic cells, the quintessential antigen-presentation cell type, might result in enhanced OVA presentation. Nevertheless, at all multiplicities of infection tested, ranging from 0.1 to 10, antigen-presentation to $CD8^+$ T cells was undetectable by the CFSE dilution method described.

7. ST fails to inhibit LM induced antigen presentation

If ST indeed inhibits antigen presentation, could it disrupt nascent antigen presentation induced against LM-OVA? I wanted to test this theory by co-infecting cultured macrophages with ST and LM and determining whether T cell priming still proceeds normally. Curiously, ST fails to halt LM-OVA induced antigen presentation, and also fails to inhibit antigen presentation when peptide is loaded externally. Upon more thorough experimentation, it was observed that infection of macrophages with very high MOIs of ST resulted in significant "inhibition" in antigen presentation. 80% of OT1 $CD8^+$ T cells divided in response to OVA presentation by LM-OVA infected cells, even when co-infected with low to intermediate MOIs of ST, but only 10% divided at high ST MOIs. However, it was revealed that in those scenarios, there is a significant reduction in the numbers of intracellular LM bacteria which suggests that ST somehow interfered with LM uptake and/or invasion. No such trend was observed in ST CFUs as a function of LM-OVA co-infection. Notably, ST interference with LM uptake does not seem to be a result of bacterial inhibition, since colonies of both bacteria can grow side by side on BHI agar. Therefore it was concluded that the apparent inhibition of antigen presentation by LM-OVA infected APCs, when high MOIs of ST were used, was due to reduced

intracellular numbers of LM-OVA and not due to active inhibition of antigen presentation by ST.

One might argue that the reduction in LM CFUs when high levels of ST are co-administered is due to reduced cell viability as a result of overwhelming bacterial load. Visually, very little cell death is observed, but to ascertain this observation I performed two reliable cytotoxicity assays 24 hours post co-infection. In MTT assays, yellow MTT is reduced to purple formazan by mitochondrial enzymes thereby giving a colorimetric measurement of mitchondrial activity. Neutral red, on the other hand, is a vital dye that is taken up by live cells and stored in the lysosmal compartment. Reduced cell viability results in loss of lysosomal integrity and therefore reduced dye uptake.

Using MTT assay, it is evident that there is no apparent reduction in cell viability. On the contrary, there seems to be slightly higher mitochondrial activity at higher co-infection doses, hinting that cells are more metabolically active. The neutral red uptake trend is virtually identical whether or not LM-OVA is present during ST infection, meaning that addition of LM did not change viability status of ST infected macrophages. Therefore, it can be concluded that the observed reduction in LM load at high ST MOIs is not due to reduced cell viability.

8. Do mutations in SPI-1 and SPI-2 enhance antigen presentation?

I documented two seemingly contradictory observations so far. First, ST infection does not yield any measurable antigen presentation, which is supposedly due to ST's inherent capacity to inhibit antigen presentation. Second, introduction of ST into the LM infection formula, did not result in inhibition of LM induced antigen presentation, contrary to what

one may expect. The next step was to test a selection of ST recombinants, mutated in key virulence genes, *in vivo* and *in vitro*, to determine whether the presumed suppression of antigen-presentation can be alleviated. A panel of mutants was created mutated in key SPI-1 and SPI-2 genes. SPI-1 is active in the acute phase of infection whereas SPI-2 is absolutely necessary for intracellular propagation and systemic persistence (131). Is the presumed inhibition of antigen presentation SPI-1 or SPI-2 restricted?

In mice, infection with these mutants did not result in any increase in the number of dividing, OVA-responsive $CD8^+$ T cells and therefore, no enhancement of antigen presentation. The infectious dose of the different mutants was successfully varied to match that of wildtype ST *in vivo* burden, to insure that any differences, or lack there of, are not due to the inherent reduced bacterial burden of the mutants. Even the highly attenuated strains *phoP* and *ssaR* did not induce any antigen presentation. It would expected that the lack of *phoP*, the master regulon that orchestrates the events of SCV formation and sustenance, would result in a massive boost in antigen presentation. Likewise, lack of *ssaR* a structural component of TTSS can result in reduced delivery of virulence factors and therefore is also expected to result in a boost of antigen presentation. Neither mutant results in a significant increase in T cell priming as determined by CFSE dilution method. The mutant *invA* behaves similarly to wild type, since it is only mildly attenuated. This is because it is defective for invasion via the oral route, but since it is used intravenously, it was interesting to see if SPI-1 has any substantial influence on antigen presentation. Infection with *invA* did not result in increased presentation to CD8 T cells. The naturally occurring strain *aroA* resulted in miniscule presentation to T cells *in vivo*, but not *in vitro*. In that case however, the burden

of *aroA* was 10 fold higher than wild type at the dose selected and therefore there was more antigen for the number of T cells present. However, when the ratio of donors to total T cells was determined, it was evident that antigen specific T cells did not increase in number in response to *aroA* infection, suggesting the reduction in CFSE could be non-specific. The strain *aroA* is documented as a good vaccine candidate (95) nonetheless, especially because it does not result in the severe inflammation and splenomagly observed in the case of wild type. These results were recapitulated *in vitro* with the same outcomes. In fact, the lack of antigen presentation was more evident, which was true of all the mutants as well as SL1344 (wild type strain) . The mutant *sifA*, which lacks structural proteins important in preserving SCV integrity (6), was also used. The result of this mutation is bacterial release into the cytoplasm. If the localization of ST in the phagosome affects antigen-presentation negatively, infection with this mutant should enhance antigen presentation. Furthermore, *sifA* was reported to be a key factor in the inhibition of antigen presentation! {{32 Brumell,J.H. 2001}}. Therefore, it can be concluded based on this representative panel of mutants that secreted virulence factors and/or phagosomal residence are not the culprit behind the evidently deficient antigen presentation during ST infection. This is in sharp contrast to what many have reported in the literature (13, 14, 132).

9. An alternative explanation: ST exhibits poor intracellular proliferation

Intracellular proliferation has been shown to be a prerequisite for proper antigen presentation and T cell activation in LM infection (133-135). Logically, bacterial proliferation directly affects antigen abundance, and therefore, antigen presentation. If

bacterial proliferation affects antigen presentation, is it possible that ST proliferates poorly in the intracellular compartment? I investigated this using my proposed *in vitro* model (Figure 6) that insures the strict evaluation of intracellular bacteria only. Infected cells were lysed at different time points and aliquots plated on BHI plates. Remarkably, ST-OVA displayed significantly reduced intracellular proliferation when compared to LM-OVA. It took 8 hours for ST to double in numbers intracellularly, versus 2.4 hours for LM. This is intriguing since the proliferation behavior of these pathogens is reversed in liquid broth where ST doubles every 38 minutes whereas LM 55 minutes!

I questioned whether the activation state of macrophages might affect proliferation of ST. Macrophages were therefore activated by overnight stimulation with *E.coli* LPS and subsequently infected with ST. The result is again the same low proliferation rate previously observed, the only difference being the number of bacteria to initially enter the cells. This is to be expected because activated macrophages are more efficient at scavenging bacteria (105, 136).

There have been an increasing number of reports emphasizing the slow proliferation rate of ST in the intracellular compartment (108-111). It appears most of the replication by Salmonella is actually undergone extracellularly, and recent work done by this group supports the notion that the perceived splenic bacterial burden is not intracellular at all (unpublished data). Furthermore, it is reported that while ST numbers increase *in vivo*, so does the number of infected macrophages, with the net numbers of ST per cell remaining low (2). Also, the infected macrophages seem to reside in distinct loci (pathological lesions) with distinct salmonella populations. These loci give rise to daughter loci as apposed to merely increasing in size (2). A revised view emerges regarding proliferation

of salmonella *in vivo*, and that is, despite the massive perceived replication of salmonella, intracellular numbers remain extremely low suggesting that its growth occurs in fits and starts, with extracellular bacteria amplifying net numbers, and intracellular bacteria contributing to chronicity and persistence.

10. Bacterial mRNA levels reassert poor intracellular proliferation of ST

I therefore determined that ST proliferates poorly in the intracellular compartment, but as a further confirmation, I proceeded to measure the amount of OVA produced during infection. Initial efforts using Western blot methodology failed because the quantities were under the sensitivity threshold (unpublished data). Alternatively, mRNA expression was quantified using real-time PCR. Even though mRNA levels do not necessarily reflect protein levels, it is nonetheless indicative of bacterial metabolism and replication.

The expression of OVA in the recombinant bacteria used herein was confirmed by performing rtPCR on liquid BHI grown bacteria. All the bacteria produced adequate and similar levels of OVA (Figures 14 and 20). To assess intracellular antigen levels, 16S rRNA and OVA expression in 24 hour ST-OVA- or LM-OVA-infected macrophages were determined. 16S rRNA is used as a positive control since its expression follows bacterial proliferation closely (137-140). In agreement with antigen presentation data, OVA expression in 24 hour ST-OVA infected macrophages was 1000-fold less than that of LM-OVA infected cells. Indeed, 16S rRNA profiles correlated with intracellular bacterial levels at 24 hours post infection. Furthermore, when OVA expression was normalized to 16S, there was still a 2-fold edge for LM-OVA versus ST-OVA.

Determination of mRNA levels *in vivo* proved very difficult considering the challenge of targeting an organism (the bacteria) within another organism (the host mouse). Furthermore, both bacteria are intracellular, and optimal infectious doses for the purposes of rtPCR, specifically using SYBR green methodology used in this study, were shown to be 10^4 CFUs previously (93). I was restricted to a maximum ST infectious dose of a 10^3 CFUs, because higher doses resulted in mice fatality. Nonetheless, I was able to extract some useful observations from those *in vivo* data. Again, the pattern of 16S rRNA expression in infected spleens correlated very well with splenic bacterial burden. Only at the peak of infection was OVA expression visible, and only in the case of LM-OVA. The numbers of detectable OVA RNA molecules was modest at best, again because of the inherent limitation of the experimental parameters. It is important to note that even though ST-OVA CFUs at the peak of infection are several folds higher than those of LM-OVA, the expression level of 16S rRNA for ST-OVA remains over 10 fold lower than that of LM-OVA at its peak. I suspect that this is not an artifact of experimentation but actually a key observation that may hint to an inherent and programmed down regulation of ST metabolism while in the chronic stage. Massive metabolic shift down by ST has been reported in the literature (108). Measured splenic bacterial burden cannot be regarded in absolute terms. This means that measured CFUs at any time point provide only a "snap shot" of what is happening during infection. It does not explain whether bacteria are dying, growing, or static, even without further complicating the picture with immune system involvement (124). Those mRNA data recapitulate the aforementioned observations regarding ST's poor intracellular growth and they forecast a significant

immune challenge; that is suboptimal antigen levels and the consequential deficient antigen presentation.

11. Surface pMHCI levels correlate with reduced antigenic load in ST infection

As an alternative to measuring mRNA levels, I was able to utilize a unique antibody that targets MHCI molecules only when loaded with SIINFEKL peptide. Therefore, using flow cytometry the frequency of H-2K^b-OVA$_{257-264}$ complexes on the surface of infected cells can be easily determined. This in turn reflects the extent of antigenic load. Henrickson et al have shown that a threshold antigenic dose is required before T cells can transition from T Cell/DC scanning, to sustained interaction and subsequent activation. Other factors included DC density and antigen affinity (141). Furthermore, it has also been shown that the magnitude of T cell response is largely affected by the antigenic dose (67).

In this study, infection with ST-OVA or any of the mutants did not result in significant elevation in the numbers of H-2K^b-OVA$_{257-264}$ complexes, all of which resided in the sub-optimal levels. LM-OVA by contrast, did induce a significant increase in numbers of complexes. Using external loading of the peptide, I was able to extrapolate that LM-OVA infection results in approximately 10 nmol of peptide, whereas that of ST-OVA or its mutants was in the 0.01-1 nmol range which in essence constitutes the noise region. It is worth noting that this peptide titration curve remarkably overlaps the one generated by the antibody (25D1.16) developer (142). These results are in line with my prediction regarding the reduced antigenic load during ST infection as a direct result of its slow intracellular proliferation. Furthermore, given that infection with the mutants resulted in

pMHCI levels comparable to that of wild type ST, the previous argument against the involvement of virulence factors in inhibition of antigen presentation holds unabated.

12. Pathogen virulence influences CD8 T cell burst size and memory phenotype

For T cell studies, I primarily compared the CD8 T cells' response against wildtype ST-OVA to that of *aroA*-OVA. The idea was to determine whether pathogen virulence influenced T cell development, and *aroA* being an attenuated strain made it an ideal candidate.

First, the endogenous response was assessed by determining the frequency of IFNγ producing $CD8^+$ cells mobilized against infection with either strain. ST virulence significantly influenced the burst size of $CD8^+$ T cells. There was over a 200 fold increase in the numbers of OVA specific T cells at the peak of ST-OVA infection. In comparison, there was a progressive "accumulation" of T cells against *aroA* infection, with no conspicuous contraction stage. This accumulation is consistent with the accumulation of memory cells documented in literature (143). After the contraction phase the numbers of IFNγ producing cells is consistently 2 folds or more higher for aroA versus wild type infection. This observation is in favor of the adoptive transfer experimental data (to be discussed shortly) as *aroA* infection results in seemingly higher numbers of central memory cells. One can argue that the ELISPOT assay involves the culturing of cells *in vitro* for 48 hours and central memory cells, which have a superior regenerative potential are favored under these conditions. Therefore any difference in the numbers of IFNγ producing cells between the two infections might be masked by the

differences in memory subtype generated for both. This naturally leads to the need to examine the phenotype of CD8+ T cells mounted during those infections.

The adoptive transfer model is a method that is well-characterized and readily used in literature to "amplify the signal" of the immune response that is otherwise difficult to visualize. Using tetramer technology I was able to track the proliferation and behavior of donor OT1 $CD8^+$ T cells that express T-cell receptor Vα2 specific to OVA peptide 257-264 (SIINFEKL) produced by recombinant ST(98). The expression of various markers of interest, using flourophore conjjuagted antibodies and flow cytometry, was also evaluated. In all, this will help determine the phenotype and magnitude of antigen specific $CD8^+$ T cell response.

As previously, the infectious dose of *aroA* was elavated to parallel splenic bacterial burden of wild type so that any differences are not attributable to reduced *aroA* burden. In blood, the magnitude of OVA specific $CD8^+$ T cell response was markedly reduced in *aroA* infection, though peaked earlier on day 21 compared to wild type. At the peak of infection, the percent tetramer positive cells were 20% and 5% for wild type and *aroA* respectively, which suggests that virulence influences burst size. More notably, *aroA* infection resulted in significantly higher expression of the memory markers IL7Rα and CD62L, at the later stages of infection. It has been shown that wild type ST infection results in predominantly effector memory populations (68). Since central memory is the primary memory pool, and as some believe, the pool from which effector memory is generated, one can argue that there is an enhancement in memory development as a result of decreased inflammation characteristic of *aroA* infection. This could be due to increased APC to T cell density ratio, which has been reported to influence APC/ T cell

interactions (141). Massive splenmegaly can be viewed as an impediment to adequate priming, since the number of hits a T cell receives is logically reduced, and proper priming translates into proper memory formation as discussed previously.

In the spleen, a significant difference in antigen specific CD8 T cells in response to either infection is again observed, with both peaks visible on day 30. These numbers are slightly less than what was observed in blood which can be attributable to splenomegaly and the fact that activated T cells leave the lymphoid organs and target the periphery to ensure the infection is universally controlled (144, 145). There was an instantaneous down-regulation of CD62L on the surface of antigen specific cells coinciding with the newly acquired homing properties of activated T cells. The divergence observed in CD62L expression in the blood in response to *aroA* and wild type infection at the memory stage is not as conspicuous in the spleen despite it being consistently 2 fold higher at the latter stage of infection with *aroA*. The IL7Rα profile however is distinctly different, with aroA responsive $CD8^+$ T cells expressing significantly higher levels of IL7Rα again hinting at a better memory pool development. Another marker that was investigated is PD-1 (programmed death receptor-1) whose higher expression has been directly correlated with T-cell exhaustion in chronic viral infections (117, 146). The PD-1 profile in both infections was virtually identical suggesting, at least, that virulence does not influence the expression of that molecule. More experiments comparing expression levels due to LM versus ST infection may be useful, but generally the highest levels of PD-1 observed was early on in both infections, and only in 25% of the OVA specific CD8 T cells pool. It has been suggested that Treg cells express higher levels of PD1 ligand and therefore regulate the antimicrobial T cell response (147). It can therefore be concluded that the magnitude

of the CD8 T cell response is contingent upon the extent of ST virulence. Furthermore, $CD8^+$ T cell response against virulent ST displays a prolonged and persistent effector-memory phenotype, whereas that against attenuated mutants display reduced numbers of effector-memory cells, which is in agreement with previous findings (94)

13. Pathogen virulence influences cytolytic function of cytotoxic lymphocyte

If pathogen virulence influences the magnitude and phenotype of responding CD8 T cell population, what are the effects, if any, of pathogen virulence on T cell cytolytic function?

I answered that question using a robust *in vivo* technique originally developed by Barber et al (118). In this method, the cytolytic function of endogenously derived antigen specific cytotoxic lymphocytes against a donor population pulsed with antigen is determined efficiently. This method is far superior to *in vitro* cytotoxicity assays because it is representative of real infections, during which cells encounter a plethora of signals, in both, micro- and macro- contexts.

At the peak of response during wildtype infection there is almost 100% effective killing of OVA flagged cells, *in vivo*. This activity remains fairly high (~90%) even at day 120 post infection. There is significantly less activity in the case of *aroA*-OVA infection that peaks only at 65% around day 90 and drops immediately to peak infection activity (40%) by day 120. An "accumulation" of memory trend is again observed with *aroA* infection. One can argue that the difference in cytolytic function of T cells during wild type and *aroA* infections are primarily due to the difference in memory pools generated. Wild type ST yields predominantly effector memory cells which have been reported to be more

efficient at cytolytic function as apposed to centrals (47). The mutant *ssaR*-OVA results in really low levels of cytolytic activity that peaks at day 90 at 20% and therefore displaying a similar accumulation pattern to *aroA*, whereas *phoP* infection results in miniscule levels of cytolytic activity. Indeed, it was shown previously that there is a general skewing towards a more central memory phenotype with increased attenuation of those identical mutants(94). These data corroborate the fact that an immune response, though significantly delayed and arguably inefficient, is ultimately mounted against Salmonella, and that pathogen virulence significantly influences T cell function. This will fundamentally influence the endeavors geared towards vaccine design and cell therapy.

CHAPTER V:
CONCLUSIONS

V. Model, future aims and conclusions

1. Model

In this study, I presented some unique and arguably controversial data. According to many studies, the dominant ingredient in salmonella virulence is its active inhibition of antigen presentation by host cells. As cited previously, many groups believe that this inhibition is attained by means of secreted virulence factors that interfere with normal antigen presentation machinery (13, 14, 132). The precise mechanism of inhibition is still at large, but one group implicated the *yej* operon in this process (148). The problem with this study is that they primarily measured enhancement of antigen presentation in terms of IL-2 secretion, and the increase in tetramer positive cell numbers was modest at best (1.1% peak from 0.2% baseline) (148). Furthermore, they used a different strain of ST (CS093) as apposed to the more commonly-used SL1344 virulent strain. T cell priming is a complex and intricate program of short brief contacts between T cells and APC followed by long stable interactions that lead to full fledged T cell activation (141). Thus, T cell division and proper function are ultimately the true measure of proper priming, and hence why CFSE-dilution was used to measure priming-induced cell division in this study.

The data presented here are in agreement with some emerging hypotheses that attribute the reduced antigen presentation during ST infection to poor intracellular proliferation of this bacterium (108-111). I have established that the massive bacterial growth observed during Salmonella infection is not occurring in the intracellular compartment. It is easy to misconstrue the lack of antigen presentation as due to active inhibition, when one believes that Salmonella's massive burden originate intracellularly. That would imply the

availability of ample amounts of antigen for processing via the MHCI pathway. Therefore, the new emerging view of Salmonella infectious cycle involves the invasion of macrophages to establish a niche in the phagosome, or more aptly, the salmonella containing vacuole (SCV) (Figure 29). This niche insures the sequestration of Salmonella away from the surveillance of the immune system (108, 149). In addition, the down regulation of bacterial metabolism (108) and reduced intracellular growth (108-111) translates into the hijacking of host cells without allowing them to commit to apoptosis immediately (74) and insures markedly reduced antigenic load. It has also been shown that the change in numbers of infected phagocytes parallels the rate of salmonella multiplication and that the numbers of intracellular bacteria remains very low (1-12 bacteria) (123, 150). More importantly, it has been recently shown that Salmonella stochastically escapes its host cell and disseminate to other uninfected cells in order to multiply and persist (150). Grant et al propose that this process of escape is not in the form of release of free bacteria but rather whole bacteria within apoptotic blebs, insuring the "silent" transfer of bacteria to new host cells (150). I believe that bacterial dissemination possibly occurs via this route, as well as in the form of free bacteria. When macrophages were purified from infected spleens, it was shown that most of the bacterial burden observed is not intracellular, indicating that some extracellular growth must occur or that most bacteria are released into the extracellular compartment (Sad et al. unpublished data). Furthermore, it has been shown that salmonella induces a unique caspase-1 dependent necrosis (151) which, along with apoptosis, explains how intracellular antigen is released to be picked up by bystander DCs and cross-presented (91, 152) (Figure 29). Necrosis may also occur due to secreted ST toxins (153, 154).

Alternatively, antigen presentation can occur by infected macrophages, though not as efficiently as DCs (54), but only when bacterial numbers intracellularly are high, which is a rare occurrence (150).

Despite the documented evidence implicating DCs in cross priming of ST antigen, I suspect that this occurs under unfavourable conditions (Figure 29). In addition to antigen paucity, ST modifies its own LPS to make it less inflammatory. LPS stimulates DCs to mature and enhance their activity (155), and cross presentation was shown to favor ubiquitous antigen (56). This may further impact the development of $CD8^+$ T cells, and may further explain why this process is delayed and skewed toward effector memory. It is has been established previously that antigen persistence influences memory development (156).

Taken together, the preceding ideas can account for the delayed priming of $CD8^+$ T cells during infection with ST. This is because antigenic load is low, the preferred host – the macrophages – is not a great antigen presenter, and finally, the release of antigen due to apoptosis is stochastic and therefore cross-presentation by DCs is suboptimal (Figure 29).

Figure 29. Proposed ST infection model

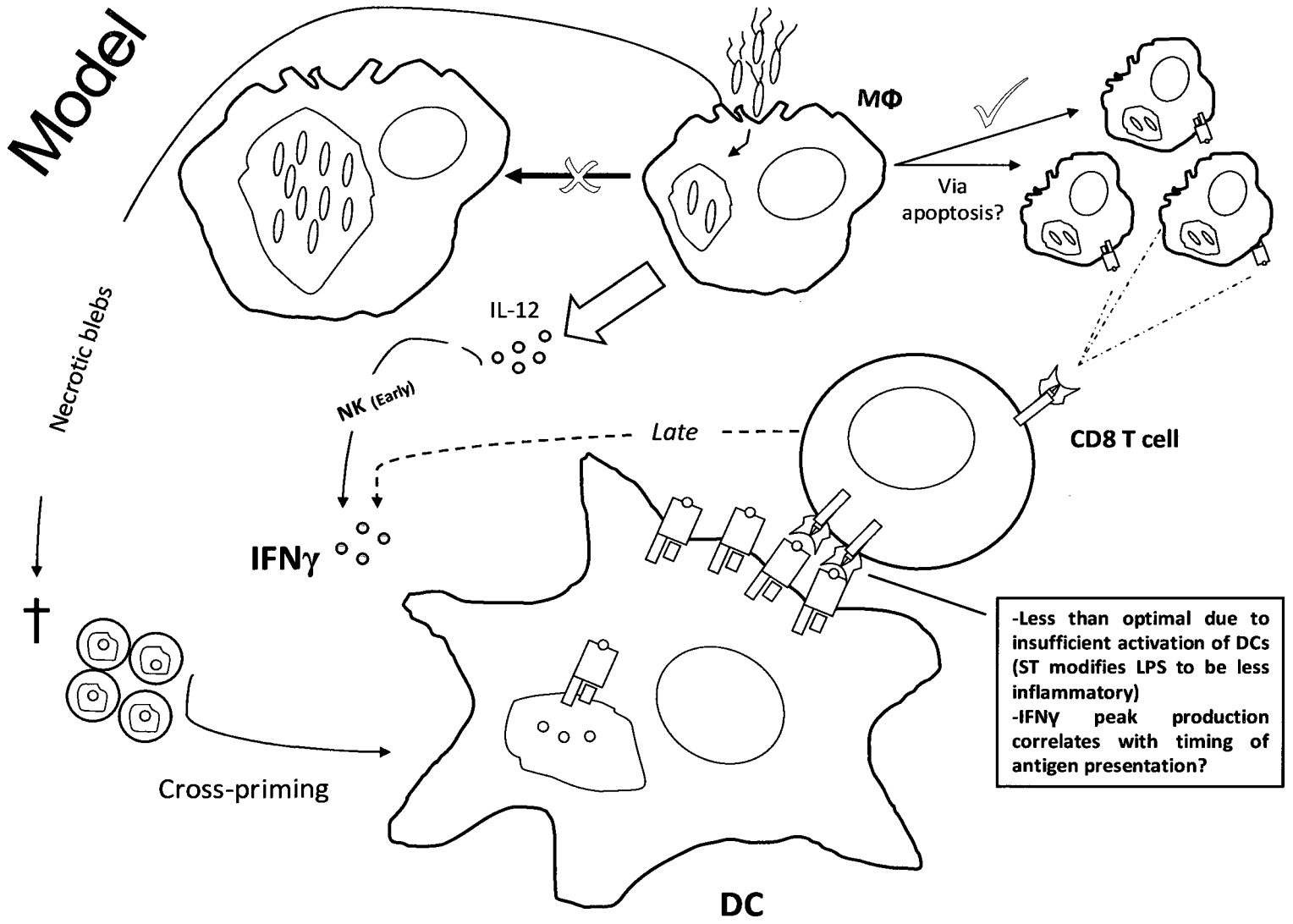
Model
Necrotic blebs
MΦ
Via apoptosis?
IL-12
NK (Early)
Late
CD8 T cell
IFNγ
Cross-priming
DC
-Less than optimal due to insufficient activation of DCs (ST modifies LPS to be less inflammatory)
-IFNγ peak production correlates with timing of antigen presentation?

2. Future directions

In order to provide further evidence for my hypothesis regarding slow intracellular growth of ST, it might be useful to extensively purify macrophages from infected spleens, and determine their bacterial content. This will establish intracellular bacterial numbers with certainty and with a simple cell count one can determine the bacterial numbers per cell. Furthermore, antigen expression levels in those purified macrophages can be determined using real-time PCR.

Since rtPCR enumeration of OVA expression proved to be challenging using SYBR green methodology, it might be valuable to attempt the procedure using TAQ MAN methodology. This procedure is much more robust compared to SYBR green given that it involves sequence specific DNA probes. Alternatively, nested PCR can be performed to amplify sequence within OVA sequence thereby significantly improving the signal to noise ratio.

To determine the precise timing of antigen presentation during ST infection, if any, it is essential to use the described *in vivo* antigen presentation model at later time points in ST infection. This is important to determine whether antigen presentation is merely delayed, or whether the cumulative sum of "silent" antigen presentation events contribute to the eventual mounting of ST-specific CD8 T cell response.

Finally, using standard intracellular staining methodology, and antibodies specific to $H2K^b$, it can be confirmed that antigen load is in fact reduced and not due to interference with pMHCI export to the surface of the cell.

3. Conclusions

I have determined that the Induction of $CD8^+$ T cell response against ST-OVA is greatly delayed and that this is due to muted antigen-presentation. This absence of early antigen-presentation is not due to the expression of various virulence genes of ST as none ofthemutants of ST used in this study induced rapid antigen-presentation *in vivo or in vitro*. In fact, poor antigen presentation is a result of poor intracellular proliferation of ST and suboptimal antigenic load as corroborated by my data and suggested by others (108-111). Theories backed by some tentative data, including the ones presented herein, all suggest that ST suppresses its own metabolism and growth (108) as it establishes its niche in the phagosome of macrophages and some other cell types. The massive numbers of bacteria seen in the spleens of infected animals, in addition to splenomegaly, might be considered incompatible with those observations. However, I and others believe that salmonella actually replicates by quickly disseminating to new host cells and multiplying intracellularly only a few folds (2-3 fold) (150). The increase in number of infected macrophages as number of ST increase (123, 150) is consistent with this hypothesis. In addition, new data in this lab strongly suggest that at any one point during infection most bacteria are actually extracellular. Whether ST replicates extracellularly *in vivo* is yet to be determined, but is conceivable given that it is a facultative-intracellular pathogen. Overall, it can envisioned that there are specialized populations of bacteria present *in vivo*, some contributing to chronicisty by hiding intracellularly and spreading to new host cells, while others preoccupy and manipulate the immune system extracellularly promoting the overall persistence of bacteria. I have indicated that ST is capable of

manipulating migration patters of cells (8), inhibiting T cells directly (132), and stimulating release of cytokines (157).

The magnitude of $CD8^+$ T cell response correlates directly with the virulence of ST. Infection of mice with virulent ST induced increased numbers of OVA-specific $CD8^+$ T cells. On the other hand, the attenuated strain *aroA*, which exhibits poor growth *in vivo*, induced reduced numbers of OVA-specific $CD8^+$ T cells. This trend held true even when the infectious dose of *aroA* was increased to match the burden seen in wild-type infection. This was previously demonstrated using the other mutants described in this study (94). Furthermore, $CD8^+$ T cells against virulent ST displayed a prolonged and persistent effector-memory phenotype; $CD8^+$ T cells against *aroA* displayed slightly reduced numbers of effector-memory cells, suggesting that pathogen virulence may influence the differentiation program of $CD8^+$ T cells. Analogous observations – using the other mutants – have also been reported, showing a progressive skewing towards a central memory phenotype of $CD8^+$ T cells, with increased attenuation of ST strain used in infection (94). In addition, the extent of virulence was also found to influence the *in vivo* cytolytic function of cytotoxic lymphocytes mounted during infection. Virulent ST induces far superior CTLs compared to *aroA*, *ssaR*, and *phoP*. I propose that this discrepancy is mostly due to differences in memory populations induced by different strains, given that effector memory $CD8^+$ T cells have been shown to have superior effector function versus the more regenerative specialization of central memory cells. Taken together, these results indicate that the delayed activation of $CD8^+$ T cells during infection with ST is mainly due to reduced antigenic load which is a consequence of poor

intracellular proliferation of ST, and that pathogen virulence influences the differentiation program of $CD8^+$ T cells.

This study aimed to elucidate the mechanisms leading up to the delayed activation of $CD8^+$ T cells during infection with Salmonella Typhimurium, and how this bacterium influences the programming of those cells. There is a clear indication that muted antigen presentation is inherently "pre-packaged" with ST infection, which was attributed to its poor intracellular proliferation rate. Whether this is a programmed process, or a side-effect of phagosomal residence is yet to be determined, but is more likely to be the former since the mutant *sifA* which resides in the cytoplasm neither improved T cell priming nor antigenic load. Despite these limitations, an ST specific $CD8^+$ T cell response, though immensely delayed, is mounted whose cytolytic function is seemingly intact. Furthermore, infection with the vaccine candidate strain *aroA* results in enhanced central memory formation, which might be perceived as an improvement, but comes at a cost of compromised cytolytic function. Such information will prove very useful in vaccine development and therapy tailoring efforts specifically targeting Typhoid disease in humans, and more universally, improving our understanding in the area of $CD8^+$ T cell response in the field of immunology.

REFERENCES

1. Raupach, B. and S. H. Kaufmann. 2001. Immune responses to intracellular bacteria. *Curr. Opin. Immunol. 13: 417-428.*

2. Mastroeni, P. and M. Sheppard. 2004. Salmonella infections in the mouse model: host resistance factors and in vivo dynamics of bacterial spread and distribution in the tissues. *Microbes Infect. 6: 398-405.*

3. Cossart, P. and A. Toledo-Arana. 2008. Listeria monocytogenes, a unique model in infection biology: An overview. *Microbes Infect.*

4. Ohl, M. E. and S. I. Miller. 2001. Salmonella: a model for bacterial pathogenesis. *Annu. Rev. Med. 52: 259-274.*

5. Jones, B. D. and S. Falkow. 1996. Salmonellosis: host immune responses and bacterial virulence determinants. *Annu. Rev. Immunol. 14: 533-561.*

6. Brumell, J. H., C. M. Rosenberger, G. T. Gotto, S. L. Marcus, and B. B. Finlay. 2001. SifA permits survival and replication of Salmonella typhimurium in murine macrophages. *Cell. Microbiol. 3: 75-84.*

7. Swanson, J. A. and S. C. Baer. 1995. Phagocytosis by zippers and triggers. *Trends Cell Biol. 5: 89-93.*

8. Zhao, C., M. W. Wood, E. E. Galyov, U. E. Hopken, M. Lipp, H. C. Bodmer, D. F. Tough, and R. W. Carter. 2006. Salmonella typhimurium infection triggers dendritic cells and macrophages to adopt distinct migration patterns in vivo. *Eur. J. Immunol. 36: 2939-2950.*

9. Galan, J. E. 2001. Salmonella interactions with host cells: type III secretion at work. *Annu. Rev. Cell Dev. Biol. 17: 53-86.*

10. Brumell, J. H. and S. Grinstein. 2004. Salmonella redirects phagosomal maturation. *Curr. Opin. Microbiol. 7: 78-84.*

11. Alpuche Aranda, C. M., J. A. Swanson, W. P. Loomis, and S. I. Miller. 1992. Salmonella typhimurium activates virulence gene transcription within acidified macrophage phagosomes. *Proc. Natl. Acad. Sci. U. S. A. 89: 10079-10083.*

12. Ernst, R. K., T. Guina, and S. I. Miller. 2001. Salmonella typhimurium outer membrane remodeling: role in resistance to host innate immunity. *Microbes Infect. 3: 1327-1334.*

13. Cheminay, C., A. Mohlenbrink, and M. Hensel. 2005. Intracellular Salmonella inhibit antigen presentation by dendritic cells. *J. Immunol. 174: 2892-2899.*

14. Tobar, J. A., L. J. Carreno, S. M. Bueno, P. A. Gonzalez, J. E. Mora, S. A. Quezada, and A. M. Kalergis. 2006. Virulent Salmonella enterica serovar typhimurium evades adaptive immunity by preventing dendritic cells from activating T cells. *Infect. Immun. 74: 6438-6448.*

15. Halici, S., S. F. Zenk, J. Jantsch, and M. Hensel. 2008. Functional analysis of the Salmonella pathogenicity island 2-mediated inhibition of antigen presentation in dendritic cells. *Infect. Immun. 76: 4924-4933.*

16. Leung, K. Y. and B. B. Finlay. 1991. Intracellular replication is essential for the virulence of Salmonella typhimurium. *Proc. Natl. Acad. Sci. U. S. A. 88: 11470-11474.*

17. Farber, J. M. and P. I. Peterkin. 1991. Listeria monocytogenes, a food-borne pathogen. *Microbiol. Rev. 55: 476-511.*

18. Edelson, B. T. and E. R. Unanue. 2000. Immunity to Listeria infection. *Curr. Opin. Immunol. 12: 425-431.*

19. Mengaud, J., H. Ohayon, P. Gounon, R. -. Mege, and P. Cossart. 1996. E-cadherin is the receptor for internalin, a surface protein required for entry of L. monocytogenes into epithelial cells. *Cell 84: 923-932.*

20. Rosenberg, S. A., J. C. Yang, and N. P. Restifo. 2004. Cancer immunotherapy: moving beyond current vaccines. *Nat. Med. 10: 909-915.*

21. Klebanoff, C. A., L. Gattinoni, P. Torabi-Parizi, K. Kerstann, A. R. Cardones, S. E. Finkelstein, D. C. Palmer, P. A. Antony, S. T. Hwang, S. A. Rosenberg, T. A. Waldmann, and N. P. Restifo. 2005. Central memory self/tumor-reactive CD8+ T cells confer superior antitumor immunity compared with effector memory T cells. *Proc. Natl. Acad. Sci. U. S. A. 102: 9571-9576.*

22. Brincks, E. L., A. Katewa, T. A. Kucaba, T. S. Griffith, and K. L. Legge. 2008. CD8 T cells utilize TRAIL to control influenza virus infection. *J. Immunol. 181: 4918-4925.*

23. Shin, H., S. D. Blackburn, J. N. Blattman, and E. J. Wherry. 2007. Viral antigen and extensive division maintain virus-specific CD8 T cells during chronic infection. *J. Exp. Med. 204: 941-949.*

24. de Alencar, B. C., A. F. Araujo, M. L. Penido, R. T. Gazzinelli, and M. M. Rodrigues. 2007. Cross-priming of long lived protective CD8+ T cells against Trypanosoma cruzi infection: importance of a TLR9 agonist and CD4+ T cells. *Vaccine 25: 6018-6027.*

25. Stenger, S. and R. L. Modlin. 1998. Cytotoxic T cell responses to intracellular pathogens. *Curr. Opin. Immunol. 10: 471-477.*

26. Guleria, I., R. Mukherjee, and S. H. Kaufmann. 1993. In vivo depletion of CD4 and CD8 T lymphocytes impairs Mycobacterium w vaccine-induced protection against M. tuberculosis in mice. *Med. Microbiol. Immunol. 182: 129-135.*

27. Kaech, S. M., E. J. Wherry, and R. Ahmed. 2002. Effector and memory T-cell differentiation: implications for vaccine development. *Nat. Rev. Immunol. 2: 251-262.*

28. Cantrell, D. A. and K. A. Smith. 1984. The interleukin-2 T-cell system: a new cell growth model. *Science 224: 1312-1316.*

29. Moriggl, R., D. J. Topham, S. Teglund, V. Sexl, C. McKay, D. Wang, A. Hoffmeyer, J. van Deursen, M. Y. Sangster, K. D. Bunting, G. C. Grosveld, and J. N. Ihle. 1999. Stat5 is required for IL-2-induced cell cycle progression of peripheral T cells. *Immunity 10: 249-259.*

30. Hinrichs, C. S., L. Gattinoni, and N. P. Restifo. 2006. Programming CD8+ T cells for effective immunotherapy. *Curr. Opin. Immunol. 18: 363-370.*

31. Intlekofer, A. M., N. Takemoto, E. J. Wherry, S. A. Longworth, J. T. Northrup, V. R. Palanivel, A. C. Mullen, C. R. Gasink, S. M. Kaech, J. D. Miller, L. Gapin, K. Ryan, A. P. Russ, T. Lindsten, J. S. Orange, A. W. Goldrath, R. Ahmed, and S. L. Reiner. 2005. Effector and memory CD8+ T cell fate coupled by T-bet and eomesodermin. *Nat. Immunol. 6: 1236-1244.*

32. Pearce, E. L., A. C. Mullen, G. A. Martins, C. M. Krawczyk, A. S. Hutchins, V. P. Zediak, M. Banica, C. B. DiCioccio, D. A. Gross, C. A. Mao, H. Shen, N. Cereb, S. Y. Yang, T. Lindsten, J. Rossant, C. A. Hunter, and S. L. Reiner. 2003. Control of effector CD8+ T cell function by the transcription factor Eomesodermin. *Science 302: 1041-1043.*

33. Piccirillo, C. A. and E. M. Shevach. 2001. Cutting edge: control of CD8+ T cell activation by CD4+CD25+ immunoregulatory cells. *J. Immunol. 167: 1137-1140.*

34. Sallusto, F., J. Geginat, and A. Lanzavecchia. 2004. Central memory and effector memory T cell subsets: function, generation, and maintenance. *Annu. Rev. Immunol. 22: 745-763.*

35. Sad, S. and L. Krishnan. 2003. Maintenance and attrition of T-cell memory. *Crit. Rev. Immunol. 23: 129-147.*

36. Harty, J. T., A. R. Tvinnereim, and D. W. White. 2000. CD8+ T cell effector mechanisms in resistance to infection. *Annu. Rev. Immunol. 18: 275-308.*

37. Yap, G., M. Pesin, and A. Sher. 2000. Cutting edge: IL-12 is required for the maintenance of IFN-gamma production in T cells mediating chronic resistance to the intracellular pathogen, Toxoplasma gondii. *J. Immunol. 165: 628-631.*

38. Flynn, J. L., J. Chan, K. J. Triebold, D. K. Dalton, T. A. Stewart, and B. R. Bloom. 1993. An essential role for interferon gamma in resistance to Mycobacterium tuberculosis infection. *J. Exp. Med. 178: 2249-2254.*

39. Bachmann, M. F., P. Wolint, K. Schwarz, P. Jager, and A. Oxenius. 2005. Functional properties and lineage relationship of CD8+ T cell subsets identified by expression of IL-7 receptor alpha and CD62L. *J. Immunol. 175: 4686-4696.*

40. Paiardini, M., B. Cervasi, H. Albrecht, A. Muthukumar, R. Dunham, S. Gordon, H. Radziewicz, G. Piedimonte, M. Magnani, M. Montroni, S. M. Kaech, A. Weintrob, J. D. Altman, D. L. Sodora, M. B. Feinberg, and G. Silvestri. 2005. Loss of CD127 expression defines an expansion of effector CD8+ T cells in HIV-infected individuals. *J. Immunol. 174: 2900-2909.*

41. Janssen, E. M., N. M. Droin, E. E. Lemmens, M. J. Pinkoski, S. J. Bensinger, B. D. Ehst, T. S. Griffith, D. R. Green, and S. P. Schoenberger. 2005. CD4+ T-cell help controls CD8+ T-cell memory via TRAIL-mediated activation-induced cell death. *Nature 434: 88-93.*

42. Badovinac, V. P., A. R. Tvinnereim, and J. T. Harty. 2000. Regulation of antigen-specific CD8+ T cell homeostasis by perforin and interferon-gamma. *Science 290: 1354-1358.*

43. Sallusto, F., D. Lenig, R. Forster, M. Lipp, and A. Lanzavecchia. 1999. Two subsets of memory T lymphocytes with distinct homing potentials and effector functions. *Nature 401: 708-712.*

44. Kaech, S. M. and E. J. Wherry. 2007. Heterogeneity and cell-fate decisions in effector and memory CD8+ T cell differentiation during viral infection. *Immunity 27: 393-405.*

45. Kaech, S. M., E. J. Wherry, and R. Ahmed. 2002. Effector and memory T-cell differentiation: implications for vaccine development. *Nat. Rev. Immunol. 2: 251-262.*

46. Chang, J. T., V. R. Palanivel, I. Kinjyo, F. Schambach, A. M. Intlekofer, A. Banerjee, S. A. Longworth, K. E. Vinup, P. Mrass, J. Oliaro, N. Killeen, J. S. Orange, S. M. Russell, W. Weninger, and S. L. Reiner. 2007. Asymmetric T lymphocyte division in the initiation of adaptive immune responses. *Science 315: 1687-1691.*

47. Reiner, S. L., F. Sallusto, and A. Lanzavecchia. 2007. Division of labor with a workforce of one: challenges in specifying effector and memory T cell fate. *Science 317: 622-625.*

48. Gett, A. V., F. Sallusto, A. Lanzavecchia, and J. Geginat. 2003. T cell fitness determined by signal strength. *Nat. Immunol. 4: 355-360.*

49. Holmes, S., M. He, T. Xu, and P. P. Lee. 2005. Memory T cells have gene expression patterns intermediate between naive and effector. *Proc. Natl. Acad. Sci. U. S. A. 102: 5519-5523.*

50. Willinger, T., T. Freeman, H. Hasegawa, A. J. McMichael, and M. F. Callan. 2005. Molecular signatures distinguish human central memory from effector memory CD8 T cell subsets. *J. Immunol. 175: 5895-5903.*

51. Zhang, Y., G. Joe, E. Hexner, J. Zhu, and S. G. Emerson. 2005. Host-reactive CD8+ memory stem cells in graft-versus-host disease. *Nat. Med. 11: 1299-1305.*

52. Lanzavecchia, A. and F. Sallusto. 2000. From synapses to immunological memory: the role of sustained T cell stimulation. *Curr. Opin. Immunol. 12: 92-98.*

53. York, I. A. and K. L. Rock. 1996. Antigen processing and presentation by the class I major histocompatibility complex. *Annu. Rev. Immunol. 14: 369-396.*

54. Guermonprez, P., J. Valladeau, L. Zitvogel, C. Thery, and S. Amigorena. 2002. Antigen presentation and T cell stimulation by dendritic cells. *Annu. Rev. Immunol. 20: 621-667.*

55. Bevan, M. J. 1995. Antigen presentation to cytotoxic T lymphocytes in vivo. *J. Exp. Med. 182: 639-641.*

56. Kurts, C., J. F. Miller, R. M. Subramaniam, F. R. Carbone, and W. R. Heath. 1998. Major histocompatibility complex class I-restricted cross-presentation is biased towards high dose antigens and those released during cellular destruction. *J. Exp. Med. 188: 409-414.*

57. Kaufmann, S. H. and U. E. Schaible. 2005. Antigen presentation and recognition in bacterial infections. *Curr. Opin. Immunol. 17: 79-87.*

58. Gromme, M. and J. Neefjes. 2002. Antigen degradation or presentation by MHC class I molecules via classical and non-classical pathways. *Mol. Immunol. 39: 181-202.*

59. Parry, R. V., J. L. Riley, and S. G. Ward. 2007. Signalling to suit function: tailoring phosphoinositide 3-kinase during T-cell activation. *Trends Immunol. 28: 161-168.*

60. Lenschow, D. J., T. L. Walunas, and J. A. Bluestone. 1996. CD28/B7 system of T cell costimulation. *Annu. Rev. Immunol. 14: 233-258.*

61. Haring, J. S., V. P. Badovinac, and J. T. Harty. 2006. Inflaming the CD8+ T cell response. *Immunity 25: 19-29.*

62. Valenzuela, J. O., C. D. Hammerbeck, and M. F. Mescher. 2005. Cutting edge: Bcl-3 up-regulation by signal 3 cytokine (IL-12) prolongs survival of antigen-activated CD8 T cells. *J. Immunol. 174: 600-604.*

63. Cousens, L. P., R. Peterson, S. Hsu, A. Dorner, J. D. Altman, R. Ahmed, and C. A. Biron. 1999. Two roads diverged: interferon alpha/beta- and interleukin 12-mediated pathways in promoting T cell interferon gamma responses during viral infection. *J. Exp. Med. 189: 1315-1328.*

64. Tian, S., R. Maile, E. J. Collins, and J. A. Frelinger. 2007. CD8+ T cell activation is governed by TCR-peptide/MHC affinity, not dissociation rate. *J. Immunol. 179: 2952-2960.*

65. Krummel, M. F. 2007. Immunological synapses: breaking up may be good to do. *Cell 129: 653-655.*

66. Quigley, M., X. Huang, and Y. Yang. 2007. Extent of stimulation controls the formation of memory CD8 T cells. *J. Immunol. 179: 5768-5777.*

67. Kaech, S. M. and R. Ahmed. 2001. Memory CD8+ T cell differentiation: initial antigen encounter triggers a developmental program in naive cells. *Nat. Immunol. 2: 415-422.*

68. Luu, R. A., K. Gurnani, R. Dudani, R. Kammara, H. van Faassen, J. C. Sirard, L. Krishnan, and S. Sad. 2006. Delayed expansion and contraction of CD8+ T cell response during infection with virulent Salmonella typhimurium. *J. Immunol. 177: 1516-1525.*

69. Canonne-Hergaux, F., S. Gruenheid, G. Govoni, and P. Gros. 1999. The Nramp1 protein and its role in resistance to infection and macrophage function. *Proc. Assoc. Am. Physicians 111: 283-289.*

70. Valdez, Y., G. E. Diehl, B. A. Vallance, G. A. Grassl, J. A. Guttman, N. F. Brown, C. M. Rosenberger, D. R. Littman, P. Gros, and B. B. Finlay. 2008. Nramp1 expression by dendritic cells modulates inflammatory responses during Salmonella Typhimurium infection. *Cell. Microbiol. 10: 1646-1661.*

71. Forbes, J. R. and P. Gros. 2001. Divalent-metal transport by NRAMP proteins at the interface of host-pathogen interactions. *Trends Microbiol. 9: 397-403.*

72. Kaufmann, S. H. 1993. Immunity to intracellular bacteria. *Annu. Rev. Immunol. 11: 129-163.*

73. McCormick, B. A., C. A. Parkos, S. P. Colgan, D. K. Carnes, and J. L. Madara. 1998. Apical secretion of a pathogen-elicited epithelial chemoattractant activity in response to surface colonization of intestinal epithelia by Salmonella typhimurium. *J. Immunol. 160: 455-466.*

74. Knodler, L. A. and B. B. Finlay. 2001. Salmonella and apoptosis: to live or let die? *Microbes Infect. 3: 1321-1326.*

75. Monack, D. M., D. M. Bouley, and S. Falkow. 2004. Salmonella typhimurium persists within macrophages in the mesenteric lymph nodes of chronically infected

Nramp1+/+ mice and can be reactivated by IFNgamma neutralization. *J. Exp. Med. 199: 231-241.*

76. Chart, H., J. S. Cheesbrough, and D. J. Waghorn. 2000. The serodiagnosis of infection with Salmonella typhi. *J. Clin. Pathol. 53: 851-853.*

77. Michetti, P., M. J. Mahan, J. M. Slauch, J. J. Mekalanos, and M. R. Neutra. 1992. Monoclonal secretory immunoglobulin A protects mice against oral challenge with the invasive pathogen Salmonella typhimurium. *Infect. Immun. 60: 1786-1792.*

78. Mittrucker, H. W., B. Raupach, A. Kohler, and S. H. Kaufmann. 2000. Cutting edge: role of B lymphocytes in protective immunity against Salmonella typhimurium infection. *J. Immunol. 164: 1648-1652.*

79. Wijburg, O. L., T. K. Uren, K. Simpfendorfer, F. E. Johansen, P. Brandtzaeg, and R. A. Strugnell. 2006. Innate secretory antibodies protect against natural Salmonella typhimurium infection. *J. Exp. Med. 203: 21-26.*

80. Thatte, J., S. Rath, and V. Bal. 1993. Immunization with live versus killed Salmonella typhimurium leads to the generation of an IFN-gamma-dominant versus an IL-4-dominant immune response. *Int. Immunol. 5: 1431-1436.*

81. Mittrucker, H. W. and S. H. Kaufmann. 2000. Immune response to infection with Salmonella typhimurium in mice. *J. Leukoc. Biol. 67: 457-463.*

82. Mittrucker, H. W., A. Kohler, and S. H. Kaufmann. 2002. Characterization of the murine T-lymphocyte response to Salmonella enterica serovar Typhimurium infection. *Infect. Immun. 70: 199-203.*

83. Sprott, G. D., S. Sad, L. P. Fleming, C. J. Dicaire, G. B. Patel, and L. Krishnan. 2003. Archaeosomes varying in lipid composition differ in receptor-mediated endocytosis and differentially adjuvant immune responses to entrapped antigen. *Archaea 1: 151-164.*

84. Sad, S. and L. Krishnan. 2003. Maintenance and attrition of T-cell memory. *Crit. Rev. Immunol. 23: 129-147.*

85. van Faassen, H., R. Dudani, L. Krishnan, and S. Sad. 2004. Prolonged antigen presentation, APC-, and CD8+ T cell turnover during mycobacterial infection: comparison with Listeria monocytogenes. *J. Immunol. 172: 3491-3500.*

86. Hayashi, F., K. D. Smith, A. Ozinsky, T. R. Hawn, E. C. Yi, D. R. Goodlett, J. K. Eng, S. Akira, D. M. Underhill, and A. Aderem. 2001. The innate immune response to bacterial flagellin is mediated by Toll-like receptor 5. *Nature 410: 1099-1103.*

87. Barsig, J., I. E. Flesch, and S. H. Kaufmann. 1998. Macrophages and hepatocytic cells as chemokine producers in murine listeriosis. *Immunobiology 199: 87-104.*

88. Hsieh, C. S., S. E. Macatonia, C. S. Tripp, S. F. Wolf, A. O'Garra, and K. M. Murphy. 1993. Development of TH1 CD4+ T cells through IL-12 produced by Listeria-induced macrophages. *Science 260: 547-549.*

89. Sun, J. C., M. A. Williams, and M. J. Bevan. 2004. CD4+ T cells are required for the maintenance, not programming, of memory CD8+ T cells after acute infection. *Nat. Immunol. 5: 927-933.*

90. Edelson, B. T., P. Cossart, and E. R. Unanue. 1999. Cutting edge: paradigm revisited: antibody provides resistance to Listeria infection. *J. Immunol. 163: 4087-4090.*

91. Yrlid, U. and M. J. Wick. 2000. Salmonella-induced apoptosis of infected macrophages results in presentation of a bacteria-encoded antigen after uptake by bystander dendritic cells. *J. Exp. Med. 191: 613-624.*

92. Srinivasan, A., J. Foley, R. Ravindran, and S. J. McSorley. 2004. Low-dose Salmonella infection evades activation of flagellin-specific CD4 T cells. *J. Immunol. 173: 4091-4099.*

93. Russell, M. S., M. Iskandar, O. L. Mykytczuk, J. H. Nash, L. Krishnan, and S. Sad. 2007. A Reduced Antigen Load In Vivo, Rather Than Weak Inflammation, Causes a Substantial Delay in CD8+ T Cell Priming against Mycobacterium bovis (Bacillus Calmette-Guerin). *J. Immunol. 179: 211-220.*

94. Sad, S., R. Dudani, K. Gurnani, M. Russell, H. van Faassen, B. Finlay, and L. Krishnan. 2008. Pathogen proliferation governs the magnitude but compromises the function of CD8 T cells. *J. Immunol. 180: 5853-5861.*

95. O'Callaghan, D., D. Maskell, F. Y. Liew, C. S. Easmon, and G. Dougan. 1988. Characterization of aromatic- and purine-dependent Salmonella typhimurium: attention, persistence, and ability to induce protective immunity in BALB/c mice. *Infect. Immun. 56: 419-423.*

96. Lyons, A. B. 2000. Analysing cell division in vivo and in vitro using flow cytometric measurement of CFSE dye dilution. *J. Immunol. Methods 243: 147-154.*

97. van Faassen, H., M. Saldanha, D. Gilbertson, R. Dudani, L. Krishnan, and S. Sad. 2005. Reducing the stimulation of CD8+ T cells during infection with intracellular bacteria promotes differentiation primarily into a central (CD62LhighCD44high) subset. *J. Immunol. 174: 5341-5350.*

98. Thanarajasingam, U., L. Sanz, R. Diaz, J. Qiao, L. Sanchez-Perez, T. Kottke, J. Thompson, J. Chester, and R. G. Vile. 2007. Delivery of CCL21 to metastatic disease improves the efficacy of adoptive T-cell therapy. *Cancer Res. 67: 300-308.*

99. Holden, D. W. 2002. Trafficking of the Salmonella vacuole in macrophages. *Traffic 3: 161-169.*

100. Lindgren, S. W., I. Stojiljkovic, and F. Heffron. 1996. Macrophage killing is an essential virulence mechanism of Salmonella typhimurium. *Proc. Natl. Acad. Sci. U. S. A. 93: 4197-4201.*

101. Salcedo, S. P., M. Noursadeghi, J. Cohen, and D. W. Holden. 2001. Intracellular replication of Salmonella typhimurium strains in specific subsets of splenic macrophages in vivo. *Cell. Microbiol. 3: 587-597.*

102. Abshire, K. Z. and F. C. Neidhardt. 1993. Growth rate paradox of Salmonella typhimurium within host macrophages. *J. Bacteriol. 175: 3744-3748.*

103. McCollister, B. D., T. J. Bourret, R. Gill, J. Jones-Carson, and A. Vazquez-Torres. 2005. Repression of SPI2 transcription by nitric oxide-producing, IFNgamma-activated macrophages promotes maturation of Salmonella phagosomes. *J. Exp. Med. 202: 625-635.*

104. Richter-Dahlfors, A., A. M. Buchan, and B. B. Finlay. 1997. Murine salmonellosis studied by confocal microscopy: Salmonella typhimurium resides intracellularly inside macrophages and exerts a cytotoxic effect on phagocytes in vivo. *J. Exp. Med. 186: 569-580.*

105. Monack, D. M., B. Raupach, A. E. Hromockyj, and S. Falkow. 1996. Salmonella typhimurium invasion induces apoptosis in infected macrophages. *Proc. Natl. Acad. Sci. U. S. A. 93: 9833-9838.*

106. van der Velden, A. W., M. Velasquez, and M. N. Starnbach. 2003. Salmonella rapidly kill dendritic cells via a caspase-1-dependent mechanism. *J. Immunol. 171: 6742-6749.*

107. Chan, S. S., P. Mastroeni, I. McConnell, and B. A. Blacklaws. 2008. Salmonella infection of afferent lymph dendritic cells. *J. Leukoc. Biol. 83: 272-279.*

108. Garcia-del Portillo, F., C. Nunez-Hernandez, B. Eisman, and J. Ramos-Vivas. 2008. Growth control in the Salmonella-containing vacuole. *Curr. Opin. Microbiol. 11: 46-52.*

109. Tierrez, A. and F. Garcia-del Portillo. 2005. New concepts in Salmonella virulence: the importance of reducing the intracellular growth rate in the host. *Cell. Microbiol. 7: 901-909.*

110. Segura, I., J. Casadesus, and F. Ramos-Morales. 2004. Use of mixed infections to study cell invasion and intracellular proliferation of Salmonella enterica in eukaryotic cell cultures. *J. Microbiol. Methods 56: 83-91.*

111. Jantsch, J., C. Cheminay, D. Chakravortty, T. Lindig, J. Hein, and M. Hensel. 2003. Intracellular activities of Salmonella enterica in murine dendritic cells. *Cell. Microbiol. 5: 933-945.*

112. Fey, A., S. Eichler, S. Flavier, R. Christen, M. G. Hofle, and C. A. Guzman. 2004. Establishment of a real-time PCR-based approach for accurate quantification of bacterial RNA targets in water, using Salmonella as a model organism. *Appl. Environ. Microbiol. 70: 3618-3623.*

113. Shi, L., R. North, and M. L. Gennaro. 2004. Effect of growth state on transcription levels of genes encoding major secreted antigens of Mycobacterium tuberculosis in the mouse lung. *Infect. Immun. 72: 2420-2424.*

114. Price, D. A., J. M. Brenchley, L. E. Ruff, M. R. Betts, B. J. Hill, M. Roederer, R. A. Koup, S. A. Migueles, E. Gostick, L. Wooldridge, A. K. Sewell, M. Connors, and D. C. Douek. 2005. Avidity for antigen shapes clonal dominance in CD8+ T cell populations specific for persistent DNA viruses. *J. Exp. Med. 202: 1349-1361.*

115. Winau, F., S. H. Kaufmann, and U. E. Schaible. 2004. Apoptosis paves the detour path for CD8 T cell activation against intracellular bacteria. *Cell. Microbiol. 6: 599-607.*

116. Yao, Z. Q., E. King, D. Praylher, D. Yin, and J. Moorman. 2007. T Cell Dysfunction by Hepatitis C Virus Core Protein Involves PD-1/PDL-1 Signaling. *Viral Immunol. 20: 276-287.*

117. Blank, C., J. Kuball, S. Voelkl, H. Wiendl, B. Becker, B. Walter, O. Majdic, T. F. Gajewski, M. Theobald, R. Andreesen, and A. Mackensen. 2006. Blockade of PD-L1 (B7-H1) augments human tumor-specific T cell responses in vitro. *Int. J. Cancer 119: 317-327.*

118. Barber, D. L., E. J. Wherry, and R. Ahmed. 2003. Cutting edge: rapid in vivo killing by memory CD8 T cells. *J. Immunol. 171: 27-31.*

119. Sun, J. C. and M. J. Bevan. 2003. Defective CD8 T cell memory following acute infection without CD4 T cell help. *Science 300: 339-342.*

120. Sun, J. C., M. A. Williams, and M. J. Bevan. 2004. CD4+ T cells are required for the maintenance, not programming, of memory CD8+ T cells after acute infection. *Nat. Immunol. 5: 927-933.*

121. Sercan, O., G. J. Hammerling, B. Arnold, and T. Schuler. 2006. Innate immune cells contribute to the IFN-gamma-dependent regulation of antigen-specific CD8+ T cell homeostasis. *J. Immunol. 176: 735-739.*

122. Godinez, I., T. Haneda, M. Raffatellu, M. D. George, T. A. Paixao, H. G. Rolan, R. L. Santos, S. Dandekar, R. M. Tsolis, and A. J. Baumler. 2008. T cells help to amplify inflammatory responses induced by Salmonella enterica serotype Typhimurium in the intestinal mucosa. *Infect. Immun. 76: 2008-2017.*

123. Johansson, C., M. Ingman, and M. Jo Wick. 2006. Elevated neutrophil, macrophage and dendritic cell numbers characterize immune cell populations in mice chronically infected with Salmonella. *Microb. Pathog. 41: 49-58.*

124. Munoz-Elias, E. J., J. Timm, T. Botha, W. T. Chan, J. E. Gomez, and J. D. McKinney. 2005. Replication dynamics of Mycobacterium tuberculosis in chronically infected mice. *Infect. Immun. 73: 546-551.*

125. Vergne, I., J. Chua, S. B. Singh, and V. Deretic. 2004. Cell biology of mycobacterium tuberculosis phagosome. *Annu. Rev. Cell Dev. Biol. 20: 367-394.*

126. van Stipdonk, M. J., E. E. Lemmens, and S. P. Schoenberger. 2001. Naive CTLs require a single brief period of antigenic stimulation for clonal expansion and differentiation. *Nat. Immunol. 2: 423-429.*

127. Dudani, R., Y. Chapdelaine, H. Faassen Hv, D. K. Smith, H. Shen, L. Krishnan, and S. Sad. 2002. Multiple mechanisms compensate to enhance tumor-protective CD8(+) T cell response in the long-term despite poor CD8(+) T cell priming initially: comparison between an acute versus a chronic intracellular bacterium expressing a model antigen. *J. Immunol. 168: 5737-5745.*

128. Mercado, R., S. Vijh, S. E. Allen, K. Kerksiek, I. M. Pilip, and E. G. Pamer. 2000. Early programming of T cell populations responding to bacterial infection. *J. Immunol. 165: 6833-6839.*

129. Kadurugamuwa, J. L. and T. J. Beveridge. 1998. Delivery of the non-membrane-permeative antibiotic gentamicin into mammalian cells by using Shigella flexneri membrane vesicles. *Antimicrob. Agents Chemother. 42: 1476-1483.*

130. Carryn, S., F. Van Bambeke, M. P. Mingeot-Leclercq, and P. M. Tulkens. 2003. Activity of beta-lactams (ampicillin, meropenem), gentamicin, azithromycin and moxifloxacin against intracellular Listeria monocytogenes in a 24 h THP-1 human macrophage model. *J. Antimicrob. Chemother. 51: 1051-1052.*

131. Coburn, B., Y. Li, D. Owen, B. A. Vallance, and B. B. Finlay. 2005. Salmonella enterica serovar Typhimurium pathogenicity island 2 is necessary for complete virulence in a mouse model of infectious enterocolitis. *Infect. Immun. 73: 3219-3227.*

132. van der Velden, A. W., M. K. Copass, and M. N. Starnbach. 2005. Salmonella inhibit T cell proliferation by a direct, contact-dependent immunosuppressive effect. *Proc. Natl. Acad. Sci. U. S. A. 102: 17769-17774.*

133. Berche, P., J. L. Gaillard, and P. J. Sansonetti. 1987. Intracellular growth of Listeria monocytogenes as a prerequisite for in vivo induction of T cell-mediated immunity. *J. Immunol. 138: 2266-2271.*

134. Brunt, L. M., D. A. Portnoy, and E. R. Unanue. 1990. Presentation of Listeria monocytogenes to CD8+ T cells requires secretion of hemolysin and intracellular bacterial growth. *J. Immunol. 145: 3540-3546.*

135. Lauvau, G., S. Vijh, P. Kong, T. Horng, K. Kerksiek, N. Serbina, R. A. Tuma, and E. G. Pamer. 2001. Priming of memory but not effector CD8 T cells by a killed bacterial vaccine. *Science 294: 1735-1739.*

136. Rabinovitch, M. 1995. Professional and non-professional phagocytes: an introduction. *Trends Cell Biol. 5: 85-87.*

137. Rogerson, B. J., Y. J. Jung, R. LaCourse, L. Ryan, N. Enright, and R. J. North. 2006. Expression levels of Mycobacterium tuberculosis antigen-encoding genes versus production levels of antigen-specific T cells during stationary level lung infection in mice. *Immunology 118: 195-201.*

138. Richardson, J., J. C. Craighead, S. L. Cao, and M. Handfield. 2005. Concurrence between the gene expression pattern of Actinobacillus actinomycetemcomitans in localized aggressive periodontitis and in human epithelial cells. *J. Med. Microbiol. 54: 497-504.*

139. Shi, L., Y. J. Jung, S. Tyagi, M. L. Gennaro, and R. J. North. 2003. Expression of Th1-mediated immunity in mouse lungs induces a Mycobacterium tuberculosis transcription pattern characteristic of nonreplicating persistence. *Proc. Natl. Acad. Sci. U. S. A. 100: 241-246.*

140. Shi, L., C. D. Sohaskey, B. D. Kana, S. Dawes, R. J. North, V. Mizrahi, and M. L. Gennaro. 2005. Changes in energy metabolism of Mycobacterium tuberculosis in mouse lung and under in vitro conditions affecting aerobic respiration. *Proc. Natl. Acad. Sci. U. S. A. 102: 15629-15634.*

141. Henrickson, S. E., T. R. Mempel, I. B. Mazo, B. Liu, M. N. Artyomov, H. Zheng, A. Peixoto, M. P. Flynn, B. Senman, T. Junt, H. C. Wong, A. K. Chakraborty, and U. H. von Andrian. 2008. T cell sensing of antigen dose governs interactive behavior with dendritic cells and sets a threshold for T cell activation. *Nat. Immunol. 9: 282-291.*

142. Porgador, A., J. W. Yewdell, Y. Deng, J. R. Bennink, and R. N. Germain. 1997. Localization, quantitation, and in situ detection of specific peptide-MHC class I complexes using a monoclonal antibody. *Immunity 6: 715-726.*

143. Sad, S., R. Dudani, K. Gurnani, M. Russell, H. van Faassen, B. Finlay, and L. Krishnan. 2008. Pathogen proliferation governs the magnitude but compromises the function of CD8 T cells. *J. Immunol. 180: 5853-5861.*

144. Berstein, G. and R. T. Abraham. 2008. Moving out: mobilizing activated T cells from lymphoid tissues. *Nat. Immunol. 9: 455-457.*

145. Sallusto, F., E. Kremmer, B. Palermo, A. Hoy, P. Ponath, S. Qin, R. Forster, M. Lipp, and A. Lanzavecchia. 1999. Switch in chemokine receptor expression upon TCR stimulation reveals novel homing potential for recently activated T cells. *Eur. J. Immunol. 29: 2037-2045.*

146. Golden-Mason, L., B. Palmer, J. Klarquist, J. A. Mengshol, N. Castelblanco, and H. R. Rosen. 2007. Upregulation of Pd-1 Expression on Circulating and Intrahepatic Hcv-Specific Cd8+ T Cells Associated with Reversible Immune Dysfunction. *J. Virol.*

147. Suvas, S. and B. T. Rouse. 2006. Treg control of antimicrobial T cell responses. *Curr. Opin. Immunol. 18: 344-348.*

148. Qimron, U., N. Madar, H. W. Mittrucker, A. Zilka, I. Yosef, N. Bloushtain, S. H. Kaufmann, I. Rosenshine, R. N. Apte, and A. Porgador. 2004. Identification of Salmonella typhimurium genes responsible for interference with peptide presentation on MHC class I molecules: Deltayej Salmonella mutants induce superior CD8+ T-cell responses. *Cell. Microbiol. 6: 1057-1070.*

149. Steele-Mortimer, O. 2008. The Salmonella-containing vacuole: moving with the times. *Curr. Opin. Microbiol. 11: 38-45.*

150. Grant, A. J., M. Sheppard, R. Deardon, S. P. Brown, G. Foster, C. E. Bryant, D. J. Maskell, and P. Mastroeni. 2008. Caspase-3-dependent phagocyte death during systemic Salmonella enterica serovar Typhimurium infection of mice. *Immunology 125: 28-37.*

151. Brennan, M. A. and B. T. Cookson. 2000. Salmonella induces macrophage death by caspase-1-dependent necrosis. *Mol. Microbiol. 38: 31-40.*

152. Sundquist, M., A. Rydstrom, and M. J. Wick. 2004. Immunity to Salmonella from a dendritic point of view. *Cell. Microbiol. 6: 1-11.*

153. Reitmeyer, J. C., J. W. Peterson, and K. J. Wilson. 1986. Salmonella cytotoxin: a component of the bacterial outer membrane. *Microb. Pathog. 1: 503-510.*

154. Ashkenazi, S., T. G. Cleary, B. E. Murray, A. Wanger, and L. K. Pickering. 1988. Quantitative analysis and partial characterization of cytotoxin production by Salmonella strains. *Infect. Immun. 56: 3089-3094.*

155. Sallusto, F., P. Schaerli, P. Loetscher, C. Schaniel, D. Lenig, C. R. Mackay, S. Qin, and A. Lanzavecchia. 1998. Rapid and coordinated switch in chemokine receptor expression during dendritic cell maturation. *Eur. J. Immunol. 28: 2760-2769.*

156. Gray, D. 2002. A role for antigen in the maintenance of immunological memory. *Nat. Rev. Immunol. 2: 60-65.*

157. Hobbie, S., L. M. Chen, R. J. Davis, and J. E. Galan. 1997. Involvement of mitogen-activated protein kinase pathways in the nuclear responses and cytokine production induced by Salmonella typhimurium in cultured intestinal epithelial cells. *J. Immunol. 159: 5550-5559.*

RESUME

HOMAM ALBAGHDADI
CURRICULUM VITAE

ACADEMICS

August 2006 – Jan 2009 The University of Ottawa/ NRC

- **Masters** Thesis in immunology and microbiology with Dr. Subash Sad at the National Research Council of Canada.
- Recipient of the Ontario Scholarship for Science and Technology **(OGSST)**
- Recipient of the **Group Achievement and Teamwork Award** from the National Research Council of Canada

September 2001 - May 2006 The University of Ottawa, Faculty of Science

- Graduated with an **B.Sc (Honours)** in **Biopharmaceutical Science** with a **Genomics** option
- Program is interdisciplinary in nature integrating studies such as molecular biology and genetics, pharmacology, biochemistry, and organic chemistry and many especially formulated courses that are genetic and biological in nature.
- Honours Research Project at Health Canada with Dr. Sean Li, M.D., Ph.D.
- Honours Research Paper: Proliferative inhibition of various strains of Influenza A Virus by Aurintricarboxylic Acid.
- $10,000 scholarship recipient.
- Dean's Honour list.
- A member of the Golden Key International Honours Society recognizing top 15% of all students.

September 1999 - June 2001 Cairine Wilson Secondary School

- Graduated and obtained **OSSD** in 2001
- **Ontario Scholar** Designation with an academic average of 89%
- Two awards for OAC **Outstanding Achievement**
- 3 **Excellence Awards** in Chemistry, Calculus, and Biology

LABORATORY EXPERIENCE

October 2008 – Present National Research Council – Montreal Rd, Ottawa
Research Assistant with the Cerebrovascular group investigating clinical imaging modalities and targeted contrast agents in brain tumor models.

August 2006 – October 2008 National Research Council – Montreal Rd., Ottawa
Masters Research Thesis investigating CD8 T cell development and response against Salmonella Typhimurium

September 2005 - May 2006 Health Canada – Tunney's Pasture, Ottawa
Honours Research Lab project investigating the anti-viral properties of Aurintricarboxylic Acid against strains of Influenza A virus

Laboratory Techniques:

- Mice handling, bleeding, and organ recovery
- Mice injections (intravenous, intracranial, intraperitoneal)

- Perfusion
- Fluorescent in vivo imaging
- MicroCT in vivo imaging
- Nanoparticle modifications and functionalization
- Liposome synthesis and functionalization
- Pharmacokinetics
- Imuunohistochemistry
- Fluorescent microscopy
- Cell Purification and Enrichment (columns, beads)
- Cell Proliferation assays
- Flowcytometry (FACS) and cell labeling
- Intracellular staining
- Tissue Culture
- In vitro and In vivo Cytotoxicity Assays
- Virus Titration, plaque assays and other virological methodologies
- Enzyme-Linked Immunosorbent Assay (ELISA)
- Eli-SPOT
- Immunoblotting (Western, Dot blots, and cell blots)
- Protein Purification
- FPLC/SEC/IMAC
- RNA extraction
- Polymerase Chain Reaction (PCR)
- Quantitiative real time PCR (QPCR)

Additional Notes

- Carried out extensive literature and resource research
- Developed familiarity with laboratory equipments such as plate washers, centrifuges, spectrophotometers and plate readers, pH meters, PCR machines.

September 2001 - May 2004 University of Ottawa

- Academic Level laboratory experiencein biology, inorganic and organic chemistry, biochemistry, molecular biology, and microbiology
- Knowledge of separation techniques (Chromatography, Electrophoresis), restriction digest and analysis, and bioinformatics.

CONFERENCES

- Attended and presented a poster at the Canadian Society for Immunology annual scientific conference in April 2008.

OTHER WORK EXPERIENCE

2001-2002	Pioneer Gas station
2002-2003	New York Fries
2003-2005	Bluenotes Outfitters
2005-2006	Mexx Boutique

Work was on a part-time basis during the school year and full-time over the summer. I acquired valuable social and public service skills due to the interactive nature of these positions. Furthermore, I learned valuable time management skills, since it is not easy to balance work and school work.

2002 (summer) Ottawa General Hospital – Eye institute

Volunteer work once a week for 3 months. It was an opportunity to get a feel for patient-physician interaction, as well as a great opportunity to give back to the community. I was lucky enough to be given the chance to converse with and witness renowned Eye surgeon Dr. Sherif El-Defrawy - currently chair of the ophthalmology department at Queens school of medicine - perform a cataract removal operation

2006-2008 University of Ottawa

Laboratory Teaching assistant: I obtained invaluable experience interacting with and coaching students through advanced lab procedures.

PUBLICATIONS

Additive inhibition of H1N1 and H3N2 influenza viruses by Aurintricarboxylic Acid with Amantadine.

Anathea S. Flaman, **Homam Albaghdadi**, Jeff McClintock, Todd Cutts, Anwar Hashem, Matt LeBrun, John Austin, Earl Brown, Runtao He, Xuguang Li

Options for the Control of Influenza Virus. Page 478-479. J. Katz (Eds). 2008, ISBN: 978-901-769-15-6. International Medical Press. London. U.K

Selectively reduced intracellular proliferation of Salmonella Typhimurium within antigen-presenting cells limits antigen-presentation and development of a rapid CD8 T cell response

Homam Albaghdadi, Brett Finlay, Lakshmi Krishnan and Subash Sad.

Manuscript has been submitted to the Journal of Immunology. ID# 09-00843-FL

REFERENCES

Available promptly upon request.

CONTACT

125 FORESTCREST ST
OTTAWA, ONTARIO, CANADA K1C 7R3
613-276-4628